



2010

Cellular effects and signalling pathways induced by MLK3 mutations

Ana Teresa Ferreira Correia. Pinto



DEPARTAMENTO DE CIÊNCIAS DA VIDA

FACULDADE DE CIÊNCIAS E TECNOLOGIA  
UNIVERSIDADE DE COIMBRA

Cellular effects and signalling pathways  
induced by MLK3 mutations

---

Ana Teresa Ferreira Correia Pinto

2010



## DEPARTAMENTO DE CIÊNCIAS DA VIDA

FACULDADE DE CIÊNCIAS E TECNOLOGIA

UNIVERSIDADE DE COIMBRA

### Cellular effects and signalling pathways induced by MLK3 mutations

Dissertação apresentada à Universidade de Coimbra para cumprimento dos requisitos necessários à obtenção do grau de Mestre em Biologia Celular e Molecular. O trabalho foi realizado sob a orientação científica da Professora Doutora Raquel Seruca (IPATIMUP) e supervisão da Professora Doutora Emília

---

Ana Teresa Ferreira Correia Pinto

2010



**This experimental work was developed in Cancer Genetics group at Institute of Molecular Pathology and Immunology of the University of Porto (IPATIMUP), Porto**

**2010**

## Acknowledgements

First of all, I would like to acknowledge to my thesis supervisor Dr. Raquel Seruca, not only for giving me the opportunity to work in her laboratory and with this project, but also for always receiving me with open arms.

To Sérgio I have also a lot to thank. She followed my work from the beginning having thus become like a shelter to me. Even with all the work she had during this year, she got time to discuss the results, plan experiments and talk with me. Thank you for these moments.

A special word to Maria for the time she spent either performing or discussing some important experiments with me. Thanks for your dedication, for your example and for your sweet words.

I have also to thank to those people who made part of my daily life in the laboratory. To those who participated in my integration thanks for the long hours you spent teaching me and answering to all my doubts and questions. To those who provided technical support thanks for your help and patience. Gratefully, I met fantastic people. Thanks you for the long conversations, for the encouragement words and for your care.

I could not end my list of acknowledgments without directing a sincerely thanks to my family. Thanks for your love and for being there whenever I need you.

## Table of contents

<b>Abbreviations</b>	<b>7</b>
<b>Resumo</b>	<b>11</b>
<b>Abstract</b>	<b>12</b>
<b>Chapter 1 Introduction</b>	<b>13</b>
1.1 <i>Mixed-lineage kinase 3 (MLK3)</i>	14
1.1.1 MLK3 structure organization	14
1.1.2 Regulation of MLK3 activity	17
1.1.2.1 Regulation through intramolecular interactions	17
1.1.2.2 Regulation through phosphorylation	17
1.1.3 MLK3 role in different physiological functions	20
1.1.3.1 MLK3 role in cell proliferation	21
1.1.3.1.1 MLK3 may contribute to microtubule instability during mitosis	22
1.1.3.2 Role of MLK3 in JNK-mediated cell death or survival	23
1.1.3.3 Role of MLK3 in intracellular trafficking and cell migration	26
1.1.3.3.1 MLK3 scaffold properties in intracellular trafficking	26
1.1.3.3.2 MLK3 regulates Rho activation	27
1.1.4 MLK3 related cancer	28
1.1.4.1 MLK3 in tumour cell proliferation.	29
1.1.4.2 MLK3 overexpression in tumours	29
1.1.4.3 Promoting MLK3 activation in tumours	32
1.1.4.4 MLK3 may potentiate taxol antitumour activity	33
1.1.4.5 MLK3 mutations in tumours	33
<b>Chapter 2 Project aims</b>	<b>37</b>
<b>Chapter 3 Material and Methods</b>	<b>39</b>
3.1 <i>Cell culture</i>	40
3.2 <i>Establishment of HEK293 stable cell lines</i>	42
3.2.1 Maxiprep preparation	43
3.2.2 Transfection	43
3.2.3 RT-PCR	43
3.2.4 PCR for MLK3 amplification	44

3.2.5	Agarose gel electrophoresis	45
3.2.6	Sequencing	46
3.3	<i>Transient transfections</i>	47
3.4	<i>Snapshot</i>	47
3.5	<i>Western Blot</i>	48
3.6	<i>Functional assays</i>	52
3.6.1	Proliferation assay	52
3.6.2	Migration assay	53
3.6.3	Viability assay	53
3.6.4	Slow aggregation assay	54
3.7	<i>Solutions recipes</i>	54
<b>Chapter 4</b>	<b>Results and Discussion</b>	<b>57</b>
4.1	<i>P252H has functional value in colorectal context</i>	58
4.2	<i>Establishment of HEK293 stable cell lines</i>	60
4.2.1	Selection after sequencing	61
4.2.2	Selection based on transfection efficiency	62
4.3	<i>Cellular effects of MLK3 mutations and of wild-type MLK3 overexpression</i>	64
4.3.1	Proliferation	64
4.3.2	Viability	66
4.3.3	Migration	71
4.3.4	Aggregation	73
4.4	<i>Signalling of P252H and R799C mutations and of wild-type MLK3 overexpression</i>	75
4.4.1	MLK3 mutations induces invasion by E-cadherin regulation	78
4.4.2	P252H and R799C mutations do not share similar patterns of p27 and cyclin D1 expression	78
4.4.3	P252H mutation induces cell migration	81
4.4.4	R799C mutation decreases cell migration	82
4.4.5	Effects of ROCK inhibitor	83
4.4.6	MLK3 mutations and WNT signalling pathway	85
4.4.7	Wild-type MLK3 overexpression	87
<b>Chapter 5</b>	<b>Concluding remarks and future perspectives</b>	<b>89</b>

<b>Chapter 6</b>	<b>References</b>	<b>91</b>
<b>Chapter 7</b>	<b>Appendix</b>	<b>101</b>

## Abbreviations

Akt	v-Akt murine thymoma viral oncogene
AP-1	Activator protein 1
APE	Alanine, proline, glutamate
A $\beta$	Amyloid- $\beta$ peptide
Bax	Bcl2-associated protein
Bcl2	B-cell lymphoma 2
Bim	Bcl2 interacting mediator
BMP-6	Bone morphogenetic protein 6
B-Raf	v-RAF murine sarcoma viral oncogene homolog B
BrdU	Bromodeoxyuridine
BSA	Bovine serum albumin
Cdc42	Cell division cell cycle 42
CDK	Cyclin-dependent kinase
CDKI	Cyclin-dependent kinase inhibitor
cDNA	Complementary deoxyribonucleic acid
CHO	Chinese hamster ovary
CK	Cytokeratin
CRIB	Cdc42/Rac interactive binding motif
DEPC	Diethyl pyrocarbonate
DFG	Aspartate, phenylalanine, glycine
DLK	Dual-leucine-zipper-bearing kinase
DMEM	Dulbecco's modified Eagle's medium
DNA	Deoxyribonucleic acid
dNTP	Deoxyribonucleotide triphosphate
DTT	Dithiothreitol
E2	17 $\beta$ -estradiol
ECL	Enhanced chemiluminescence
EDTA	Ethylenediaminetetraacetic acid
EGF	Epidermal growth factor
EGFR	EGF receptor
ER <sup>-</sup>	Estrogen receptor-negative
ERK	Extracellular signal-regulated kinase
FBS	Fetal bovine serum
FZD10	Frizzled homologue 10
G17	Gastrin-17



GAPDH	Glyceraldehyde 3-phosphate dehydrogenase
GCK	Germinal center kinase
GDP	Guanosine diphosphate
Gly	Glycine
GnRH-a	Gonadotropin releasing hormone analogs
GPCR	G protein-coupled receptor
GRP	Glycine-rich protein
GSK-3 $\beta$	Glycogen synthase kinase-3 beta
GTP	Guanosine triphosphate
GTPase	Guanosine triphosphatase
HEK293	Human embryonic kidney 293
HNSCC	Head and neck squamous cancer
HPK	Hematopoietic kinase
H-Ras	Harvey rat sarcoma virus oncogene
HRP	Horseradish Peroxidase
Hsp90	Heat-shock protein 90
IgG	Immunoglobulin G
IKB	Inhibitor of NF-KB
IKC	I $\kappa$ B kinase complex
IKK	I $\kappa$ B kinase
IL-1	Interleukin-1
JIP	JNK-interacting protein
JNK	c-Jun N-terminal kinase
KIF	Kinesin superfamily protein
K-Ras	Kirsten rat sarcoma virus oncogene
LEF1	Lymphoid enhancer-binding factor-1
LZK	Leucine zipper-bearing kinase
MAPK	Mitogen-activated protein kinase
MEK	MAPK/ERK kinase
MEKK	Erk kinase kinase (=MAP3K=MAPKKK)
MKK	Mitogen-activated protein kinase
MLK3	Mixed-lineage kinase 3
MMP7	Metalloproteinase 7
mRNA	Messenger ribonucleic acid
MSI	Microsatellite instability
NAD+	Nicotinamide adenine dinucleotide
NADH	Reduced nicotinamide adenine dinucleotide

NADPH	Reduced nicotinamide adenine dinucleotide phosphate
NF	Neurofibromatosis
NF-kB	Nuclear factor kappa-light-chain-enhancer of activated B cells
NGF	Nerve growth factor
NIH3T3	Mouse embryo fibroblast cell line
NIMA	Never-in-mitosis in <i>Aspergillus nidulans</i>
NMDA	N-methyl-D-aspartic acid
P/S/T	Proline/Serine/Threonine
p63RhoGEF	p63 Rho guanosine nucleotide exchange factor
PARP	Protein poly (ADP-ribose) polymerase
PBS	Phosphate buffered saline
PCR	Polymerase chain reaction
PDPKs	Proline-directed protein kinases
Phospho	Phosphorylated
PI	Propidium iodide
PI3K	Phosphatidylinositol 3-kinase
Pin1	Peptidylprolyl cis/trans isomerase, NIMA-interacting 1
POSH	Plenty of SH3s
PR <sup>-</sup>	Progesterone receptor-negative
PRDs-	Proline-recognition domains
PS	Penicillin–streptomycin
PTEN	Phosphatase and tensin homologue deleted on chromosome ten
PTK1	Protein-tyrosine kinase 1
Raf-1	v-raf-1 murine leukemia viral oncogene homolog 1
Rho	Ras homologue gene
RNA	Ribonucleic acid
RNAi	RNA interference
ROCK	Rho-associated coiled-coil forming kinase
ROS	Reactive oxygen species
RT-PCR	Reverse-transcriptase PCR
SCG	Superior cervical ganglion
SH3	Src homology 3
siRNA	Small interfering RNA
Slpr	Slipper
SPRK	SH3-containing proline-rich protein kinase
Taq	<i>Thermus aquaticus</i>
TBE	Tris-borate-EDTA

TGF- $\beta$	Transforming growth factor-beta
T <sub>m</sub>	Melting temperature
TNF- $\alpha$	Tumour necrosis factor-alpha
UV	Ultraviolet
WNT	Wingless and INT1
WT	Wild-type
ZAK	Zipper-sterile- $\alpha$ -motif kinase

## Resumo

A proteína *mixed-lineage kinase 3* (MLK3) é uma cinase de serina/treonina vastamente expressa que está envolvida em diferentes funções fisiológicas como proliferação, apoptose, sobrevivência e migração celular. Ao responder a mitogénios e estímulos de stress regula a sinalização das MAPK através da activação das vias da ERK, JNK e p38. O seu domínio cinase é crucial para fosforilar e conseqüentemente activar moléculas alvo. Contudo, a activação da MLK3 nem sempre é requerida para a modulação de algumas funções por ela induzidas. A MLK3 pode ainda funcionar como proteína *scaffold*, ligando diferentes vias de sinalização.

Mutações na *MLK3* foram descritas, pela primeira vez, em 2010 pelo nosso grupo. Nesse mesmo trabalho, foi demonstrado que mutações missense na *MLK3* possuíam potencial transformante e tumorigénico. Duas dessas mutações (P252H e R799C) mostraram um comportamento invasivo. Tendo em conta estas informações nós estabelecemos linhas celulares (HEK293) que expressam de uma forma estável estas mutações para assim identificar os efeitos celulares a elas associados e avaliar quais os alvos moleculares dependentes desses dois mutantes da MLK3. Verificámos que a mutação no domínio cinase da MLK3 (P252H) confere propriedades diferentes quando comparada com a mutação localizada no domínio rico em prolina. A mutação P252H parece induzir uma maior migração celular, enquanto a mutação R799C parece interferir com a diferenciação celular. Além disso, nós verificámos que ambas as mutações regulam a via do WNT de maneira distinta, seja através da activação da via canónica ou da não canónica. Em resumo, o trabalho descrito nesta tese mostra que duas das mutações na MLK3, previamente descritas, interferem com vias de sinalização cruciais do desenvolvimento colorectal e neste sentido contribuem para a tumorigénese colorectal.

**Palavras-chave:** MLK3, mutações; HEK293

## Abstract

Mixed-lineage kinase 3 (MLK3) is a serine/threonine kinase widely expressed and involved in different physiological functions, such as proliferation, apoptosis, cell survival and cell migration. Responding to mitogens and stress stimuli it regulates MAPK signalling through activation of ERK, JNK, p38 pathways. Its kinase domain is crucial to phosphorylate and thus activate downstream targets. However, MLK3 activation is not always required to MLK3-induced modulation of some cellular functions. MLK3 may indeed function as a scaffold protein, linking different signalling pathways.

*MLK3* mutations were reported, for the first time, in 2010 by our group. Missense *MLK3* mutations were found to be able to harbour transforming and tumourigenic potential. Two of the mutations (P252H and R799C) were found to show an invasive behaviour. Taking this data into account we generated HEK293 stable cell lines harbouring these mutations in order to identify associated cellular effects and evaluate which molecular targets were dependent of these two MLK3 mutants. We found that a mutation in MLK3 kinase domain (P252H) confers different properties when compared to a one localized in the proline-rich domain. P252H mutation seems to induce increased cell migration, while R799C seems to interfere with cell differentiation. Furthermore, we verified that both mutations regulate the WNT pathway in distinct manner, either through the activation of the canonical or non-canonical pathway. In summary, we showed that two of the *MLK3* mutations previously described interfere with crucial pathways of colorectal development and in this way contribute to colorectal tumourigenesis.

Chapter 1

Introduction

## 1.1 Mixed-lineage kinase 3 (MLK3)

MLK3, also designated MEKK11, SPRK or PTK1, is a mitogen activated protein kinase kinase kinase (MAP3K) involved in the cellular response to mitogen and stress stimuli, through activation of extracellular signal-regulated kinase (ERK), p38 and c-Jun N-terminal kinase (JNK). *MLK3* gene is mapped at 11q13.1-q13.3 and encodes a cytoplasmatic protein of 847 aminoacids, with 95KDa [1, 2]. Although this protein presents a markedly perinuclear along with punctate, vesicular patterns and limited diffuse cytosolic pattern its cellular localization also changes during cell cycle phases as will be further described [3, 4].

MLK3 belongs to the MLK family, which has an important role in response to environmental stress, inflammatory cytokines and growth factor and whose members are activated by upstream G-proteins including Cdc42 and Rac1 [5]. MLKs were first characterized as dual specificity kinases, i.e. kinases with both serine/threonine and tyrosine kinase activity [6]. However, tyrosine kinase activity has never been reported [7]. In mammals MLKs cluster is composed of seven proteins divided into three subgroups, according to their structure similarities: MLKs (MLK1 - 4), the dual-leucine-zipper-bearing kinases (DLKs – DLK and LZK) and the zipper-sterile- $\alpha$ -motif kinase (ZAK) [8]. Some of these proteins are tissue-specific, while MLK3 is ubiquitously expressed, either in fetal or adult tissue [1, 9].

### 1.1.1 MLK3 structure organization

MLK3 shares most of its structure features with MLKs proteins subgroup (MLK1-4) [9]. MLK3 structure (Figure 1) is composed of a NH<sub>2</sub>-terminal glycine-rich region, an amino-terminal Src homology 3 (SH3) domain, a kinase catalytic domain, two leucine zippers domain, a Cdc42/Rac interactive binding (CRIB) motif and a COOH-terminal proline/serine/threonine-rich region [6, 9, 10]. These domains will be described with more detail.



**Figure 1- Schematic representation of MLK3 protein structure.** In this figure are represented the domains above mentioned and the position number of the initial and final aminoacid for each domain [11].

Glycine-rich region. Glycine-rich proteins (GRPs) are characterized by the presence of Glycine-rich domains that are arranged in (Gly) $n$ -X repetitions. This type of domain was first discovered and well characterized in proteins from plants, but nowadays proteins with this kind of repetition are reported in a wide variety of organisms, from cyanobacterias to animals (reviewed in [12]). Thus, depending on the context GRPs exert different physiological roles, such as signal transduction, stress response, transcriptional regulation and development [13]. Contrarily to other members of MLK subfamily, MLK3 harbours a glycine-rich region, whose longest stretch has 9 continuous glycine residues [1, 9]. However, the biological relevance of this region in MLK3 remains unknown.

SH3 domain. SH3 domain makes part of the superfamily of proline-recognition domains (PRDs) and is one of the most abundant PRDs in vertebrates. SH3 domain is not quite selective, as it binds to various peptides and protein ligands (reviewed in [14]). In MLK3 this domain contains three extremely conserved aromatic residues (Tyr<sup>52</sup>, Trp<sup>83</sup> and Tyr<sup>99</sup>). Specific intramolecular interactions may occur between a domain and its binding sequence when they coexist in a single polypeptide chain and this is what happens in MLK3 [10]. The SH3 domain of MLK3 promotes an autoinhibitory interaction that will be described in chapter *Regulation through intramolecular interactions*. As SH3 domains commonly bind to proline-rich regions, it is possible that in MLK3 it also binds to the large COOH-terminal proline-rich tail of this protein

Kinase domain. Protein kinases harbour an ATP-binding region within its kinase domain, also known by catalytic domain [15]. In MLK3 ATP-binding site comprises a region from aminoacid 123 to 131. The kinase domain usually folds into a two-lobed structure, composed of different subdomains. Between the two lobes there is a highly conserved loop and ATP sits beneath it. This loop, also designated as the “activation loop”, has typically 20–30 residues in length and is crucial to substrate recognition and kinase activation [15]. Many kinases are phosphorylated (either by itself



(autophosphorylation) or by other kinases) in this centrally located loop, localized between the conserved motifs DFG (Asp184PheGly – located at the base of the loop) of subdomain VII and APE (Ala206, Pro207 and Glu208) of subdomain VIII [16]. In MLK3, the activation loop was also proved to be crucial for MLK3 autophosphorylation and its subsequent activation [17].

The construct of a kinase-deficient mutant of MLK3, through replacement of lysine 144 (which is a highly conserved residue among catalytic domains of most protein kinases and is known to be critical for binding of ATP) for an arginine residue is commonly used to study the role of MLK3 kinase domain [5, 18]. One of these studies describes a drastic reduction on JNK activation when cells expressing this mutant are stimulated by the GTPases Cdc42 and Rac1 [5].

Leucine zippers. The leucine-rich domains mediate protein dimerization or oligomerization. In MLK subfamily, MLK1-MLK4 share about 70% sequence identity [9]. The predicted helix-turn-helix conformation for double zipper region allow for an interaction between the two zippers of one MLK3 molecule to form a uniquely folded zipper-turn-zipper domain [6].

CRIB motif. The CRIB motif was first termed like that because it confers binding to the Cdc42 and/or Rac GTPases [19]. It contains eight core amino acids with the sequence I-S-X-P-(X)<sub>2-4</sub>-F-X-H-X-X-H-V-G and is not exclusive of kinases. Like other kinases, MLK3 significantly binds to Cdc42-GTP, but not to Cdc42-GDP. It also binds to Rac, but to a less extent than to Cdc42, either to its wild type or constitutively active form [19].

Proline/Serine/Threonine-rich region. This is the less conserved region between MLK family members and thus it might be associated to different regulatory functions (reviewed in [9]). In COOH-terminal of MLK3, proline residues contribute 24% of the total number of amino acids in that region. They present a uniform distribution along the COOH-terminal region with stretches no longer than three residues [1]. Proline-rich region present in MLK3 could bind to the SH3 domain either in MLK3 itself or in other proteins [1]. Although some phosphorylation sites were already identified in MLK3 proline/serine/threonine-rich region [20] (Figure 4), specific regulatory functions conferred by this domain to each of MLK kinases remain unknown.

## 1.1.2 Regulation of MLK3 activity

Protein kinases are involved in many critical physiological roles and thus the regulation of its protein activity is fundamental. The mechanisms for protein kinases regulation falls into two categories: regulation by pseudosubstrate autoinhibitory domains, and remodelling of the catalytic core in response to phosphorylation and/or protein/protein interactions [21].

### 1.1.2.1 Regulation through intramolecular interactions

**SH3-mediated autoinhibition.** Through a series of mapping experiments it was identified a region in MLK3 with which the SH3 domain of MLK3 itself interacts: a sequence located between zipper and CRIB motifs, that contains a single proline residue at position 469 (which is conserved in MLK1, 2, 3 and in slpr) (Figure 2) [9, 10]. Replacement of this proline by an alanine increases the catalytic activity of MLK3, which is in agreement with the autoinhibition of MLK3 by an SH3-mediated intramolecular interaction.

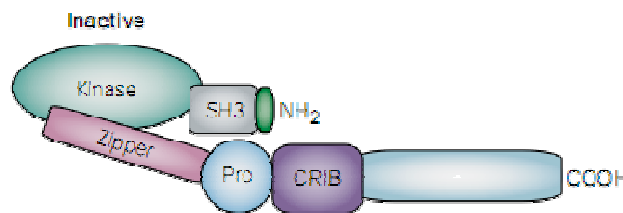


**Figure 2 - Representation of the SH3-mediated intramolecular interaction that leads to MLK3 autoinhibition [9].**

**Leucine zipper homodimerization.** Dimerization of MLK3 via the leucine-zippers domain and subsequent autophosphorylation was shown to be critical for proper interaction with and phosphorylation of downstream targets [22, 23].

### 1.1.2.2 Regulation through phosphorylation

MLK3 may be phosphorylated by itself or other kinases. Two residues seem to be critical for MLK3 autophosphorylation, thus to its efficient activity: Thr<sup>277</sup> (which is conserved in MLK1 and MLK2) and Ser<sup>281</sup>, that is conserved among all MLK family members [17]. The commercial available antibodies for phospho-MLK3 were designed

to only recognize these to residues. When any of these residues are mutated to alanine, MLK3 autophosphorylation levels alter, namely in mutant Thr<sup>277</sup> that displays a significantly reduced MLK3 autophosphorylation activity [17]. However, when Thr<sup>277</sup> and Ser<sup>281</sup> are mutated to negatively charged glutamic acid, mimicking phosphorylated serine/threonine residues, they retain MLK3 kinase activity, indicating that they serve as MLK3 (auto)phosphorylation sites [17]. Taken together these data and the previous one about MLK3 dimerization, we can predict that activation of MLK3 requires at an initial step an induced-homodimerization, which then leads to protein autophosphorylation and subsequent activation [17].

Additional *in vivo* MLK3 phosphorylation sites were identified through mass spectrometry techniques: Arg<sup>37</sup>, Ser<sup>524</sup>, Ser<sup>555</sup>, Ser<sup>556</sup>, Ser<sup>654</sup>, Ser<sup>705</sup>, Ser<sup>724</sup>, Ser<sup>727</sup>, Ser<sup>740</sup>, Ser<sup>758</sup>, Ser<sup>770</sup> and Ser<sup>793</sup> (Figure 4) [20]. Due to technical limitations this study could not possible identify very stable MLK3 phosphorylation sites. Of the twelve sites identified, eight are localized in the COOH-terminal region of MLK3 and three are in the region immediately following the CRIB domain (including the two Cdc42-inducible sites Ser<sup>555</sup> and Ser<sup>556</sup>) [20]. As most of MLK3 phosphorylation sites are followed by a proline residue and proline-directed protein kinases (PDPKs) phosphorylate Ser/Thr residues that are immediately followed by a proline residue, it is suggested that MLK3 could be a target of this type of kinases, which include for instance the glycogen synthase kinase-3 (GSK-3) that is a protein involved in different pathways, namely in wingless and INT1 (WNT) signalling and phosphatidylinositol 3-kinase (PI3K) pathway [20, 24]. Curiously, the beta isoform of GSK-3 was found to phosphorylate MLK3 in residues Ser<sup>789</sup> and Ser<sup>793</sup> [25].

**Binding to RhoGTPases.** In MLK3 the binding of Cdc42 or Rac, both in their GTP form, to CRIB motif competes with SH3-mediated autoinhibition, inducing a conformational change and thereby allowing the activation of MLK3 kinase activity (Figure 3) [3, 9].

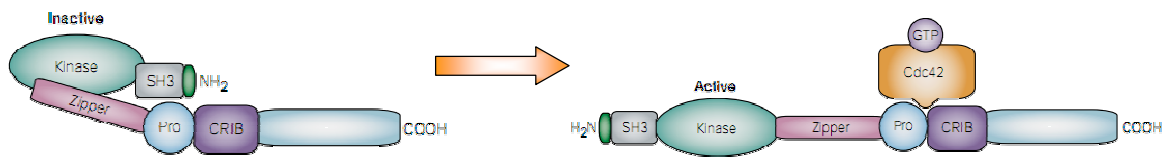


**Figure 3 - Inactivation of SH3-induced autoinhibition in MLK3, through binding of Cdc42-GTP to CRIB motif [9].**

Cdc42-GTP binding disrupts MLK3 autoinhibition, and then induces MLK3 dimerization and subsequent phosphorylation within the activation loop. However, this binding does not lead to the immediately fully activation of MLK3 [3]. Besides an intact CRIB motif to a correct Cdc42-GTP association with MLK3, which leads to its partial activation, the Cdc42 geranylgeranylation (which is a subtype of lipid posttranslational modification essential for proteins localization to cell membrane and hence for their biological function [26]) is also required to Cdc42 and MLK3 co-localization at plasma membrane and consequently for fully MLK3 activation and signalling to JNK [3].

**Binding to other upstream molecules.** MLK3 interacts with germinal center kinase (GCK) and hematopoietic kinase (HPK) which are two yeast Ste20 homologues that directly phosphorylate MLK3 and promote its activation [27, 28] Ser<sup>281</sup> residue, located in MLK3 activation loop, was identified as the HPK1-phosphorylation site [17].

Two important triggers of cell death were also reported to act upstream MLK3: tumour necrosis factor-alpha (TNF- $\alpha$ ) and ceramide, which is a lipid molecule that makes up sphingomyelin, one of the major lipids in the lipid bilayer. TNF- $\alpha$  and ceramide-induced MLK3 activation leads to JNK pathway activation, without affecting ERK and p38 pathways [29]. In MLK3-deficient fibroblasts it was observed a suppression of TNF-stimulated JNK activation and so MLK3 requirement to JNK activation appears to be selective to TNF [30].

Besides the mentioned MLK3 upstream activators there are two more that regulate in opposite ways its activity: Akt and GSK-3 $\beta$  [25, 31]. Akt is able to suppress MLK3 activity by phosphorylating it in Ser<sup>674</sup>, what leads to inhibition of MKK7 and JNK activities and consequently promotes cell survival [31]. GSK-3 $\beta$  phosphorylates MLK3 in its C-terminal, more precisely in Ser<sup>789</sup> and Ser<sup>793</sup> residues, leading to MLK3 activation [25].

Taking into account all data about the yet identified residues that might be phosphorylated in MLK3, a more detailed schematic representation of its structure is represented (Figure 4).

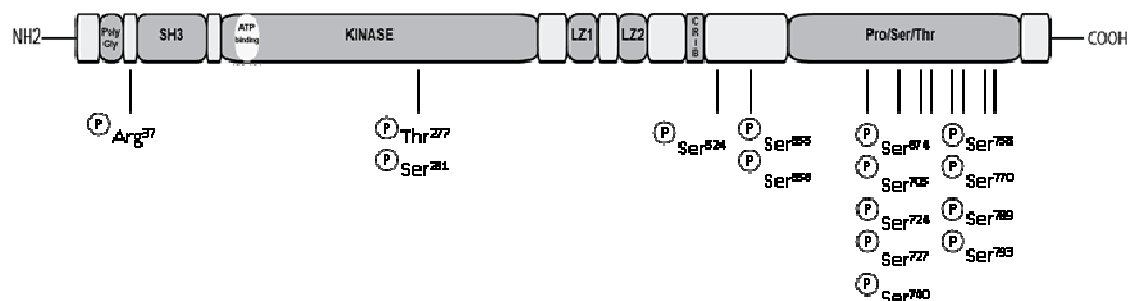


**Figure 4 - Localization of the already discovered MLK3 (auto)phosphorylation sites in MLK3 schematic structure.** Ser<sup>281</sup> is phosphorylated by HPK1, Ser<sup>555</sup> and Ser<sup>556</sup> by Cdc42, Ser<sup>674</sup> by Akt, Ser<sup>789</sup> and Ser<sup>793</sup> by GSK3 $\beta$ . [17, 20, 25, 28].

**Binding to JNK.** Although JNK is a downstream target of MLK3, it may also controls MLK3 levels, by phosphorylating and activating it, through a positive-feedback loop [32]. Thus, when JNK activity is diminished there is a decrease in hyperphosphorylated, active MLK3 and the opposite also happens. JNK inhibition leads to a change in MLK3 cellular distribution, i.e. MLK3 shifts from a Triton-soluble form to a Triton-insoluble fraction, which largely lacks the association with heat shock protein Hsp90 and co-chaperone p50<sup>cdc37</sup> and thus inactivates MLK3, but this effect can be reversed [9, 33]. Many kinases that interact with Hsp90/p50<sup>cdc37</sup> are stabilized by this association [33]. A final model suggests that MLK3 is first phosphorylated by JNK at the COOH-terminal and then a phosphatase may target the same sites. So, MLK3 cellular levels are, at least in part, regulated by the balance between these two activities [34].

### 1.1.3 MLK3 role in different physiological functions

MLK3 directly interacts with many different molecules (Figure 5). Some are upstream activators that were already mentioned. Like others MLK family members, MLK3 also respond to some stimuli that causes cellular stress, activating JNK and p38 pathways by directly phosphorylating and activating MKK4/MKK7 (JNK kinases) and MKK3/MKK6 (p38 MAP kinases), respectively [7, 9, 35, 36]. Some authors found that *MLK3* silencing, using MLK3 RNAi, suppressed mitogen and cytokine activation of JNK, ERK and p38 [37]. Thus, depending on the cellular context, MLK3 has been

implicated in different cellular responses such as apoptosis, proliferation, migration and survival. As will be described along this chapter, MLK3 kinase activity is essential to activation of downstream targets, but its scaffold property is also important.

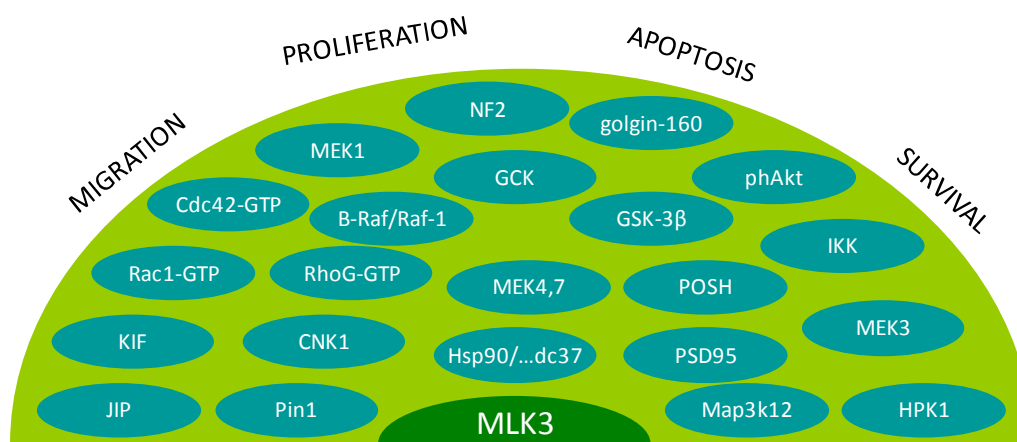


**Figure 5 - Summary of proteins with which MLK3 interacts.** (udapted from UCSD- Nature Molecule Page. doi:10.1038/mp.a001551.01. and [25])

### 1.1.3.1 MLK3 role in cell proliferation

The fact that *MLK3* silencing prevented serum-stimulated cell proliferation suggests a possible role for MLK3 in ERK activation [37]. As widely known ERK proteins are essential for cell proliferation induced by mitogens [38].

MLK3 has the ability to regulate either positive or negatively the ERK pathway, depending on the stimulus and duration of the exposure. Some extracellular factors induce sustained activation of MLK3 and JNK pathway leading to attenuation of ERK pathway activation, which implicates Jun transcription, while MLK3 short phase activation may lead to the opposite effect. ERK activation occurs through MLK3-mediated phosphorylation and consequent activation of mitogen-activated protein kinase 1 (MEK1) [39].

In 2004, MLK3 was implicated in the regulation B-Raf-Raf-1 complex (Figure 6) [37, 40]. Both B-Raf and Raf-1 undergo Ras-dependent phosphorylation, but formation of a B-Raf–Raf-1 complex *in vivo* enables B-Raf to transactivate Raf-1 [41]. MLK3 is required for B-Raf phosphorylation in an indirect manner, by maintaining the integrity of the complex. The levels of the MLK3-B-Raf-Raf-1 complex are then regulated by the tumour suppressor merlin (protein encoded by neurofibromatosis 2 gene - *NF2*). It

interacts with MLK3, disrupting the complex integrity. Therefore, merlin protein is able to decrease ERK activation and negatively interferes with other MLK3 associated pathways, like JNK pathway [40].

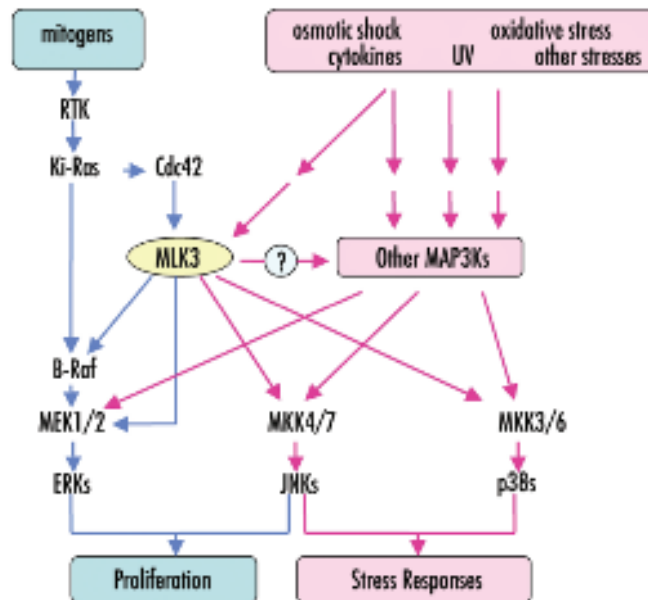


Figure 6 – MLK3 interactions in mitogen-activated protein kinases (MAPK) signalling [42].

### 1.1.3.1.1 MLK3 may contribute to microtubule instability during mitosis

Interestingly, MLK3 was found to have homology with C-terminal extension of NIMA, a serine/threonine mitotic kinase, which is present in the filamentous fungus *Aspergillus nidulans* [4]. This kinase is essential for correct G2/M transition and was found to interact with the human protein Pin 1, that is a peptidyl-prolyl cis/trans isomerase. Pin 1 ability to regulate mitosis is presumably related to this interaction [43, 44]. MLK3 was also found to interact with the peptidyl isomerase Pin1, being its Pin1-binding properties similar to those of NIMA [4].

Although MLK3 protein levels remain constant throughout the cell cycle, there is a hyperphosphorylation and an increase in kinase activity (in similar levels to NIMA), both in G2/M. MLK3 distribution changes from interphase to cytokinesis and was found to be dependent on microtubule organization. During interphase MLK3 staining appears as numerous foci proximal to the nucleus, which becomes more intense around centrosomes in prophase. In metaphase and anaphase MLK3 appears to be uniformly distributed through the cell. However, after cytokinesis the centrosome-associated

sprinkle distribution is reestablished [4]. Curiously, the subcellular localization of both NIMA and MLK3 is associated with centrosome-nucleated microtubules as well as with centrosome-itself. Overexpression of wild-type MLK3 leads to the disruption of microtubule organization in interphase and mitotic cells, what was also observed for NIMA overexpression [4].

Despite similarities between NIMA and MLK3, MLK3 does not trigger a cell cycle arrest at G2 as NIMA does [4]. Taking together NIMA and MLK3 similarities, and despite MLK3-Pin1 interaction is not well known, we can predict an important role for MLK3 in mitosis.

### ***1.1.3.2 Role of MLK3 in JNK-mediated cell death or survival***

Characterization of MLK3 physiological function has primarily evolved around its role in regulating the activity of JNK, which, in turn, mediates the apoptosis of different cell types, particularly neurons. Thus, MLK3 has been suggested as a pharmacological target for treatment of neurodegenerative disorders such as Parkinson's and Alzheimer's diseases, which are associated with dysregulation of apoptosis [45-47]. Some of these studies are reviewed below.

In rat adrenal pheochromocytoma (PC12) cells and superior cervical ganglion (SCG) neurons, nerve growth factor (NGF) deprivation leads to a rapid increase in MLK3 activity and apoptosis that can be reversed when MLK3 is blocked by overexpression of MLK3 kinase dead [46]. When cortical neuronal cultures are treated with amyloid- $\beta$  peptide (A $\beta$ ), apoptotic cell death increases and a concomitantly increase in MLK3, MKK7, and JNK3 phosphorylation is also observed [47]. K252a, a potent inhibitor of MLK3, is able to decrease A $\beta$ -induced cortical neuron apoptosis when added either before or after A $\beta$  treatment. MLK3 was also found to be involved in the neuroprotective mechanism of exogenous estrogen against transient global cerebral ischemia, through inhibition of MLK3-MKK4/7-JNK1/2 pathway by Akt1 [48].

The role of MLK3 in modulating apoptosis events is also corroborated by other evidences. For instance, MLK3 directly phosphorylates golgin-160, a Golgi-associated protein, and its overexpression enhances the susceptibility of golgin-160 to caspase dependent-cleavage [49]. The cleavage of several Golgi-proteins contributes to breakdown of the Golgi apparatus, which is an early event during apoptosis [50].



MLK3 activity is not exclusively related to its kinase activity as we already realized by its scaffold function in B-Raf-Raf-1 complex. MLK3 is also able to regulate JNK pathway, through its scaffold properties. It binds to a pro-apoptotic scaffolding protein with plenty of SH3s (POSH) that facilitates JNK signalling. The complex POSH-MLK-MKK-JNK is negatively regulated by Akt2, that phosphorylates and inhibits MLK3, leading to complex disassembly and subsequent down-regulation of JNK pathway. Thus, POSH-MLK3 interaction increases when PI3K/Akt pathway is inhibited [51].

From all these studies a model for the apoptotic and survival signalling pathways, through modulation of MLK3 activity by PI3K/Akt pathway was created (Figure 7).

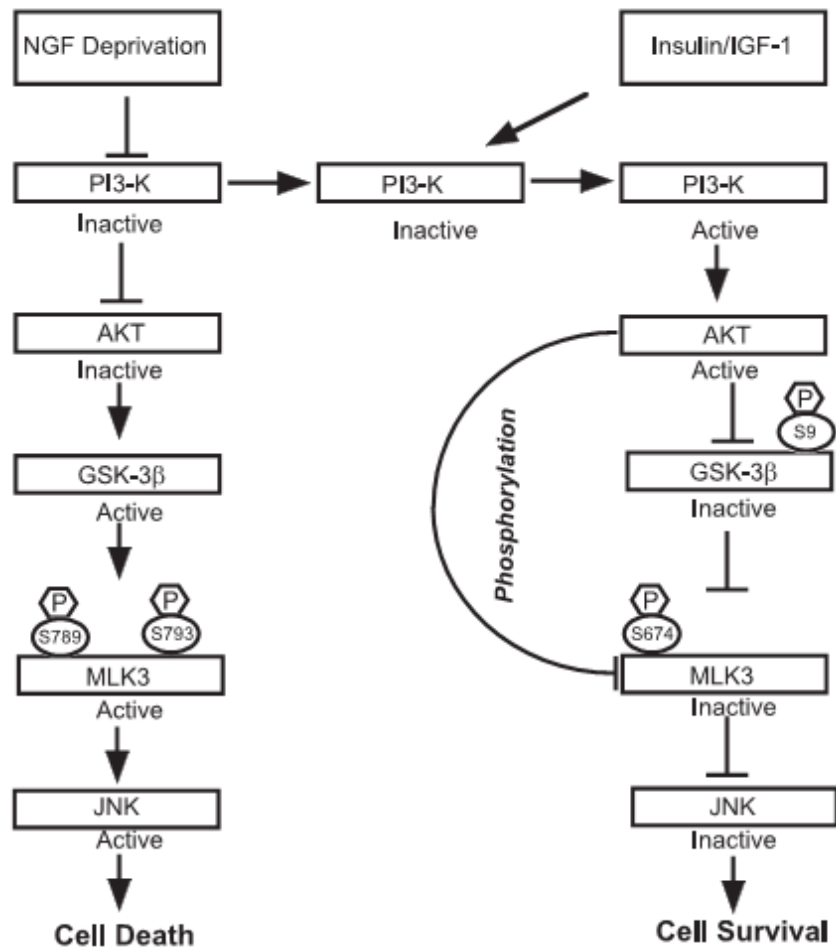


**Figure 7 - A model for the apoptotic and survival signalling pathways, mediated by MLK3 phosphorylation.** The inhibition of PI3K/Akt pathway by NGF deprivation leads to activation of GSK-3 $\beta$ , which in turn phosphorylates its downstream substrate, MLK3 on Ser<sup>789</sup> and Ser<sup>793</sup>, leading to MLK3 activation and consequently to JNK-mediated apoptosis. On the other way, survival agents such as insulin and insulin-like growth factor 1 lead to the opposite effect by activating PI3K-Akt pathway. It causes GSK-3 $\beta$  phosphorylation at Ser<sup>9</sup> and MLK3 phosphorylation at Ser<sup>674</sup>, leading to MLK3 inactivity and consequent cell survival, through JNK activity attenuation [25].

MLK3 may also mediate cell survival, through NF- $\kappa$ B pathway activation. Upon T-cell co-stimulation, MLK3 phosphorylates and thus activates both I $\kappa$ B kinase alpha (IKK $\alpha$ ) and IKK $\beta$ , which are the two catalytic subunits of the multisubunit I $\kappa$ B kinase complex (IKC) capable of phosphorylating I $\kappa$ B proteins. Therefore I $\kappa$ B proteins are degraded, allowing the migration of NF- $\kappa$ B dimmers to the nucleus and consequently activation of NF- $\kappa$ B-dependent transcription [52]. Curiously MLK3-induced NF- $\kappa$ B activation is

dependent on the type of stimulus, seeing that upon TNF- $\alpha$  or interleukin-1 (IL-1) T cells stimulation MLK3 does not play an important role in NF- $\kappa$ B activation [52]. NF- $\kappa$ B activation seems to have an important role in cells survival, for instance it is associated to the response of tumour cells to hypoxic stress [53]. Therapeutic approaches implying IKK inhibitors as an adjuvant therapy have been suggested to overcome tumours cells resistance [54]. However other paper shows that inhibition of *MLK3* expression leads to an increase of IKK activity levels, a decrease of I $\kappa$ B $\alpha$  protein levels and to *NF- $\kappa$ B* dependent gene expression in both mouse embryo fibroblast cells (NIH3T3) and ovarian carcinoma cells (SKOV39) cells. Thus, in these cells MLK3 may confer resistance to ectoposide-induced apoptotic cell death [55]. On the other way, overexpression of wild-type MLK3 or MLK3 kinase dead enhanced etoposide-induced apoptotic cell death and cleavage of PARP, an enzyme involved in DNA repair. Maybe the cell lines studied and the kind of stimulus used in each experimental work may account for the variations in the results and for the role of MLK3 in NF- $\kappa$ B pathway activation.

### **1.1.3.3 Role of MLK3 in intracellular trafficking and cell migration**

#### **1.1.3.3.1 MLK3 scaffold properties in intracellular trafficking**

Again MLK3 kinase-independent activity may confer MLK3 involvement in different physiological functions. JNK-interacting proteins (JIP) proteins are other important scaffold proteins for JNK and p38 pathways. MLK3 interacts only with three members of this family: JIP1-3, which are widely expressed in nervous system [56-59]. JIP1 and JIP3 act exclusively to facilitate JNK pathway signalling, while JIP2 is both a p38 and JNK scaffold protein. Curiously, JIP1 and JIP2 interact, trough its COOH terminal with the proline-rich region of MLK3, while JIP3 binds selectively to MLK3, through its NH2 terminal, and not to any other member of MAP3K [57-59].

Also interesting is that JIP1 and JIP2 exist in peripheral cytoplasmic projections, indicating a possible association with cytoskeletal proteins [59]. Accordingly, JIPs were found to interact directly with kinesins, which are motor proteins that transport cargos along microtubules in a specific direction - anterograde transport and in an ATP-dependent manner [60]. This model for the transport of cargo by kinesin I involving JIP and MLK3 was already described for the transport of Reelin (extracellular matrix protein involved in neuronal migration during brain development) receptor [60]. MLK3

also interacts with kinesin superfamily proteins (KIF): KIF3A, KI3B, KIF17 and KIFAP3 [61]. KIF17 was indeed described to efficiently transport NMDA receptor 2B subunits along microtubules [62]. All these MLK3 interactions prove the interesting role of MLK3 in cellular trafficking.

#### **1.1.3.3.2 MLK3 regulates Rho activation**

JNK-deficient mouse and *Drosophila melanogaster* show defects in dorsal epidermis due to neural tube closure defects and to dorsal closure defects, respectively [63, 64]. Thus, JNK signalling, which is very conserved among vertebrates and *Drosophila*, has a critical role in epithelial cell migration that promotes dorsal closure [65]. Curiously MLK3-deficient mouse shows no developmental abnormalities, despite the reduction of the thickness of the dorsal epidermal tissue [30]. A homolog of mammalian MLK gene called slipper (slpr) was shown to be involved in dorsal closure in *Drosophila* [64]. Together these data suggest an interesting role for MLK3 in the migratory events induced by JNK signalling.

Indeed MLK3 is required for cell migration but again in a kinase activity-independent manner. In MLK3-depleted cells the chemotactic index was very low compared with the control ones, but this level could be, at least, partially rescued by ectopic expression of nondepletable MLK3 [66]. The defects in cell migration were also translated into an increase in the thickness and number of stress fibers, as well as enlarged focal adhesions and absence of lamellipodial protrusions and were proved not to be related with inhibition of JNK, ERK or p38 phosphorylation. Interestingly, these MLK3-depleted cells presented high levels of activated Rho [66]. Increased activated Rho results in increased microtubule stability [67], a phenotype also observed following MLK3 depletion [4].

The mechanism of MLK3-mediated Rho inhibition is downstream of active Gαq. The authors found that MLK3 interacts with the p63 Rho guanosine nucleotide exchange factor, p63RhoGEF, through its kinase domain and that this interaction is positively modulated after acute activation of a Gαq-coupled G protein-coupled receptor (GPCR). When MLK3 binds p63RhoGEF, it compromises the interaction of Gαq with p63RhoGEF, which is required for p63Rho-GEF activation and consequently for full activation of Rho downstream of Gαq (Figure 8). MLK3 phosphorylation on Thr<sup>277</sup>/ Ser<sup>281</sup> (residues localized within MLK3 kinase domain) and also Rac binding promote MLK3 interaction with p63RhoGEF, while MLK3 phosphorylation by JNK decreases binding to

p63RhoGEF [66]. Thus, MLK3 seems to have a crucial role in regulation of Rho-mediated migratory events.

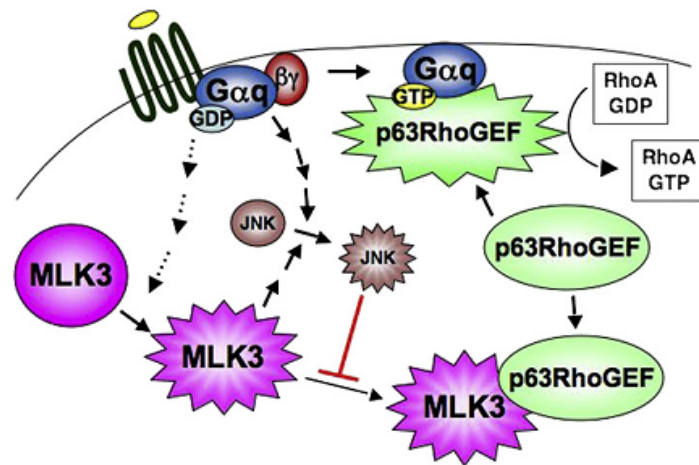


Figure 8 - Inhibition of Gαq-mediated Rho activation, by MLK3 binding to p63RhoGEF [66].

#### 1.1.4 MLK3 related cancer

In this chapter we will describe some of the few evidences in the literature that point MLK3 as being involved in tumour development and progression or as an interesting target for cancer therapy. Most of the data is still very inconsistent and controversial. The first evidence that MLK3 induces transformation was presented by Hartkamp and colleagues. In this report, overexpression of MLK3 results in the transformation of NIH3T3 fibroblasts and anchorage-independent growth, an ability that transformed cells acquired *in vitro* and is correlated with the potential of tumour cells to survive far away from each other without depending on interactions with extracellular matrix (a phenotype that is crucial to induce metastasis) [36]. However, in another study with NIH3T3 cells that co-expressed wild-type MLK3 and a Rac mutant, the MLK3 kinase activity was reported to inhibit Rac1 transforming activity and wild-type MLK3 alone had not the ability to transform these cells [68]. The inconsistency between results can be due to the different MLK3 constructs used or to the different susceptibilities of NIH3T3 strains to transformation [68].

#### **1.1.4.1 *MLK3 in tumour cell proliferation.***

It was demonstrated that MLK3 is not only required for normal cell proliferation but also for tumour cell proliferation. *MLK3* silencing, through RNAi, was shown to prevent proliferation of tumour cells harbouring either oncogenic K-Ras or loss-of-function *NF1* or *NF2* mutations [37]. *NF2* gene encodes merlin, a protein that binds MLK3 and consequently disrupts the interaction between the members of B-Raf-Raf-1-MLK3 complex. On the other hand, *MLK3* silencing in tumours cells bearing either *B-Raf* or *Raf-1* mutations did not affect proliferation [37], demonstrating that MLK3 is an upstream molecule of B-Raf and Raf-1

Curiously the MLKs inhibitor CEP-11004, which was proved to target MLK3 more specifically than other isoforms of MLK family, was able to inhibit mitotic transitions and cell proliferation in transformed cells, such as human epithelial cervical cancer HeLa cells, human lung adenocarcinoma epithelial cells (A549), ER negative SUM159 breast cancer cells or human embryonic kidney 293 (HEK293) cells but not in non-transformed NIH 3T3 or normal diploid human MRC-5 lung fibroblasts [69]. The effect of this inhibitor on mitotic arrest in pro-metaphase could be explained by the observed defects in microtubule organization and aberrant spindle formation induced by the inhibitor. At least in HeLa cells the arrest in pro-metaphase was partially reversed by overexpressing MLK3. Knowing that MLK3 is related to NIMA, which phosphorylates histone H3 Ser<sup>10</sup> *in vitro*, it is interesting to observe a delay of histone H3 phosphorylation in early mitosis, upon treatment with CEP-11004 [4, 69, 70]. Because MLK3 is thought to be a more specific target of CEP-11004 than others MLKs, it was suggested a direct or indirect involvement of MLK3 in the reported events.

Maybe pharmacological inhibition of MLKs, namely MLK3, could be a good therapeutic approach to prevent cancer cell proliferation in at least cases without alterations of B-Raf or Raf-1.

#### **1.1.4.2 *MLK3 overexpression in tumours***

Our group has recently investigated the levels of *MLK3* expression in human breast and gastric cancer cell lines, by real-time polymerase chain reaction (Real-time PCR) and found that a large number of breast and gastric cancer cell lines show a higher level of *MLK3* expression when compared to the normal breast and normal stomach, respectively (data not published and related results will be discussed later in this

thesis). But this increased level of MLK3 in tumours was also described in other models like in pancreas.

**Pancreatic cancer cells.** MLK3 protein levels were found to be three-fold higher in pancreatic cancer cell lines, when compared to an immortalized pancreatic epithelial cell line. The inhibition of MLK3 expression in pancreatic cancer cell lines either through siRNA or by using K252a lead, in both cases, to a reduction of cell proliferation and a decreased activation of ERK, JNK and Akt. Taking into account that most of pancreatic cancers harbour oncogenic *K-Ras* [71] mutations and knowing that in those cases MLK3 inhibition prevents cell proliferation [37] it makes sense that inhibition of MLK3 alone blocks pancreatic cell proliferation. However, pancreatic cancer cell lines also overexpress epidermal growth factor (EGF) receptors (EGFR), so coupling EGFR inhibition to MLK3 inhibition may cause a dramatic decrease in phosphorylation of Akt, an increased cleavage of PARP and an increase in cleaved caspase-3 activity that is not verified in MLK3 inhibition alone. In fact, the inhibition of both MLK3 and EGFR lead to apoptosis of pancreatic cancer cells [72]. New clinical trials are evaluating the presumable more effective action of combined therapies against advanced pancreatic cancer [73]. Maybe the use of both EGFR and MLK3 inhibitors would lead to pancreatic cancer cells death and could herein be a good combined therapeutic approach.

**Head and neck squamous cancer (HNSCC) cells.** Curiously MLK3 is also overexpressed in malignant HNSCC cell lines, compared to normal tonsil lysate [74]. MLK3 was inhibited, as described for pancreatic cancer cells, and the results were very similar. It was observed a downregulation of phospho-Akt and phospho-ERK and a decrease in cell proliferation. As HNSCC cells also overexpress EGFR, the same therapeutic approach as used above was performed: MLK3 inhibition coupled to EGFR inhibition. This combination induced less phospho-Akt expression and increased apoptosis (caspase 3 or PARP cleavage) compared with EGFR inhibition alone. From these results we may say that MLK3 has probably a role in avoiding apoptosis in HNSCC cells.

Thus, MLK3 inhibition may enhance the effects of EGFR inhibition either in pancreatic cancer cells or in HNSCC cells.

**Breast cancer cells.** According to our group results, breast cancer cell lines present high levels of MLK3 protein, comparing to non-tumorigenic ones, what was also verified by Chen and colleagues [75]. MLK3-induced expression leads to an increase of

migration either of the poorly invasive MCF7 breast cancer cells or of MCF10A mammary non-tumourigenic epithelial cells. This effect was accompanied by JNK and p38 activation, but not ERK one, despite basal ERK activation being necessary to migration [75]. Curiously, *MLK3* gene was also identified as a modulator of migration, among over 60 genes, in a wound healing screen, using a siRNA approach, with MCF10A cells [76]. MCF10A cells overexpressing wild-type MLK3 were three-fold more invasive than those expressing the control vector. Activation of JNK pathway, through c-Jun phosphorylation and activation of AP-1 transcription factor seems to be crucial to the acquisition of this aggressive and consequently malignant phenotype. Thus MLK3-JNK-AP-1 signalling seems to develop a crucial role in carcinogenesis of breast cells [75].

**In gastric cancer cells this effect of MLK3 in cell migration was determined.** Over the past two decades it has been established a link between high expression levels of gastrin, which is a gastrointestinal peptide hormone produced by the gastric G cells and gastrointestinal cancer (reviewed in [77]). Amidated gastrin (G17), the fully processed amidated form of gastrin, was demonstrated to induce gastric cancer cells migration [78]. This effect was preceded by an activation of ERK, JNK and p38. Besides the well-known JNK1 role in apoptosis its activation was already shown to be crucial for both tumour initiation and promotion in gastric cancer [79]. In agreement, inhibition of JNK was shown to be more critical to G17-induced migration than the inhibition of the other MAPKs. Not only JNK1 but also MLK3, which activity is induced up to 1h after G17 addition, seem to be involved in this migratory process. JNK downstream mediators of migration are not well known, but this study point c-Jun as one of them. The activation of MLK3/JNK/c-Jun induced by G17 also leads to an increase of the metalloproteinase 7 (MMP7) promoter activity. Increased expression of MMP7 was found to stimulate gastric epithelial cell migration in a subset of gastric epithelial cells infected with the gastric oncogenic pathogen *Helicobacter pylori* [80]. MMP7 transcriptional activation was abolished after knocking down of MLK3 expression [78]. Together these data seem to pinpoint a role for MLK3 in mediating G17-induced migration in gastric cancer cells, through JNK activation.



#### **1.1.4.3 Promoting MLK3 activation in tumours**

Surprisingly, the promotion of MLK3 activity could also be an adjuvant strategy to treat tumours.

**Breast cancer cells.** MLK3 kinase activity was found to be about five-fold higher in breast tumours with both estrogen and progesterone receptor-negative (ER<sup>-</sup>, PR<sup>-</sup>), than in ER<sup>+</sup>, PR<sup>+</sup> ones. Such data suggests that estrogen might be negatively interfering with MLK3 activity [81]. Thus, 17 $\beta$ -estradiol (E2), which is the predominant estrogen form that binds strongly to ER $\alpha$ , was proved to be negatively regulating MLK3 kinase activity as well as its downstream activation of JNK, but only in ER<sup>+</sup> breast cancer cells. This inhibition is ER-dependent and occurs via PI3K/Akt pathway, being Akt the kinase responsible for MLK3 phosphorylation at Ser<sup>674</sup>. This phosphorylation reduces MLK3 proapoptotic activity, through attenuation of JNK activity. So, in ER<sup>+</sup> tumours, E2 promotes cell survival and proliferation probably by downregulating the proapoptotic activity of MLK3 [81]. Therefore antiestrogen treatment of breast cancer cells remains a mainstay of therapy for tumours expressing ER $\alpha$  [82] and agents that can activate MLK3 and at the same time block Akt phosphorylation might also have a beneficial effect.

**Prostate cancer cells.** In patients with prostate cancer in the early, androgen-responsive stages of the tumour, androgen ablation and consequent administration of gonadotropin releasing hormone analogs (GnRH-a) is the standard therapeutic approach, due to GnRH-a antiproliferative effect [83]. However, in hormone-refractory prostate cancer cell lines, GnRH-a was also able to induce apoptosis. GnRH-a-induced apoptosis leads to JNK and ERK1/2 activation and to Akt dephosphorylation. It was also confirmed a significantly reduction of MLK3 phosphorylation on the Akt phosphorylation site. The authors suggest that MLK3 may mediate this increase in JNK activity after the reduction of MLK3 phosphorylation on its inhibitory site, by Akt [84].

Genipin is a natural compound that has been implicated in apoptosis of hepatoma cells. Its action is mediated via NADPH oxidase-dependent generation of reactive oxygen species (ROS), which leads to downstream activation of JNK [85]. MLK3 was also found to be a link between ROS signalling and JNK activation in genipin-induced apoptosis in PC3 human prostate cancer cells. It appears that genipin induces ROS formation, which then induces MLK3 phosphorylation and activation and finally leads to cells apoptosis, through downstream activation of JNK. When ROS generation is

inhibited in the genipin-treated cells MLK3 phosphorylation was blocked. MLK3 activity was proved to be important for genipin-induced apoptosis as cells expressing a dominant-negative MLK3 mutant (K144R) were less susceptible to this effect. This was demonstrated by an impairment of cytochrome *c* content, no changes in mitochondrial membrane potential and less stimulation of caspase-3 activity. So, MLK3 seems to be an important mediator of genipin-induced apoptosis PC3 cells [86].

#### **1.1.4.4 *MLK3 may potentiate taxol antitumour activity***

Paclitaxel (taxol) acts as an anti-cancer drug in many tumours, such as breast tumours [87]. Its effect was first attributed to microtubules stabilization, through direct binding to them, what consequently avoids mitosis and stops cell proliferation [88]. As already mentioned MLK3 seems to cause microtubules disruption when ectopically expressed and if its depletion increases cellular sensitivity to taxol at low concentrations it suggests that MLK3 absence results in a partial stabilization of the microtubule network and as it is non toxic to cells MLK3 depletion/targeting could be an interesting adjuvant therapy to taxol treatment [4].

On the other hand, taxol also activates the JNK signalling, inducing cell death [89]. However when ER<sup>+</sup> cells were first stimulated with E2 and then with taxol, cell death was reduced [81]. This happens due to the probably MLK3 down-regulation induce by E2. In this case MLK3 depletion would not probably be a good option. In particular, in the case of estrogen-dependent breast cancer tumours agents that could active MLK3 and inhibit Akt simultaneously might have clinical relevance [81].

Together all data indicate that, depending on the cellular context, MLK3 depletion or its increased activation could increase cells sensitivity to taxol, thus becoming the treatment more effective. However, before defining the best therapeutic strategy it is crucial to determine the role of MLK3 in each specific situation, as MLK3 induces different cellular effects according to the cell line and tumour model.

#### **1.1.4.5 *MLK3 mutations in tumours***

The investigation that our group was taking on about gene expression of *MLK3* in human cancer cell lines was extended to the identification of *MLK3* mutations in colorectal cancer lines. As verified for gastric and breast cancer cell lines, also colorectal cancer cell lines present high levels of *MLK3* expression. However, some

colorectal cancer cell lines show similar levels of *MLK3* expression when compared to normal tissue. This is the case for two colorectal carcinoma cell lines (RKO and CO115). As widely known, mutations in many genes may strongly alter signalling pathways and by this way interfere with different physiological functions such as proliferation or apoptosis, two important processes in a carcinogenic process. For instance *B-Raf* mutations are known to be prevalent in many human cancers such as colorectal cancer (5%-22%) and most of these mutated genes are translated into mutant B-Raf proteins that present high levels of kinase activity, which stimulate ERK signalling in cells (reviewed in [90]). In the same way it is well possible that also *MLK3* mutations are an alternative mechanism to maintain cell survival in tumours or induce other functional effects pivotal for tumour progression, namely migration.

In fact in 2010 our group described for the first time *MLK3* gene structural mutations in cancer [11]. In the case of gastrointestinal cancer *MLK3* mutations were related to the microsatellite instability (MSI) phenotype. Mutations were also found in colorectal cancers cell lines with MSI (RKO and CO115), mimicking what was observed for primary tumours. Curiously, in half of the MSI primary gastrointestinal tumours tested, *MLK3* mutations were found together with wild-type *B-Raf* and *K-Ras* genes. In the series of cases studied, somatic missense mutations were more prevalent than frameshift ones. Most of them occurred in functional domains of the protein and affect amino acids that are evolutionary conserved (Figure 9). To better understand the potential impact of some of these mutations, 3D protein predictive studies were performed using the crystal structure of the kinase domain of MLK1 as a model. They all seem to interfere with scaffold properties of MLK3, rather than with its kinase activity. After, the transforming potential of mutations localized in different domains was tested either *in vitro* or *in vivo*. P252H and R799C mutations had the highest fold (4x) increase in focus assay, compared to Mock, despite all the mutations analysed presented significant transforming potential *in vitro*. P252H mutation is localized in MLK3 kinase domain, while R799C localizes in the P/S/T-rich domain. These two mutations were inoculated in nude mice and tumours were developed within five weeks, while Mock and wild-type MLK3 expressing cells were not able to generate tumours not even after six weeks. The tumours were analysed and a high number of mitotic figures and an infiltrative pattern of growth was observed for tumours expressing MLK3 mutant cells. The ability to invade was also proved *in vitro* in a matrigel assay. So, this paper reveals an important role for cancer-related *MLK3* mutations, but more studies are required to understand the signalling pathways associated to them.

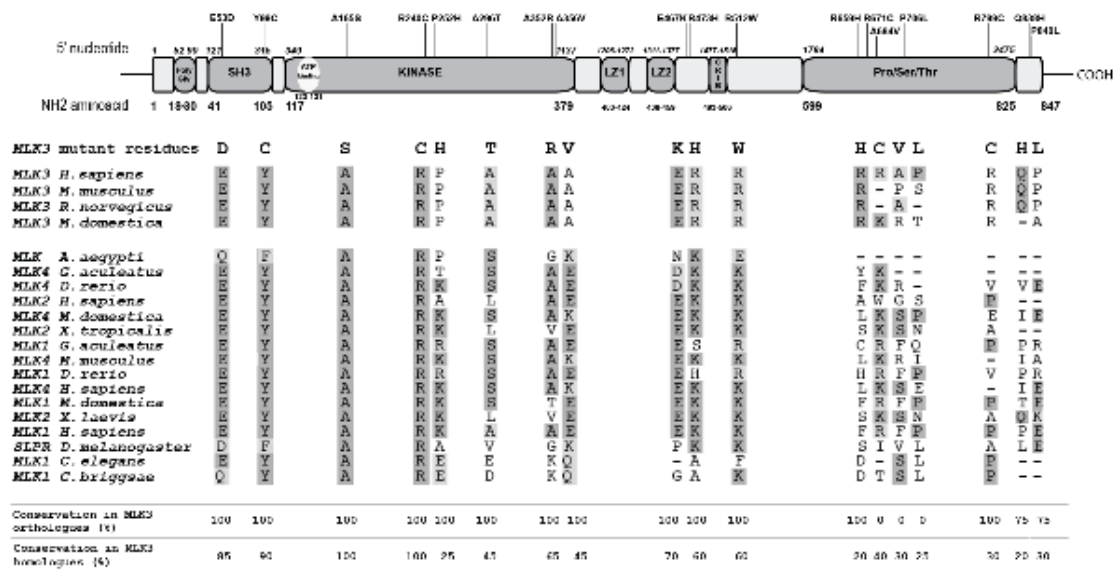


**Figure 9 - Summary of the localization of missense mutations in *MLK3* gene found in MSI primary carcinomas and cell lines and the mutated aminoacid residues they originated.** The evolutionary conservation of the correspondent wild-type amino acid residues was studied within mammalian orthologues and within eukaryotic homologues [11]

Later on to understand the role of P252H mutation, which seems to have the most aggressive phenotype either *in vitro* or *in vivo*, the same authors performed a microarray expression profiling of biological triplicates of HEK293 cells transfected with mutant, wild-type and empty vector (Mock) (data not published). The expression profiles allowed the identification of genes at least 2 log-fold differentially expressed between wild-type and Mock, as well as between P252H and Mock. It was found a significant differential expression between P252H and wild-type in 445 genes. Curiously, the colorectal pathway, which encompasses several relevant pathways such as WNT, MAPK, NOTCH, transforming growth factor-beta (TGF- $\beta$ ) and P53, was significantly over-represented, what corroborates with the discovery of P252H mutation in a colorectal tumour. Together these data suggest that mutant *MLK3* deregulates important pathways involved in colorectum differentiation.

The expression of some of those genes was confirmed by Real-time PCR. Cyclin D1 (*CCND1*), lymphoid enhancer-binding factor-1 (*LEF1*) and bone-morphogenetic protein 6 (*BMP6*) genes were confirmed to be down-regulated, while frizzled homologue 10 (*FZD10*) was confirmed to be up-regulated in P252H, always comparing with wild-type *MLK3* expressing cells. *CCND1* and *LEF1* are associated to the activation of the

canonical WNT pathway, while FZD10 is involved in the non-canonical one [91]. This was the first time that MLK3 is reported to be related to WNT pathway.

So regarding all data about MLK3 role in tumours we may suggest *MLK3* as novel oncogene, often mutated in mismatch repair deficient tumours, where it confers transforming and invasive potential by deregulating several fundamental colorectal cancer-related pathways. From now on it is important to understand, not only the signalling pathways associated to *MLK3* mutations, but also the cellular effects induced by them.

Chapter 2

Project aims

The purpose of this thesis is included in the objectives of the FCT project entitled “*MLK3*, a new mutated gene in MSI colorectal cancer”, that is being developed in our laboratory. This project is related to the tumorigenic role of MAPkinases in MSI cancer, namely the role of MLK3. As already mentioned *MLK3* mutations were described for the first time by Raquel Seruca’s group. However, we urge to understand the importance of these mutations in cancer development and progression. In order to achieve that it was important to evaluate the cellular effects and activated signalling pathways mediated by those mutations. So, this experimental work intends to be a scientific approach to better understand the role of MLK3 in cancer. For that, different aims were proposed.

1) To evaluate the cellular effects associated to P252H mutation and which signalling pathways could it be interfering with.

3) To understand if the observed effects were independent or not on the localization of the mutation in the different MLK3 domains. In order to verify the putative genotype-phenotype correlations we studied another MLK3 mutations localized in a distinct domain of the protein – R799C.

4) Finally we want to verify if wild-type MLK3 overexpression leads, in similar or distinct manner, to the effects and signalling alterations verified for the previous *MLK3* mutations.

Chapter 3

Material and Methods



The Figure 10 represents an overall view of the different assays performed, as well as cell lines used in each one, during this work to better understand and correlate all data.

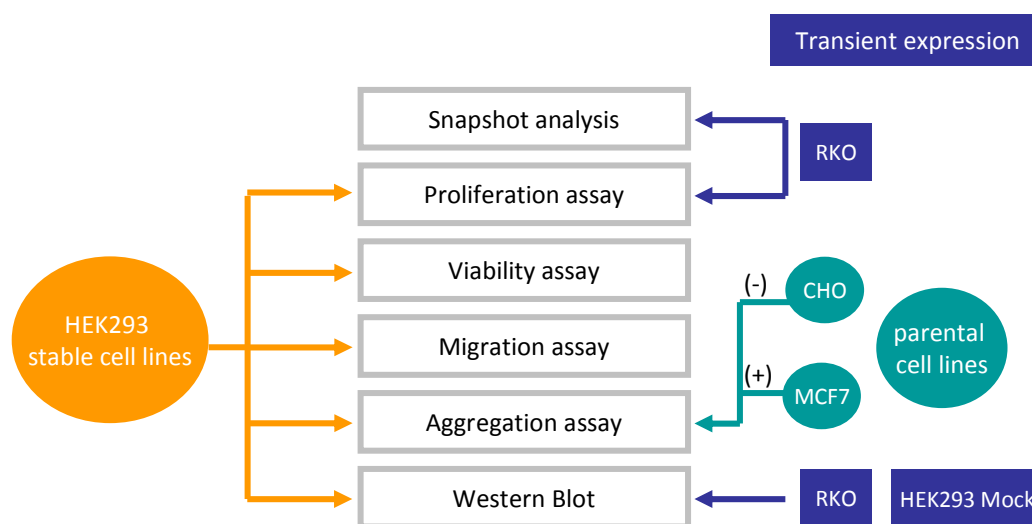


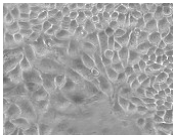
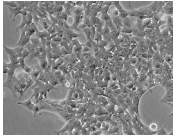
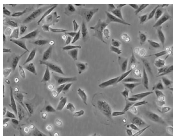
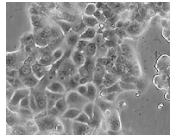
**Figure 10 - Schematic representation of this experimental work.**

## 2.1 Cell culture

In this experimental work four epithelial cell lines from human origin: RKO, HEK293, BT20 and MCF7, and one epithelial-like of hamster origin – CHO were used. All of them were cultured in Dulbecco's modified Eagle's medium - DMEM (High Glucose) (Gibco, Invitrogen) or in Minimum Essential Medium Eagle with Alpha Modification –  $\alpha$ -MEM (Gibco, Invitrogen). The supplements used depended on the specificities of each cell line: fetal bovine serum – FBS (HyClone, Perbio), penicillin–streptomycin - PS (Gibco, Invitrogen), sodium bicarbonate 7,5% (Gibco, Invitrogen), sodium pyruvate MEM 100mM (Gibco, Invitrogen) and blasticidin (Gibco, Invitrogen). These and other details are described in Table I.

**Table I - Detailed information of the cell lines used in this experimental work.**

Some data was provided by ATCC, <http://www.lgcstandards-atcc.org/>.

Designation	Source	Culture medium –	Observations
<p><b>RKO<sup>1</sup></b></p> 	colon (carcinoma)	DMEM supplemented with 10%FBS , 1% PS, 1mM sodium pyruvate, 150mg/mL sodium bicarbonate	Biosafety Level:1 Cell line with multiple genetic alterations (ex: <i>B-Raf</i> and <i>MLK3</i> mutations)
<p><b>HEK293</b></p> 	embryonic kidney	<p>• <u>parental cell line</u></p> DMEM supplemented with 10%FBS , 1% PS <p>• <u>stable cell lines</u></p> DMEM supplemented with 10%FBS , 1% PS, blasticidin (8µg/mL)	Biosafety Level:2 [cells contain adenovirus ]
<p><b>CHO</b></p> 	ovary	α-MEM (Gibco)	Biosafety Level:1
<p><b>MCF7</b></p> 	breast (adenocarcinoma from metastatic site)	DMEM supplemented with 10%FBS , 1% PS	Biosafety Level:1

Cells were grown at 37°C in a humidified atmosphere of 5% CO<sub>2</sub>. When cells needed to be divided, they were washed in physiological serum and incubated with trypsin-EDTA (Gibco, Invitrogen) to detach them and then were resuspended in medium. Before freezing cells, they were first trypsinized and centrifuged at 1200rpm for 5 minutes, then they were resuspended in FBS with 10% DMSO (Sigma) and finally the content was divided by cryovials (CRYOVIAL®) and kept at -80°C in a cryogenic freezing container (Nalgene) that contains 100% isopropanol (Merck). This box system allows a slow cooling rate of -1° per minute.

## 2.2 Establishment of HEK293 stable cell lines

The Figure 11 represents an overview of all procedures we performed to obtain HEK293 stable cell lines.

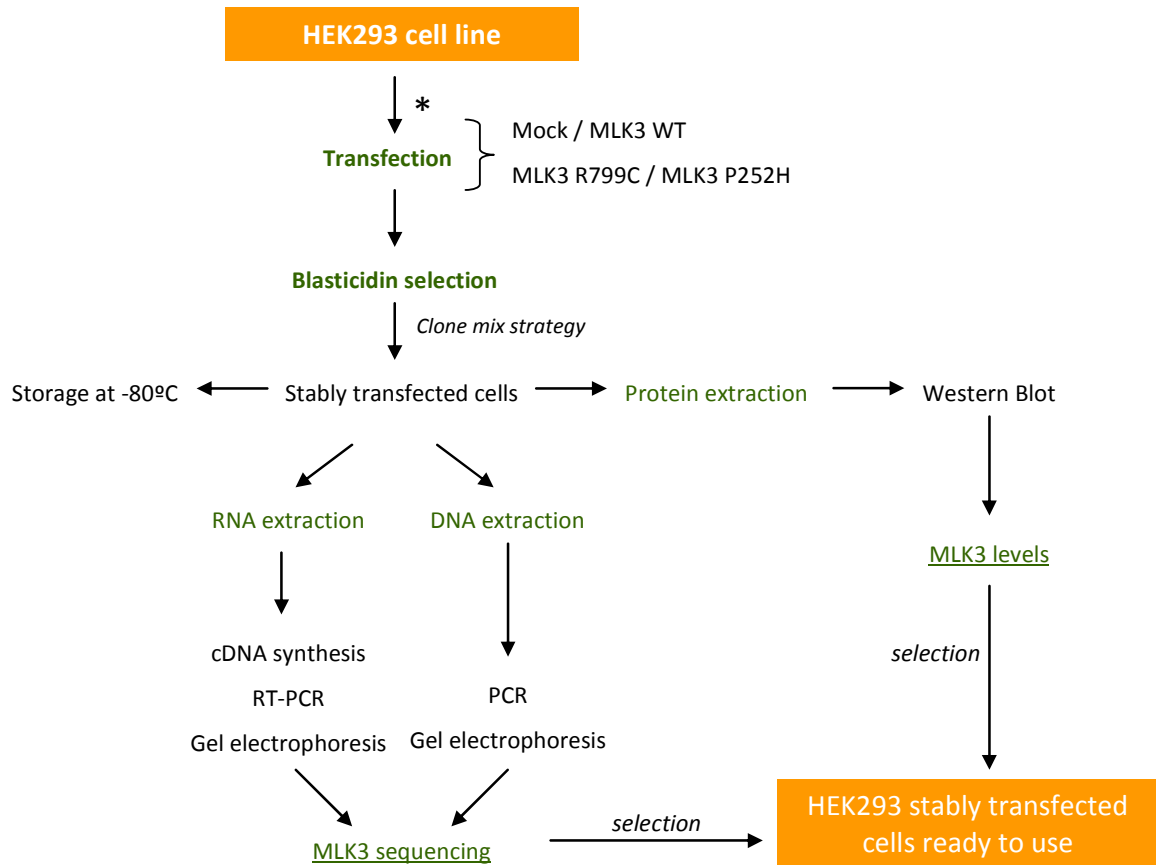


**Figure 11 - Schematic representation of the establishment of HEK293 stable cell lines.**

(Steps before HEK293 transfection, indicated in the figure as an asterisk (\*), were previously performed by our group. [11]. First, wild-type and mutants sequences were generated by site-directed mutagenesis, cloned into pLENTID6/V5 vector and the empty vector (Mock) was obtained by the insertion of a small fragment of cDNA. After, *Escherichia coli* cells were transformed with the constructs generated, colonies were then selected, plasmids were purified and the sequence cloned was confirmed by direct sequencing. If the sequence was correctly inserted, then glycerol stocks with the selected clones were prepared.) Finally, the different vectors were inserted in HEK293 cell line and transfected cells were selected with blasticidin. *MLK3* sequence and *MLK3* levels were analysed, before performing functional assays and testing expression levels of target proteins, to guarantee that everything was according to what was expected.

### 2.2.1 Maxiprep preparation

A maxiprep was prepared using Plasmid Maxi Kit (QIAGEN) to increase the amount of the empty vector. The protocol used was based on manufacturer's instructions but with some alterations. Seventy  $\mu\text{L}$  of the glycerol stock, which is composed of a culture of *Escherichia coli* that harbours the empty vector, was grown into 300mL of Lysogeny Broth/ Ampicilin medium at 37°C overnight. The material was then separated in six Falcons of 50mL and centrifuged at 4000g for 20 minutes at 4°C. The supernatant was poured off and Buffers P1, P2 and P3 were added. Other centrifugations at 14000g for 40 minutes and at 14000g for 20 minutes, both at 4°C, were performed. After equilibrating and washing the QIAGEN column, the DNA was eluted by adding 15mL of Buffer QF, precipitated with isopropanol and centrifuged at 9000g for 50 minutes at 4°C. After washing DNA pellet with etanol 70% it was centrifuged at 9000g for 30 minutes. DNA pellet was air-dried and resuspended in water. Its concentration was measured at 260nm.

### 2.2.2 Transfection

HEK293 cell line was transfected with empty vector (Mock) and wild-type MLK3 and mutant (P252H and R799C) sequences in triplicate, using Lipofectamine™ 2000 Transfection Reagent (Invitrogen) according to manufacturer's instructions. Transfected cells were selected through its resistance to 8 $\mu\text{g}/\text{mL}$  of blasticidin (Invitrogen) and a group of resistant clones was mixed together. In the end of all process three replicas per each vector sequence were obtained and termed T1, T2 and T3, except for empty vector that had only one replica. HEK293 MLK3 R799C and HEK293 wild-type MLK3 stable cell lines were previously prepared in our laboratory.

### 2.2.3 RT-PCR

**RNA extraction.** RNA extraction was performed with TriPure Isolation Reagent (Roche) according to the instruction manual. RNA was quantified with NanoDrop ND-1000 (Alfagene) and water with DEPC, in which RNA was diluted after extraction procedure, was used as a negative control.

**Priming.** First, 2 $\mu\text{g}$  of RNA, 0,1ng of Random Primers 100ng/ $\mu\text{L}$  (Invitrogen) and water with DEPC (inhibitor of ribonucleases), in a final volume of 12 $\mu\text{L}$ , were put together in a

microcentrifuge tube that was incubated at 70°C for 10 minutes. After that, samples had to be kept on ice for 2 minutes.

**cDNA production.** The following mix was prepared and added to the previous one: 1x first strand buffer (Invitrogen), 10mM DTT 0,1M (Invitrogen), 0,5mM dNTPs 10mM (Bioron), 8U of rRNasin® (Promega), 150U of SuperScript™ II Reverse Transcriptase (Invitrogen) and water with DEPC. A final volume of 20µL was incubated at 37°C during 1 hour, in the termocycler.

#### **2.2.4 PCR for MLK3 amplification**

**DNA extraction.** DNA extraction was performed with Spin Tissue Mini Kit (Invisorb) according to the instruction manual. DNA was quantified with NanoDrop ND-1000 (Alfagene) and the elution buffer D from the DNA extraction kit mentioned above was used as a negative control.

**PCR.** In a microcentrifuge tube was prepared a mix with the following components: 1x PCR Amp Buffer (Invitrogen), 0,8mM dNTP 10mM (Bioron), 0,4µM of each forward and reverse primers 10µM (Sigma) (Table II), 1U of Taq DNA Polymerase (GE Healthcare), DNA or cDNA and water, in a final volume of 25µL. The PCR-reaction occurred then in a thermocycler beginning with the denaturation of DNA or cDNA molecule at 95°C for 5 minutes, followed by 35 cycles of the combination of a denaturation step - 95°C for 30 seconds -, an annealing step - 60°C for 45 seconds - and an extension step - 72°C for 1minute -, finishing with a final elongation step at 72°C for 10 minutes and a final hold of 15°C.

**Table II - Primers used in amplification of *MLK3* gene.** Abbreviation: T<sub>m</sub>, melting temperature

Primer name	Sequence 5'-3'	T <sub>m</sub>	PCR-fragment size (KDa)
MLK3_Ex1F1	GCTTTGGCAAGGTGTACAGG	62	278
MLK3_Clon1R	ATGTGCTGGTCAACTGGGCT	67,0	
CMV Fw	CGCAAATGGGCGGTAGGCGTG		503
MLK3_Ex1R	CAGCTGCCCTGTACACCTT	64	
MLK3_Clon1F	ATGGAGCCCTTGAAGAGCCTC	75,1	657
MLK3_Clon1R	ATGTGCTGGTCAACTGGGCT	67,0	
MLK3_Clon1F CACC	CACCATGGAGCCCTTGAAGAGCCTC		661
MLK3_Clon1R	ATGTGCTGGTCAACTGGGCT	67,0	
MLK3_Clon2F	CTGTGCCTGGTGATGGAGTATG	66,6	470
MLK3_Clon2R	CTCACACTGCCCATCCCATC	67,9	
MLK3_Clon3F	GCAGTGACGTCTGGAGTTTTG	64,8	457
MLK3_Clon3R	AGTGGGAGCTAGAGGTGTTCTGA	66,2	
MLK3_Clon4F	CGAGCCAAGGAAAAGGAACTAC	64,8	450
MLK3_Clon4R	ACTCAAGCAATGGAGAGCGG	66,6	
MLK3_Clon5F	ACGTCTGGAGGACTCAAGCAA	66,1	892
MLK3_Clon5R	GGGTGCCGGAAGCGGGGCCT	80,5	
MLK3_Clon5F	ACGTCTGGAGGACTCAAGCAA	66,1	602
MLK3_2725_Rv	GACATCACGCTCTGCTCCTG	66,3	
MLK3_2725_Fw	GACATCACGCTCTGCTCCTG	66,3	
p_LENTI_V5b =	CGGGCCCTCTAGACTCGA	65,5	

## 2.2.5 Agarose gel electrophoresis

The result of the PCR reaction was visualized in a 2% agarose gel. To prepare the gel, SeaKem® LE Agarose (Lonza) was dissolved in 1x Tris-borate-EDTA (TBE) buffer and 1,5µL/50mL of the GelRed™ Nucleic Acid Gel Prestaining Kit with “50bp” Tracking Dye were added before solidification of the gel. After it, a volume of 28µL per sample (already containing bromophenol blue) and 5µL of the 1Kb Plus DNA Ladder (Invitrogen) were loaded and the gel ran at 120V. An image of the gel was captured with the Molecular Imager® Gel Doc™ XR+ system (BioRad). As the final purpose of

these agarose gels was to purify the PCR products, the bands were cut with a surgical blade (Sofdan) in the ultraviolet (UV) transilluminator and then kept in eppendorfs at 4°C until use.

## 2.2.6 Sequencing

**Agarose bands purification.** PCR product from the cut bands was purified with illustra GFX PCR DNA and Gel Band Purification Kit (GE Healthcare), according to the manufacturer's protocol.

**Sequencing reaction.** Two mixes were prepared: one with the forward primer and the other with the reverse one (the primers used were those mentioned above to amplify *MLK3* fragments). The common components of each mix were: 0,8µL of Big Dye Terminator v3.1, 1,67x of Big Dye Terminator sequencing buffer (Applied Biosystems), 1µM of forward or reverse primers 10µM (Sigma), purified cDNA or DNA and water. After preparing two mixes per each DNA or cDNA, samples were incubated in the thermocycler at 96°C for 2 minutes (denaturing step), followed by 25 cycles of three steps (96°C for 30 seconds, 54°C for 15 seconds and 60°C for 3 minutes), finishing with a step of 60°C for 10 minutes and a final hold at 10°C.

**Reaction Purification with Sephadex.** Sephadex is a gel composed of macroscopic beads that allows the purification of DNA/cDNA after labelling reactions, i.e. removal of un-incorporated dyes or dye terminators. As it is supplied as a dry powder, it must be allowed to swell in water before use (6,6g/100mL). To initiate purification first the columns were washed at least twice: a GFX Microspin Column (GE Healthcare) was placed into one Collection tube, and water was added to the top and it was centrifuged at 14000rpm for 10 minutes. After that the Sephadex G-50 Fine (GE Healthcare) was added to the Microspin columns and centrifuged at 4400rpm for 4 minutes, resulting in the formation of a porous column. Then, the collection tube was changed by an eppendorf and finally the sample was added to the center of the sephadex column and centrifuged at 4400rpm for 4min, which allowed the elution of the purified product into the collection tube. After adding 12µL of Hi-Di™ Formamide (Applied Biosystems), which denatures the DNA/cDNA template from the newly synthesized strands, increases sample preservation and dissolves local secondary structures, the samples were ready to be sequenced.

**Detection on an automated sequencer.** Samples reading was done with the Genetic Analyzer 3130 (Applied Biosystems) and data was edited with Sequencing Analysis v5.2 software (Applied Biosystems).

## 2.3 Transient transfections

Cells were transiently transfected either with a siRNA targeting a mutation in *MLK3* sequence – P252H (QIAGEN) or siRNA targeting wild-type *MLK3* (Dharmacon) (details in Table III). Cells were counted using a 0,0025 cm<sup>2</sup> Neubauer chamber (Marienfeld) and plated in a 6-well plate. The transfections were performed in the next day using Lipofectamine™ 2000 Transfection Reagent (Invitrogen) (6µL/mL and 2,5µL/mL for RKO and HEK293 cell lines, respectively), according with the instructions manual. Three controls were used: blank (cells cultured without any reagents), siRNA control (cells cultured only with a non specific siRNA – AllStars negative control (QIAGEN)) and lipofectamine control (cells cultured only with the lipofectamine reagent). Opti-MEM® I Reduced Serum Media (Gibco, Invitrogen) was used in the blank control and to dilute siRNA in the others samples. The medium was changed 4 to 6 hours after transfection and protein extraction or cellular assays were performed 48 hours after transfection.

**Table III – Details of the transfection with siRNA of RKO and HEK293 cell lines.**

Cell line	Cells per well	[siRNA] (nM)		
		siRNA non- specific	siRNA wild-type <i>MLK3</i>	siRNA <i>MLK3</i> P252H
RKO	1,7 x 10 <sup>5</sup>	250	-	250
HEK293 Mock	4 x 10 <sup>5</sup>	150nM	50,100 and 150nM	-

## 2.4 Snapshot

**PCR to amplify GAPDH and *MLK3* cDNA flanked P252H regions.** Mixes for the housekeeping gene (*GAPDH*) and for the cDNA of interest (*MLK3*) had the following components in common in a final volume of 25µL: 1x of Buffer Taq (GE Healthcare), 0,8mM of dNTPs 10mM (Bioron), 800nM of both forward and reverse primers for RKO or *GAPDH* 10µM (Sigma) (Figure 12), 0,5 U of Taq DNA polymerase (GE Healthcare), 2µL of cDNA, and water. A mix for negative control was also prepared. The PCR programme used consisted of a first step at 95°C for 5 minutes to denature the cDNA template; followed by a cycle repeated 35 times (95°C for 30 seconds, 58°C for 30 seconds and 72°C for 30 seconds), a final extension step at 72°C for 7 minutes and a final hold of 15°C.



**PCR products purification.** After amplification the products were loaded in an agarose gel, previously prepared, and were purified with Gel Band Purification Kit (GE Healthcare), according to the manufacturer's protocol.

**Snapshot reaction** Purified products from both GAPDH and MLK3 mixes were put together in equal volumes (1 $\mu$ L of each one). To 1 $\mu$ L of this mix were added 600nM of RKO Snapshot primer, 600nM of GAPDH Snapshot primer (Figure 12), 1 $\mu$ L of Snapshot mix (Applied Biosystems) and water. The PCR programme used consisted of a cycle repeated 25 times, divided in three steps: 95°C for 15 seconds, 50°C for 5 seconds and 60°C for 30 seconds and a final hold of 4°C.

**Purification of Snapshot PCR products.** 1 $\mu$ L of the previous mix was added to 1U FastAP™ Thermosensitive Alkaline Phosphatase (Fermentas). Then the following three-step PCR programme was performed: 37°C for 15 minutes followed by 85°C for 15 minutes and a final hold at 4°C.

**GenScan analysis.** Finally, 0,5 $\mu$ L of 120 LIZ GeneScan size standard (Applied Biosystems) and 11 $\mu$ L of formamide (Applied Biosystems) were added to 0,5 $\mu$ L of the previous mix. The samples were then read in the ABI PRISM® 310 Genetic Analyzer (Applied Biosystems).

**Figure 12 - Primers sequences used in snapshot procedure.**

Primer	Primer sequence 5' - 3'	PCR fragment size (bp)
GAPDH Fw	TCAAGGCTGAGAACGGGAAG	456
GAPDH Rv	CAGTAGAGGCAGGGATGATG	
RKO Fw	CCCTGGTGCC CGTCATCCA	227
RKO Rv	AAAACCTCCAGACGTCCTGACC	
GAPDH Snapshot	GCGAGATCCCTCCAAAATCAA	-
RKO Snapshot	TCCAACAACATTTTGCTGCTGCAGC	-

## 2.5 Western Blot

**Protein extraction.** Cells from T-25 or 6-well plate were grown until subconfluence. To perform protein extraction cells were put on ice, the medium was removed and cells were washed twice with PBS1x. The cell lysis occurred when the lysis buffer was added to the cells monolayer. It was composed of RIPA buffer enriched with a protease inhibitor cocktail (Roche) and a phosphatase inhibitor cocktail (Sigma). The lysis

content was removed with a cell scraper, collected, transferred to a tube and then centrifuged at 14000rpm for 10 minutes at 4°C. The resulting supernatant, which corresponds to the total cell lysate, was kept at -20°C. Protein quantification was performed in 96-well plate with detergent-compatible protein assay (BioRad) which is a colorimetric assay similar to Lowry assay. The assay was performed according to the manufacturer's instructions. To construct the standard line bovine serum albumin (Sigma) standards were previously prepared with the following concentrations: 0,25 ; 0,5 ; 0,75 ; 1; 1,5 and 3mg/mL. The absorbance was read on the spectrophotometer (BioRad) at 655nm.

**Sample preparation.** After quantification, 25µg of protein were used to perform western blot. The correspondent volume was mixed with water and 4x Laemmli buffer and boiled at 95°C for 5min.

**Electrophoresis.** After mounting the Mini-PROTEAN 3 cell (BioRad) the separating gel monomer solution was poured between the glasses. After its polymerization, the resolving gel was plated above together with the comb. Samples and PageRuler™ Plus Prestained Protein Ladder (Fermentas) were loaded and the gel ran immersed in 1x TGS Tris/Glycine/SDS buffer (BioRad) for about 1h30 at 120V and 400mA.

**Immunoblotting.** The proteins were transferred from the gel to a nitrocellulose membrane (Amersham Hybond™ ECL™ (GE Healthcare)) with Mini Trans-Blot® Electrophoretic Transfer Cell (BioRad) during 1h30 at 100V and 400mA, according to the instruction manual. To confirm the transference efficiency, nitrocellulose membrane was stained with Ponceau S dye (Sigma) and bands were rapidly visualized.

**Membrane blocking and antibody incubations.** The membranes were blocked in 5% powdered milk (Nestlé Molico) in PBS-Tween 0,5% during 1 hour at room temperature or at 4°C during overnight. Then they were incubated with primary antibodies (listed on the Table IV) during overnight. Most of the antibodies were diluted in milk 5%-PBS-Tween 0,5%, exceptions for phosphorylated ones that were diluted in bovine serum albumin (BSA) 4% and for RhoE antibody that was diluted in both solvents. In the next day the membrane was washed with PBS-Tween 0,5% and incubated with secondary antibody against mouse, rabbit or goat species (sheep anti-mouse immunoglobulin G (IgG) Horseradish Peroxidase linked (HRP) (GE Healthcare), donkey anti-rabbit IgG-HRP (GE Healthcare), donkey anti-goat IgG-HRP (Santa Cruz Biotechnology), respectively).

**Detection.** After some washings the membrane was incubated with ECL Plus Western Blotting Detection Reagents (GE Healthcare) and, in a dark room, an Amersham Hyperfilm™ ECL (GE Healthcare) was put in contact with membranes. After some seconds or minutes of exposure the film was revealed with a 1:5 diluted solution of Developer and replanisher (Kodak GBX), washed and then fixed with 1:5 diluted solution of Fixer and replanisher (Kodak GBX). When membrane reprobing was intended it was made a first washing with PBS1x for 15 minutes, then membrane was incubated for other 15 minutes with a soft stripping solution, which contains acetic acid instead of  $\beta$ -mercaptoethanol to better preserve proteins integrity and finally it was washed again for 15 minutes to remove that solution.

**Quantification.** Protein bands were quantified through the Quantity One 1-D Analysis Software (BioRad). The background value was deducted on the value of each band. The final value corresponds to a normalization to the tubulin value of same the gel.

**Statistical analysis.** Student's t-test was performed to compare the means of the different experiments. P values of 0,5 or less were considered.

**Table IV – Characterization of the antibodies used in western blot.**

PROTEINS			PRIMARY ANTIBODIES		
Name	Molecular weight (KDa)	Dilution	Species	Company/Reference	
Actin	45	1:1000	goat	Sta Cruz Biot (#sc-1616)	
Akt (total)	60	1:1000	rabbit	Cell Sign (#9272)	
Akt (ph)	60	1:1000	rabbit	Cell Sign (#3787S)	
Bcl2	26	1:100	mouse	Dako (F7053)	
Cyclin D1	38	1:500	mouse	Sta Cruz Biot (#sc-20044)	
E-cadherin	135	1:1000	rabbit	Cell Sign (#3195)	
ERK (total)	42/44	1:1000	rabbit	Cell Sign (#9102)	
ERK(ph)	42/44	1:1000	rabbit	Cell Sign (#4377)	
JNK (total)	46/54		rabbit	Cell Sign (#9252)	
JNK (ph)	46/54	1:1000	mouse	Cell Sign (#9255S)	
MLK3 (total)	95	1:1000	rabbit	Sta Cruz Biot (#sc-536)	
MLK3 (ph)	95	1:1000	rabbit	Upstate	
p21	21	1:250	mouse	BD Biosciences (554228)	
p27	27	1:1000	rabbit	Sta Cruz Biot (#sc-528)	
p38 (total)	43	1:500	mouse	Cell Sign (#9212)	
p38 (ph)	43	1:500	mouse	Cell Sign (#9216S)	
p53	53	1:1000	rabbit	Cell Sign (#9282)	
PI3K p110 $\alpha$	110	1:1000	rabbit	Cell Sign (#4249)	
PI3K p85 $\alpha$	85	1:2500	mouse	BD Biosciences (610046)	
PTEN	55	1:100	rabbit	Sta Cruz Biot (#sc-6817-R)	
RhoE	27	-	mouse	Abcam	
ROCK I	160	1:500	mouse	BD Biosciences (611137)	
$\alpha$ -tubulin	50	1:10000	mouse	Sigma	
$\beta$ -catenin	92	1:2000	rabbit	BD Biosciences (610153)	

## 2.6 Functional assays

### 2.6.1 Proliferation assay

The proliferation assay performed was based on the incorporation of Bromodeoxyuridine (BrdU), which is a thymidine analogue, during DNA synthesis (phase S of cell cycle).  $2,5 \times 10^5$  cells per well were plated in 6-well plates, with or without coverglasses Ø10mm (Sofdan) (the evaluation of this assay by flow cytometry does not require coverglasses), and grown in the CO<sub>2</sub> incubator at 37°C. After 48h, 10µM of BrdU stock solution were added and cells were then incubated for 1 hour at 37°C. After that, medium with BrdU was removed and cells were washed twice in PBS1x. From here two different procedures were undertaken to fix cells and stain them with anti-BrdU, because at the end proliferation levels were evaluated by different methods: immunocytochemistry and flow cytometry.

**Immunocytochemistry.** Cells were fixed in paraphormaldehyde 4% for 30 minutes, followed by PBS1x washing. To denature DNA, HCl 2M was added for 20 minutes and then coverglasses were washed in PBS1x and in PBS-0,5% Tween20 – 0,05% BSA. Details about antibodies incubation characteristics are described in Table V. Coverglasses were mounted on microscope slides with a drop of Vectashield Mounting Medium with DAPI (Vector Laboratories, Inc.), covered with a coverslip (BioSigma) and counted on the microscope DM2000 (Leica) at 400x magnification.

**Flow cytometry.** Cells were detached with trypsin-EDTA (Gibco, Invitrogen), resuspended in medium and the content was centrifuged twice at 1500rpm for 5 minutes with an intermediate washing in PBS1x. Cells were then fixed with 70% ethanol in PBS1x for 30 minutes. After fixation procedure, cells were centrifuged again in the same conditions to remove fixation solution. After washing in PBS1x with 0,5% BSA cells were resuspended and 2M of HCl was added for 20-30 minutes to denature DNA. After new centrifugation the pellet was dissolved and incubated with primary and secondary antibodies in conditions described in Table V. Samples were read by Epics XL-MCL™ Flow Cytometer (Beckman Coulter) and analysed with WinMDI 2.9 software.

The viable cell population was delimited through the definition of a gate in a dotplot, where the events were distributed by size (forward scatter) and complexity (side scatter). Inside that gate, definition a new gate to select the singlet population was

created in a dotplot, where propidium iodide (PI) fluorescence was represented. Based on another dotplot containing both BrdU and PI fluorescences three regions were created corresponding to G<sub>0</sub>, S and G<sub>2</sub>/M phases and a final histogram was created (where M1 includes G<sub>0</sub> and G<sub>2</sub>/M phases, and M2 includes S phase).

**Table V – Antibodies used in proliferation assay.**

Antibody	Designation	Dilution	Incubation
<b>Primary</b>	Monoclonal Mouse Anti-BrdU (Dako)	1:10 PBS-0,5%Tween20 – 0,05% BSA	1h
<b>Secondary</b>	Polyclonal Rabbit Anti-Mouse IgG/FITC (DakoCytomation)	1:100 in PBS-0,5%Tween20 – 0,05% BSA	30 minutes in the dark

### 2.6.2 Migration assay

Cells were plated, in duplicates, in 12-well plates until confluence. When they reached it, a pipete tip was used to make a scratch in the monolayer of cells. Immediately after that, in only one of the plates, ROCK inhibitor – Y27632 was added at a final concentration of 10µM, after removing the medium. Cell migration was photographically recorded in an automated way during 14 hours in time-lapse (Zeiss). Photos were taken each 5 minutes at 20x magnification. Films were analysed with Lsmib software (Zeiss). Cell migration was measured as the distance from the monolayer wall to the leading edge of the wound in three aleatory positions.  $3 \times 10^4$  cells per well were also plated in a 24-well plate. After a few hours ROCK inhibitor was added to some wells to evaluate its action on cells morphology (comparative photos were taken).

### 2.6.3 Viability assay

This assay was performed in triplicate in 96-well plates.  $4 \times 10^3$  and  $8 \times 10^3$  cells were plated in each well (both in duplicates in each plate). In the next day, the medium was replaced by medium with 1% FBS instead of 10% as usually, in half of the wells. After 8, 24 and 48 hours, 20µL of the MTS reagent from CellTiter 96® AQueous One Solution Cell Proliferation Assay (Promega) was added to each well. After these time-points cells were incubated at 37°C for 1–4 hours in a humidified, 5% CO<sub>2</sub> atmosphere and absorbance was recorded at 490nm using a 96-well plate reader (BioRad). The

cell morphology was documented using an inverted bright field microscope, at 8 and 24 hours upon culture with 1% FBS.

## 2.6.4 Slow aggregation assay

A slow aggregation assay was performed for HEK293 stable cell lines, using MCF7 cells as a positive control and CHO cells as the negative one. Three replicas per sample were performed.

Each well of a 96-well plate was coated with 50 $\mu$ L of agar medium previously prepared (100mg Bacto™ Agar (BD Biosciences) were dissolved in 15mL of PBS1x, that was boiled three times to sterilize the solution). This agar layer prevents cell-substratum adhesion. After its gelification, 100 $\mu$ L of a single-cell suspension ( $1 \times 10^5$  cells/mL) was seeded onto the semisolid agar of each well. Cultures were incubated for 44 hours in a humidified atmosphere of 5% CO<sub>2</sub> in air at 37°C. The aggregate formation was evaluated with an inverted microscope (40x magnification) after 15, 22 and 44 hours of incubation.

## 2.7 Solutions recipes

**Table VI - Recipes of the solutions used in this experimental work.** Distilled water was the solvent used. Solutions pH was measured with sympHony Multiparameter Research Meters SB90M5 (VWR). The pH was adjusted to the desired value with HCl 4M (Merck) and NaOH 5M (Merck).

Solution	Components	pH	Storage
DNA ladder	Bromophenol blue 6x	80 $\mu$ l	-
	Xylene blue 6x	80 $\mu$ l	
	DNA marker	100 $\mu$ l	
Laemmli Buffer4x	Tris-HCl 0,5M	0,25M	6,8
	C <sub>3</sub> H <sub>8</sub> O <sub>3</sub> (glycerol)	40%	
	SDS	0,319M	
PBS stock solution 20x	NaCl	2,74M	7,4
	KCl	54nM	
	Na <sub>2</sub> HPO <sub>4</sub> .2H <sub>2</sub> O	0,145M	

	KH <sub>2</sub> PO <sub>4</sub>	35mM		
<b>RIPA buffer</b>	C <sub>4</sub> H <sub>11</sub> NO <sub>3</sub> HCl (Tris HCl)	50mM		
	NP-40	1%	7,5	4°C
	NaCl	150mM		
	EDTA	1,65mM		
<b>Separating buffer</b>	C <sub>4</sub> H <sub>11</sub> NO <sub>3</sub> (Tris)	1,5M	8,8	room temperature
	SDS 10%	0,4%		
<b>Separating gel (10% acrylamide)</b>	Separating buffer	24,8%		
	Solution d'acrylamide	33%	-	prepared when used
	TEMED	0,2%		
	Persulfate d'ammonium 10%	1%		
<b>Soft stripping solution</b>	Acetic acid	10%	-	room temperature
	Methanol	10%		
<b>Stacking buffer</b>	C <sub>4</sub> H <sub>11</sub> NO <sub>3</sub> (Tris)	0,5M	6,8	room temperature
	SDS 10%	0,4%		
<b>Stacking gel</b>	Stacking buffer	20,6%		
	Solution d'acrylamide	13,22%	-	prepared when used
	TEMED	0,2%		
	Persulfate d'ammonium 10%	0,99%		
<b>TBE 10x stock solution</b>	C <sub>4</sub> H <sub>11</sub> NO <sub>3</sub> (Tris-base)	0,87M		
	H <sub>3</sub> BO <sub>3</sub> (boric acid)	0,89M	8,0	room temperature
	EDTA 0,5M pH=8	2mM		
<b>Transfer Buffer10x</b>	C <sub>4</sub> H <sub>11</sub> NO <sub>3</sub> (Tris-base)	0,48M	-	room temperature
	C <sub>2</sub> H <sub>5</sub> NO <sub>2</sub> (Glycine)	0,39M		
<b>Transfer Buffer1x</b>	Transfer buffer 10x	10%	9,2	room temperature
	Methanol	20%		





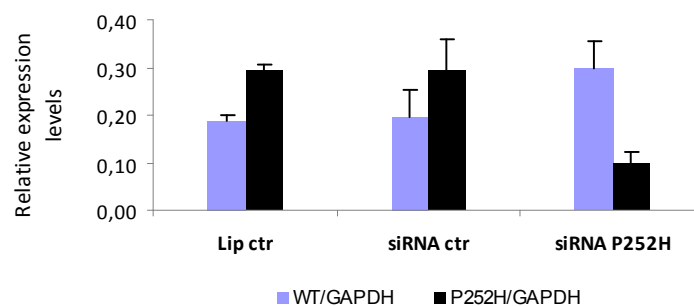
Chapter 4

Results and Discussion

### 3.1 P252H has functional value in colorectal context

In 2010 *MLK3* missense mutations were described for the first time by our group in colorectal carcinomas and protein predictive models, *in vitro* and *in vivo* experiments demonstrated that these mutations were functionally important. One of the described *MLK3* mutations (P252H) became especially important, not only because it was shown to be associated to an aggressive phenotype, but also because it was constitutionally present in a colorectal cell line (RKO). That gave us the possibility to determine the role and the signalling pathways associated to this *MLK3* mutation in its specific context. In order to access the functional role of *MLK3* P252H in colorectal cancer, we transiently transfected RKO cell line with siRNA. RKO presents two *MLK3* alleles, a wild-type *MLK3* allele and P252H mutation. Furthermore, it presents multiple genetic alterations and that is a clear limitation in our study. However, taking this problem in consideration we proceeded with our study and transfected RKO with siRNA for the *MLK3* mutated allele.

The specificity of the siRNA to inhibit only the mutated allele and not the wild-type allele too, was confirmed by snapshot analysis (Graphic 1). So, any data that comes from this condition is only due to the inhibition of the P252H allele.



**Graphic 1 - Snapshot results representing the allelic mRNA ratio.** The values are normalized to GAPDH. The ratio between two alleles in both lipofectamine and siRNA controls was similar. However, in the third condition we verified a higher level of the wild-type allele comparing to the mutated one, what was in accordance with what we expected.

We also confirmed *MLK3* protein inhibition, by western blot, and evaluated the effect of the mutation in some targets: phosphorylated ERK, cyclin D1 and p21. The mutation appear to be downregulating these targets (Figure 13).

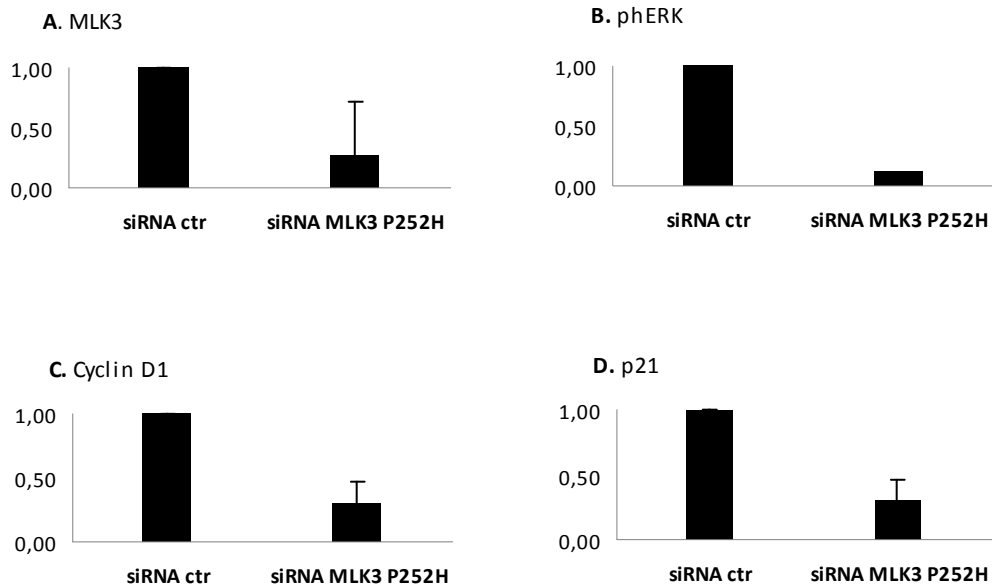
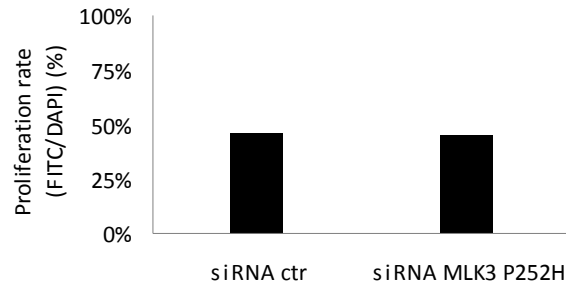


**Figure 13 - Effect of P252H inhibition in expression levels of some proteins.** The values are normalised to siRNA control. A) MLK3. B) pERK (note that this antibody was only tested once, that is why the bar in graphic does not have standard deviation). C) cyclin D1. D) p21.

With these experiments, we could prove that P252H inhibition in colorectal cancer context interferes with targets related to the MAPKinase and WNT pathway. However, we also aimed to verify if the silencing of P252H lead to a decrease in RKO proliferation rate. In order to study this hypothesis we performed proliferations assays with BrdU incorporation more than once, but the presented data (Graphic 2) results only from a unique transfection that conjugates information from snapshot, western blot and proliferation assay.

In spite to what has been previously shown for wild-type *MLK3* silencing prevented serum-stimulated cell proliferation [37], and confirmed in our previous results, P252H silencing does not seem to have the same effect. It seems that alterations on the levels of the mutant protein on proliferation related targets is not reflected in the proliferation rate of the cells where P252H allele was inhibited. However, we need to confirm this result by performing again a new siRNA transfection followed by a snapshot analysis and a western blot to confirm the efficiency of the inhibition before performing the proliferation assay.



**Graphic 2 - Results from proliferation assay in RKO transfected with either siRNA control or siRNA MLK3 P252H.** BrdU-positive cells were counted and the value was normalised to siRNA control.

Overall, we demonstrated that P252H mutation perturbs the expression of some targets in colorectal cancer cells thus this *MLK3* mutation harbours a functional value and not a by passenger effect.

### 3.2 Establishment of HEK293 stable cell lines

After proving the functional value of P252H, it was important to evaluate the associated cellular effects *per se* and the signalling pathways that this *MLK3* mutant could be affecting. To do so, we established *MLK3* mutant stable cell lines. In order to have a clear cellular model, without multiple genetic alterations that could mask the function of *MLK3* we choose HEK293 cell line and transfected it with *MLK3* mutations (P252H and R799C), Mock vector and wild-type *MLK3*. As P252H and R799C *MLK3* mutants were the most *in vitro* transforming mutations [11] and were also localized in two distinct key functional domains (the kinase and the P/S/T rich domains, respectively) we had a chance of studying genotype-phenotype correlations. In fact we aimed at verifying whether mutations in *MLK3* localized in distinct domains lead to distinct or similar cellular effects and activated signalling pathways. Further, the wild-type *MLK3* vector will allow us to understand if wild-type *MLK3* overexpression causes the same effects as mutations do. At the same time it could also give us a hint about what happens in many tumours, where *MLK3* protein was found to be overexpressed.

### 3.2.1 Selection after sequencing

After transfection, HEK293 cells were subjected to a blasticidin selection, allowing the resistant ones, those with the vector, to survive. However, to guarantee that every replica had the right sequence in their vector, *MLK3* gene was sequenced in all samples. The entire coding sequence of *MLK3* (ENSG00000173327 – Appendix I) was screened for mutations. HEK293 *MLK3* R799C was the first HEK293 stable cell line to be sequenced together with the parental one. Its *MLK3* sequences were analysed in both DNA and cDNA.

Some silent mutations were detected only in the cDNA of HEK293 *MLK3* R799C T1 (Figure 14) and because of that this replica was excluded from further experimental works.

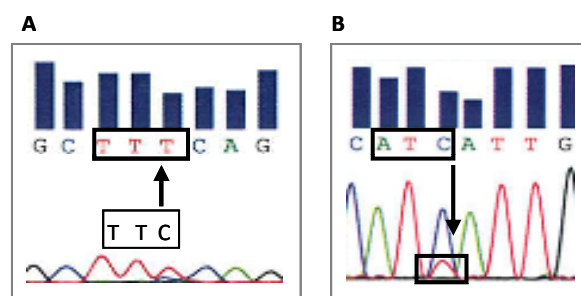


**Figure 14 – Examples of two unexpected mutations in R799C T1.** A) The sample contains a –C-to-T substitution, localized at nucleotide position number 835, which does not alter the aminoacid phenylalanine localized at aminoacid position number 114 (code number in PUBMED’s protein database CAI94235). B) There are two peaks at nucleotide position number 1021. The nucleotide C is the right one and the nucleotide T, that appears in heterozigoty, is a silent mutation, thus not alter the aminoacid isoleucine at aminoacid position number 176.

R799C T2 and R799C T3 had the desired mutation correctly inserted, comparing to wild-type sequence

Until here, the entire coding sequence of *MLK3* was screened for mutations either in DNA or cDNA of *MLK3* R799C stable cell lines. However, contrarily to what happened in cDNA, as in the DNA there were not found any mutations, we decided to screen for mutations only the cDNA of the other established stable cell lines, thus we were able to detect any mutation that could appear.

In P252H T2 we identified a deletion in the sequence between nucleotide position numbers 2366 and 2695 (Figure 15). Instead of the normal 330bp sequence there were only 13bp, without any identified homologue sequence. So, P252H T2 was also excluded.

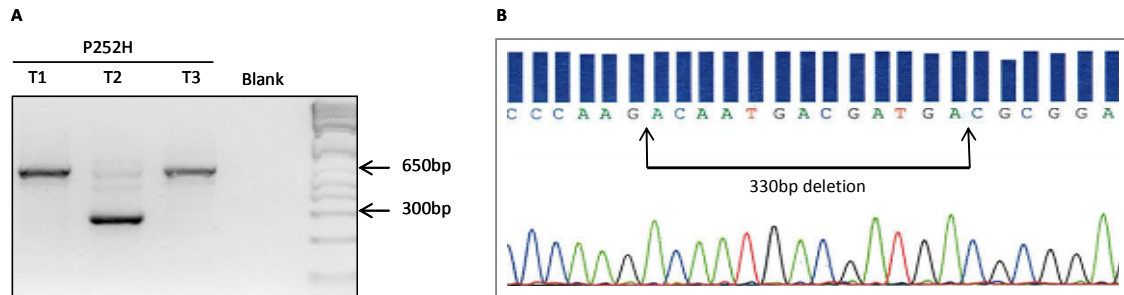


**Figure 15 - Deletion in P252H T2.** A) Agarose gel electrophoresis of PCR products from *MLK3* exon 9 amplification of P252H replicas. The expected band had 602bp size and the one below, near 300bp, corresponds to a deletion in P252H T2. B) Confirmation of P252H T2 deletion by sequencing the lower band.

Those mutated stable cell lines that were not excluded presented the right insertion of the expected mutations (Figure 16).

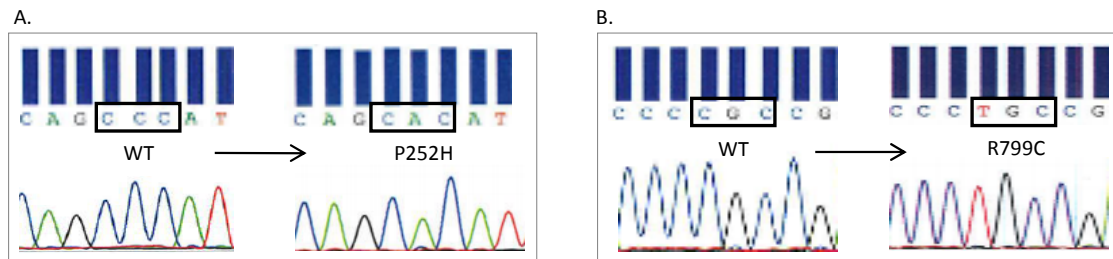


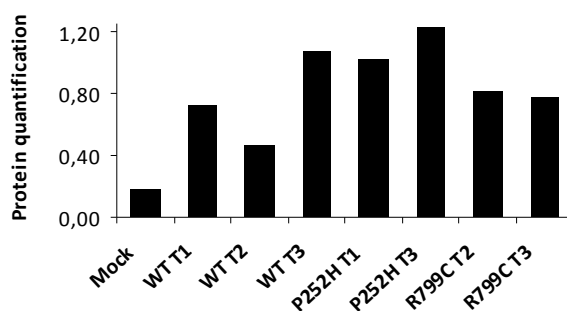
**Figure 16 - Correct insertion of the mutations into the *MLK3* sequence.** A) Comparison between *MLK3* sequences from wild-type *MLK3* and *MLK3* P252H cell lines. B) Comparison between *MLK3* sequences from wild-type *MLK3* and *MLK3* R799C cell lines.

The Mock vector was also sequenced to confirm that there was not any undesired sequence in it.

### 3.2.2 Selection based on transfection efficiency

The level of transfection efficiency corresponded to the amount of protein expressed, which was evaluated by western blot analysis. From the previous step of selection we excluded two mixes of clones, each of one from a stable cell line with a different

mutation. To further perform comparative studies between wild-type MLK3 and mutant MLK3 it was imperative to determinate eventual expression gaps between replicas that could justify eventual differences in cellular effects. The results of the first western-blot for MLK3 expression are shown in the Graphic 3. As what was expected, Mock cell line had the lowest MLK3 expression. However, wild-type MLK3 stable cell lines had some differences of expression between them. So, from the graphic we excluded WT T2 because we could not pare its MLK3 expression levels with those of any mutation.



**Graphic 3 - MLK3 protein expression levels from the first western-blot after HEK293 transfection.** Bands quantification was done with Quantity One software.

From now on and due to the similarity of MLK3 expression levels and also to simplify the data, the results will be presented in the following manner:

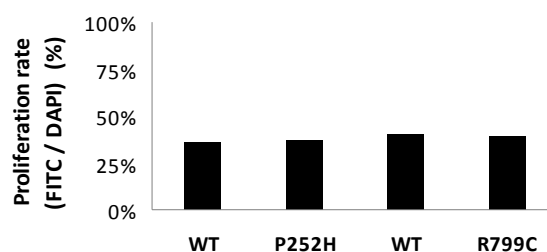
- Wild-type (average value between T1 and T3 transfections) will always be compared to Mock, allowing the evaluation of the effect of wild-type MLK3 overexpression;
- The P252H mutation (average value of T1 and T3 transfections) will always be compared with WT T3 (abbreviated to WT), allowing the evaluation of the effect of P252H mutation in comparison to wild-type MLK3;
- The R799C mutation (average value of T2 and T3 transfections) will always be compared with WT T1 (abbreviated to WT), allowing the evaluation of the effect of R799C mutation in comparison to wild-type MLK3.



### 3.3 Cellular effects of *MLK3* mutations and of wild-type *MLK3* overexpression

#### 3.3.1 Proliferation

In order to evaluate the effect of the mutant forms of *MLK3* in comparison to wild-type *MLK3* on proliferation rate, the stable transfected HEK293 cell lines were studied and performed a BrdU immunocytochemistry. According to the Graphic 4 no differences were found between the proliferation rates of P252H and R799C, when compared with the respective wild-type control. However, the meaning of this result is still debatable since we only performed a single experiment and this was due to a technical limitation.



**Graphic 4 - Proliferation rate of *MLK3* mutations compared to the respective WT.**

HEK293 cells have very low adherence to coverslips and consequently a very low number of cells per coverslip is obtained in the end of an immunocytochemistry, thus it was difficult to repeat this experience. As an alternative approach we evaluated the proliferation by flow cytometry (Figure 17). However, the results seem to confirm the previous ones, no significant differences were found between mutations and their respective wild-types or between wild-type and Mock. Both results suggest that *MLK3* does not play a major role in cell proliferation control.

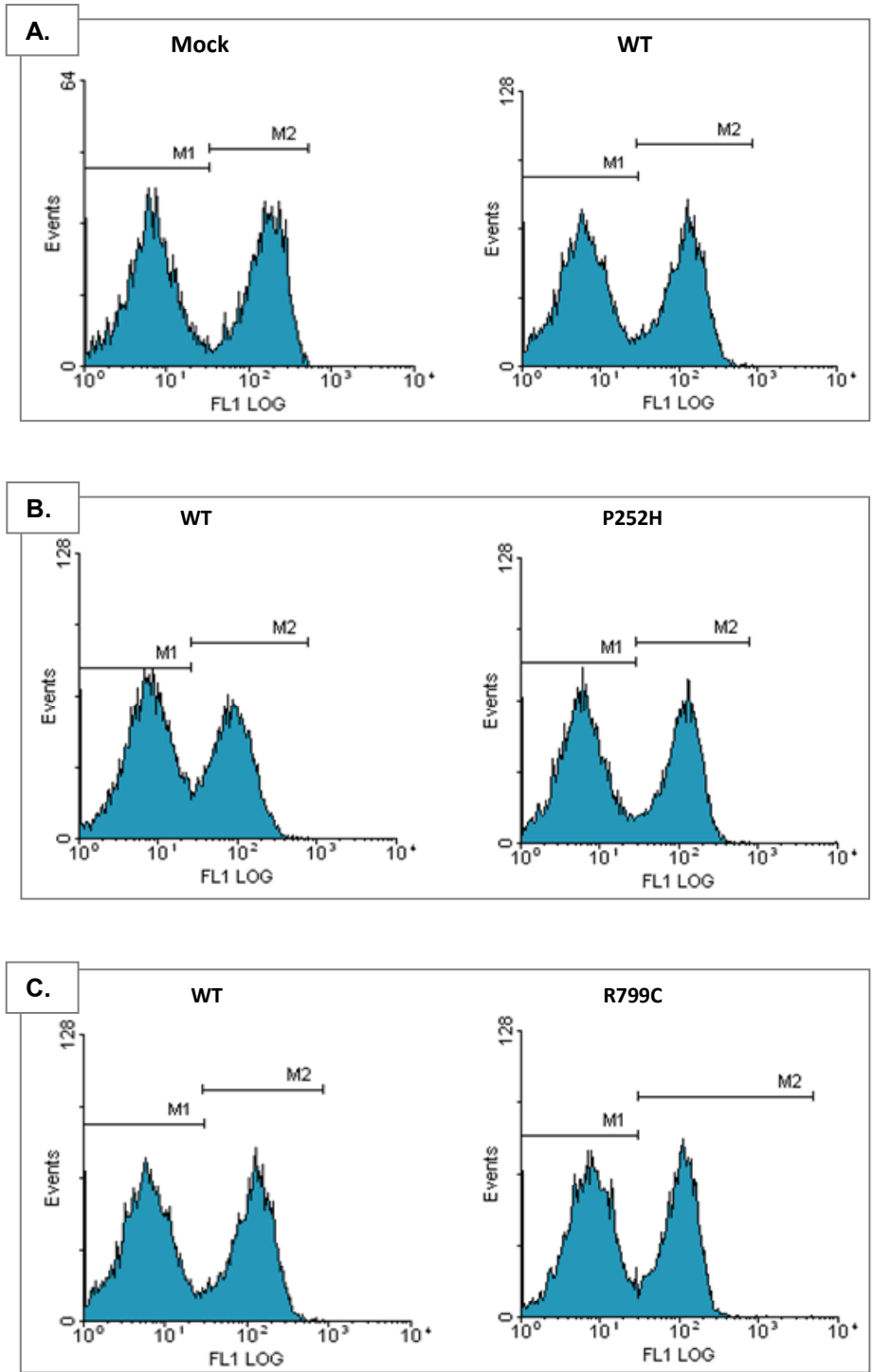


**Figure 17 - Histogram representation of the cell cycle of HEK293 stable cell lines.** It shows the number of cells in G0, G2/M phases (M1) and S phase (M2). Comparisons between WT and Mock (A), P252H mutation and respective WT (B) and between R799C and respective WT (C).

### 3.3.2 Viability

The viability assays performed allows the determination of the number of viable cells in proliferation or cytotoxicity effects and consists in the reduction of a tetrazolium compound named MTS into the colored formazan product [92]. This conversion is presumably accomplished by NADPH or NADH produced by dehydrogenase enzymes in metabolically active cells [93]. The quantity of formazan product formed is measured, after 1-4 hours of the addition of the reagent, by the absorbance at 490nm and is directly proportional to the number of living cells in culture. So, this assay allows the indirect measurement of viable cells in culture.

The manufacturer advises to first perform a cell titration to choose an optimal cell number of cells to initiate the assay. They also recommend an initial number of 5000 cells per well to initiate proliferation studies with most tumour cells, hybridomas and fibroblast cell lines. In our study we only tried two different initial conditions: 4000 and 8000 cells per well.

Graphics A, B and C from Figure 18 shows the absorbance at 490nm of HEK293 stable cell lines (Mock, wild-type MLK3, P252H, R799C) upon 8(A), 24 (B) and 48 hours (C) of culture with either 10% FBS or 1% FBS, which is directly proportional to the number of living cells in culture. The increased absorbance observed along time in any stable cell line was independently on the percentage of FBS in culture and could be attributed to an increase in the number of cells and not to an increase in cell viability. Anyway, this indicates that 1% FBS is not affecting cell metabolism to a great extent and that a stronger stimulus must be used to provoke a decrease in cell viability along time.

Now, looking at the absorbance values of cells exposed to 1% FBS after 8 and 24 hours we realize that sometimes they are similar or even higher than those grown with 10% FBS. Values are not yet stabilized and that increase could probably be attributed to an adaptation process. It is known that nutrient deprivation causes an upregulation of NAD<sup>+</sup> levels in mitochondria, which determines cell survival [94].

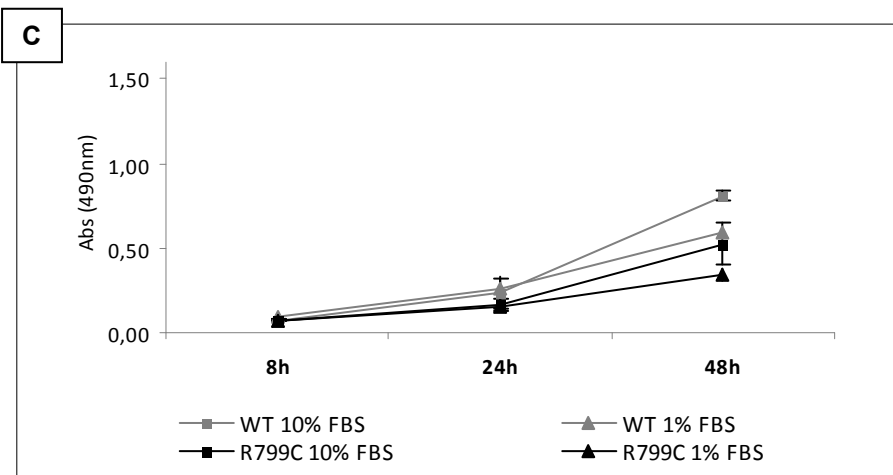
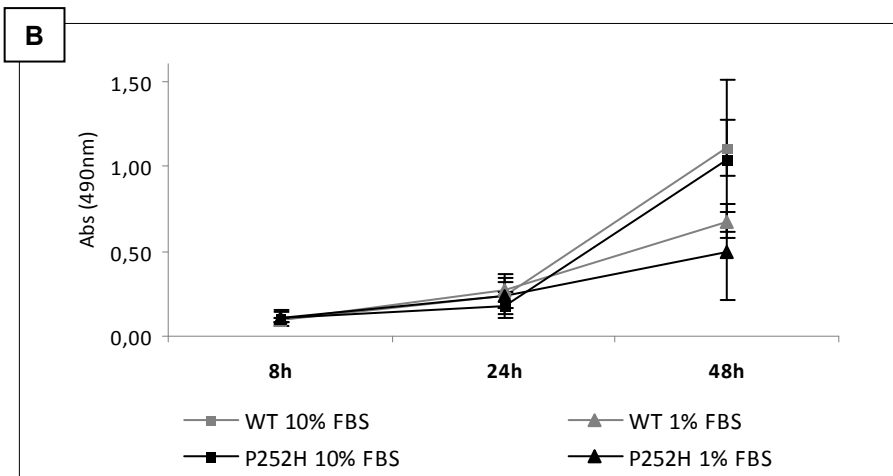
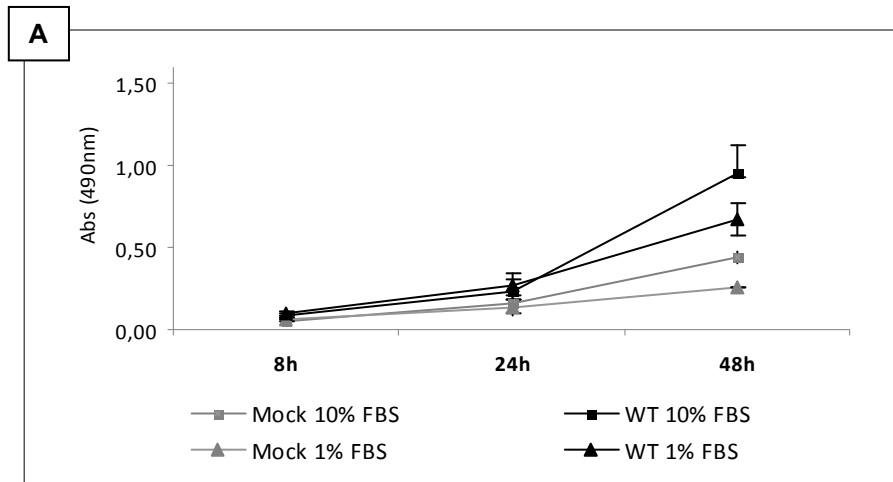


**Figure 18 - Cell viability of HEK293 stable cell lines, upon 8 (A.), 24 (B) and 48 hours (C) of culture with either 10% FBS or 1% FBS.**

Figure 19 shows the influence of 48 hours of culture with 1% FBS on cell viability, with either 4000 or 8000 cells per well, as initial conditions. As proliferation does not seem to be altered, the observed differences between stable cell lines, upon treatment with

1% FBS, should not be attributed to differences in proliferation rate. In both initial conditions, wild-type MLK3 overexpression itself caused a decrease of almost 20% in cell viability and R799C mutation presented viability values lower than wild-type control in graphic I, but similar in graphic II. In cells expressing P252H mutation it is not very clear if the mutation provokes a decrease in cell viability or not, because the standard deviations are too big. Such big standard deviations could be due to mistakes in the number of cells plated in each well. However, this MLK3 mutant seems to be more resistant, at least to 1% FBS, than the other mutant.

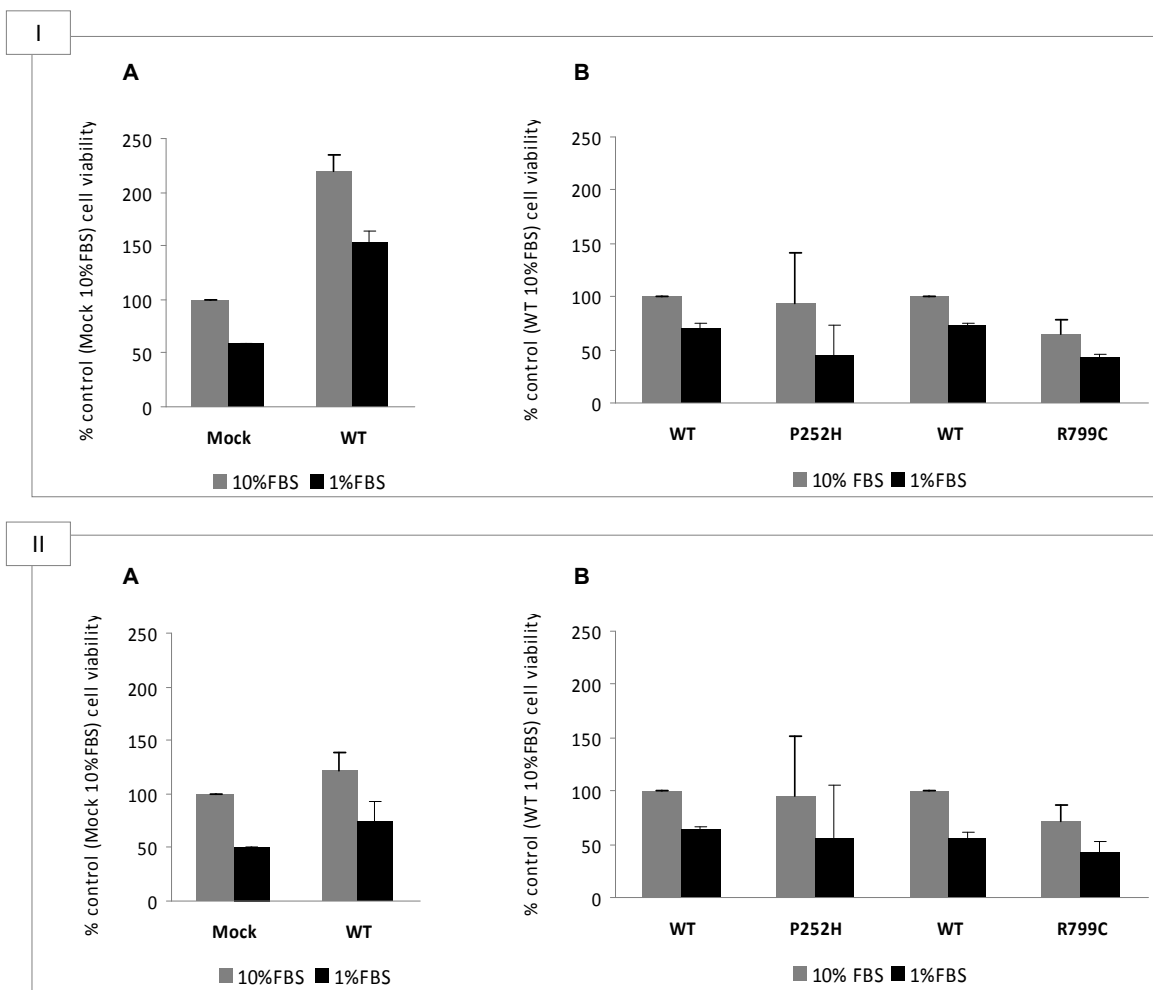


**Figure 19 - The effect of culture with 1% FBS and wild-type MLK3 overexpression (A) or MLK3 mutations (B) on viability of two different initial conditions (I – 4000 cells per well; II – 8000 cells per well). The values are normalised to the control either to Mock 10% FBS (A) or to WT 10% FBS (B)). Cells were incubated in normal culture conditions in the presence of 10% FBS (graybars) or presence of 1% FBS (black bars) for 48 hours. After treatment, the MTS reduction assay was used to determine the level of cell survival, compared with controls.**

Upon 48 hours of culture, cells subjected to 1% FBS not only dye more than those grown with 10% FBS as they develop a different morphology. Looking only to pictures of cells treated with 1% FBS for 48 hours (Figure 20) we observe that MLK3-mutated and Mock cells present a round-shape morphology with reduced area, losing the majority of the cellular extensions, while wild type cells retained their morphology, with differences in cell number.

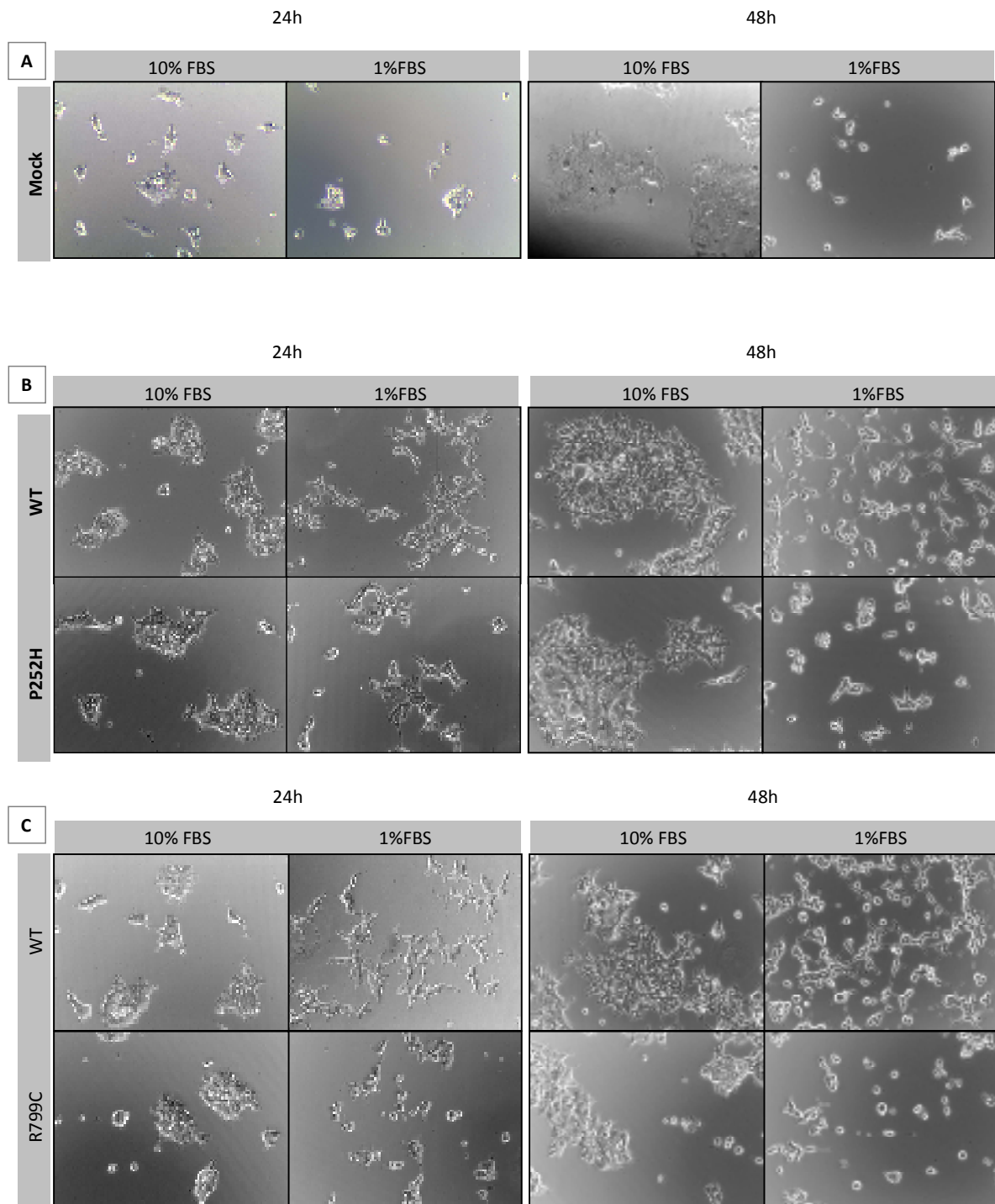


**Figure 20 - Cells morphology after 24 and 48 hours of culture with either 10 or 1% FBS (data from an initial number of 4000 cells per well).** (A) Mock pictures; comparisons between (B) P252H and WT, (C) R799C and WT.

In spite of the well accepted number of replicas used per each stable cell line, which indeed increases the reliability of the results, this assay was only performed once. In future experiments it must be followed by a western blot analysis to evaluate the expression of some apoptosis and proliferation-related proteins, such as Bcl2 or caspase-

3 and cyclin D1 or p21. Depending on the type of stimulus applied, both P252H and R799C mutations may confer different resistance to cells. However this should be proven, subjecting cells to more aggressive stimuli. More cell numbers in the beginning of the assay have also to be tested to take more clear conclusions about, at least, the effect of P252H mutation on cell viability. To complement these studies in the future cell death should be also evaluated by flow cytometry, using annexin V.

### 3.3.3 Migration

Cell migration was recorded for 14h. After that, both WT seem to have differences in the establishment of cells protrusions, because WT T1 presents more and longer protrusions than WT T3 (Figure 21). This effect may be related to the level of expression of wild-type MLK3 since WT T1 and WT T3 present different levels of MLK3 protein expression. However, this hypothesis needs to be proven by additional experiments.

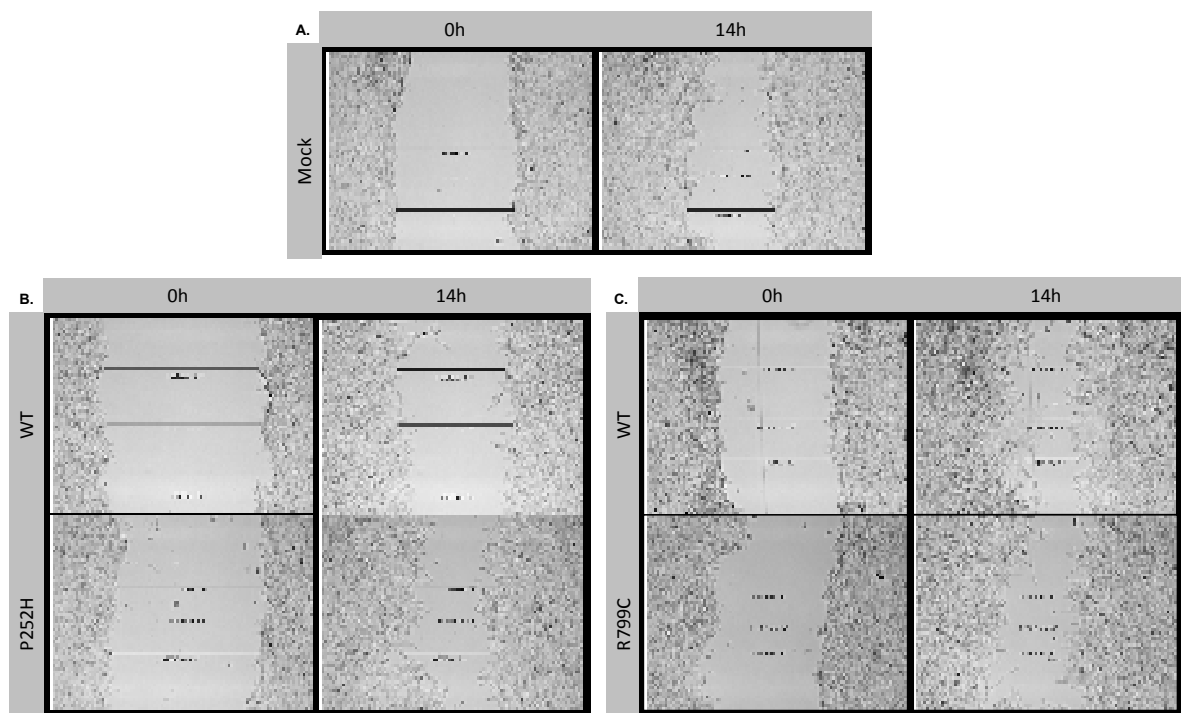


**Figure 21 - Photos of migration assay at 0 and 14 hours. (A) Mock cells. Comparisons between (B) P252H and WT, (C) R799C and WT.**

Data resuming the measures made in every films are presented in Figure 22. Interestingly, the mutation R799C leads to an impairment of cell migration levels, comparing to WT. Otherwise, P252H mutation seems to have the opposite effect. The



overexpression of wild-type MLK3 also leads to an increase in cell migration levels, comparing to Mock. The differences in the migrated distance should not be attributed to differences in cell proliferation since the proliferation rate of mutant MLK3, wild-type MLK3 and Mock cells were very similar (results presented above).

Migration assays could have been better explored. For instance, to guarantee that any observed effect was due to cell proliferation, we could prolong the assay for 24 hours using mitomycin-C, which inhibits cell proliferation [75]. To minimize the eventual effect on cells communication of the different wound sizes created by manual scratching we could experiment the CytoSelect™ 24-Well Wound Healing Assay (Cell Biolabs), where defined wound fields are created. However, the results can not be directly compared since in the case of CytoSelect™ 24-Well Wound Healing Assay there is not cell damage and that the lack of this damage stimulus could alter the results.

The velocity of migration is another important parameter that we could also evaluate. The distance migrated along time could be graphically represented, given the idea of migration or contraction of cells from the monolayer. Indeed cells trajectories could also be evaluated in cells plated with lower confluence. Together these data would bring valuable clues to better understand the observed differences in the distance migrated by HEK293 stable cell lines.

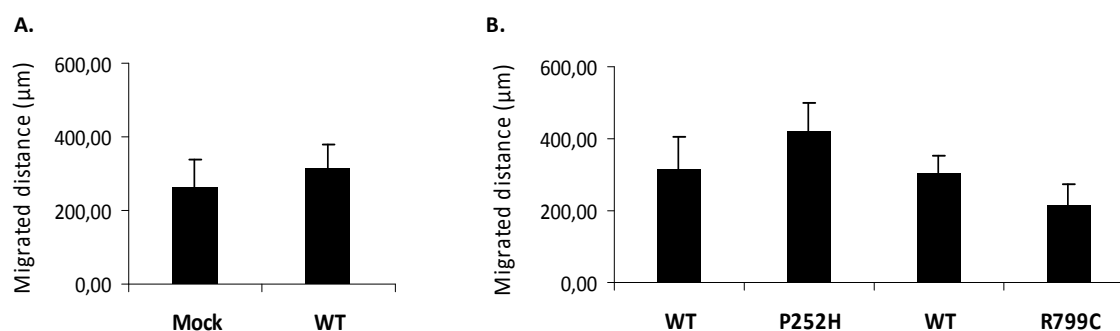


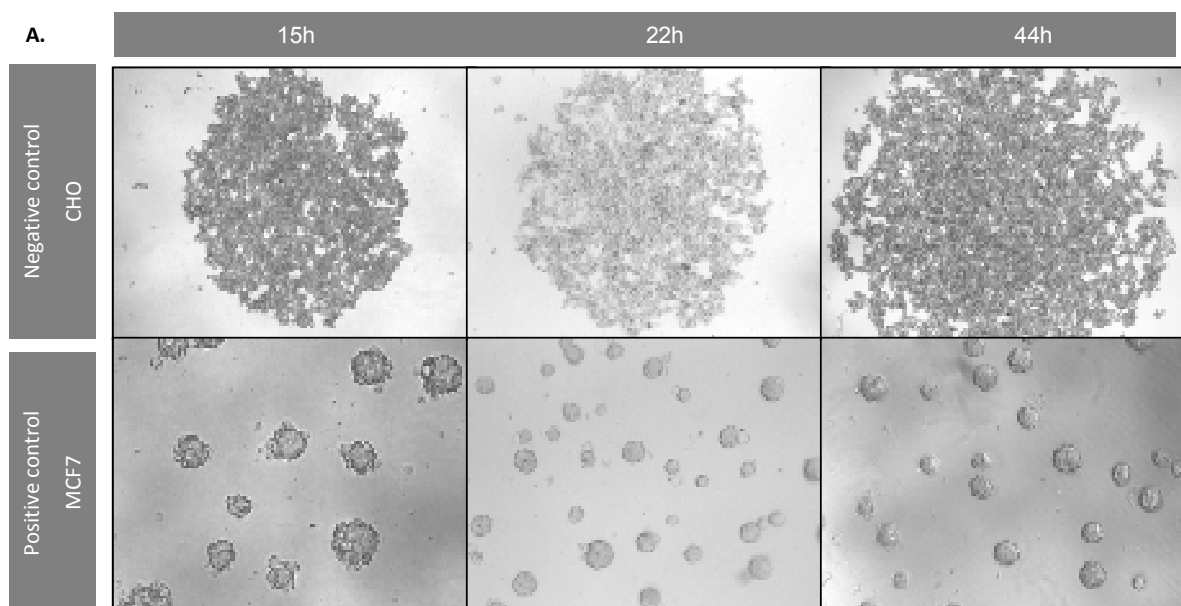
**Figure 22 - Migrated distance by each HEK293 stable cell line after 14 hours.** Cell migration was calculated by subtracting the leading edge distance from the starting position of the leading edge. (A) MLK3 WT versus Mock, (B) MLK3 mutants versus MLK3 WT.

### 3.3.4 Aggregation

In general, cell aggregation assays are designed to test the functionality of cell to cell adhesion and indirectly to access the status of the E-cadherin/catenin complex. Cell-cell adhesion is mostly dependent on the integrity of this complex. This assay allows to study the capacity of the cells to adhere to the neighbouring cell in a cohesive status [95]. In slow aggregation assays cells are seeded on a semisolid agar substrate in a 96-well plate and the cells spontaneously aggregate.

As a negative control for this experimental assay CHO cells were used since these cells are cadherin-negative and fail to aggregate homotypically, despite forming a single central cluster. MCF7 cells were used as a positive control since they express E-cadherin and make multiple and disperse aggregates around the well. The level of aggregation was photographically registered at different time points (Figure 23A).

At 15 hours, there were differences in the pattern of slow aggregation between Mock and all the other stable cell lines. Mock cells already presented a large, compact and central-positioned aggregate, while the other stable cell lines do not present a cohesive one (Figure 23B-D). At 22 hours those differences were a bit attenuated. Mock cells developed a perfect round-shaped aggregate while the other stable cell lines are acquiring that phenotype in a slower way. At 44 hours all stable cell lines present a similar pattern of aggregation, despite the delay observed in wild-type and mutated cells in the initial time points.



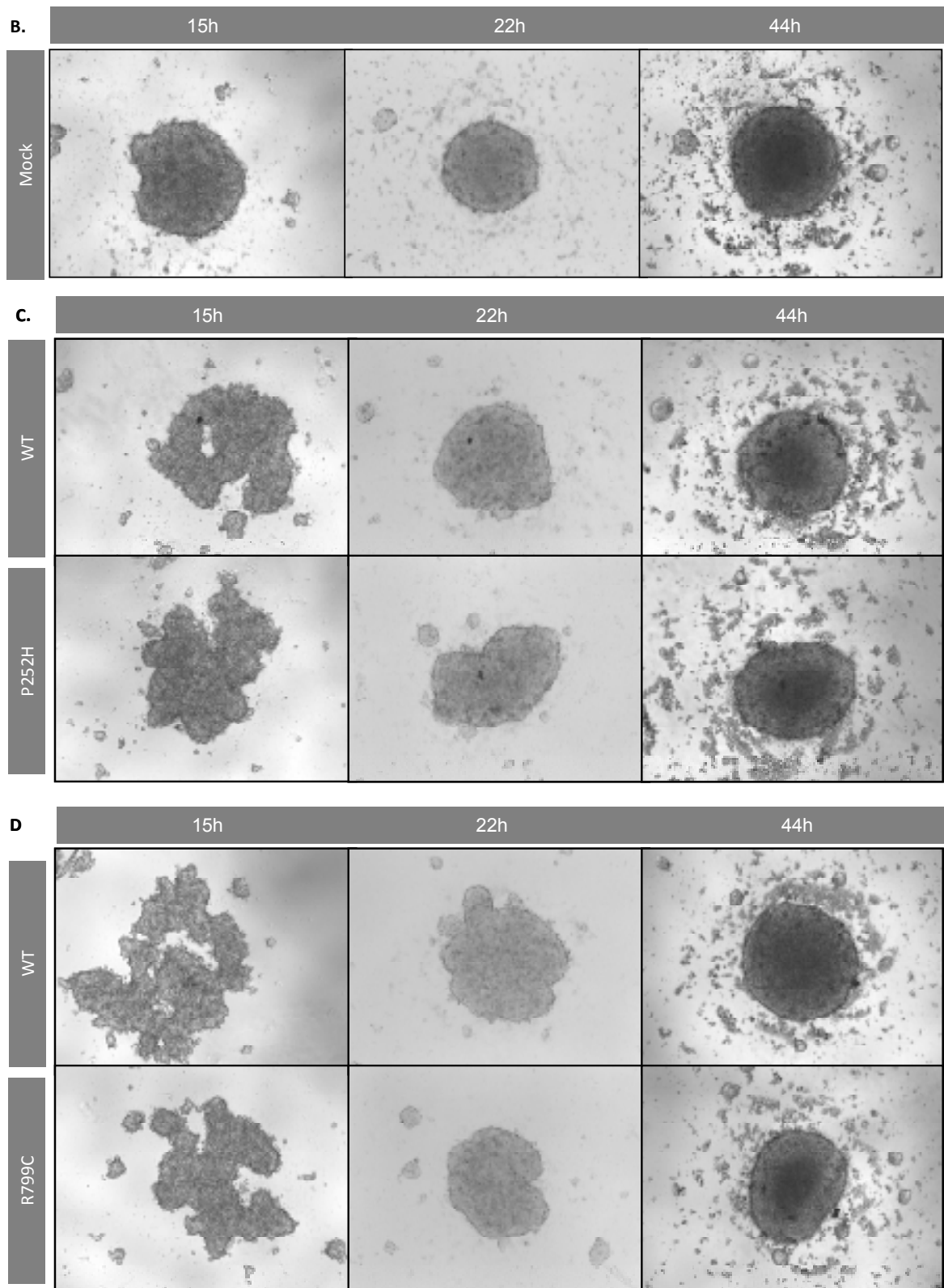


**Figure 23 - Cell aggregation captured at different time points: 15, 22 and 44 hours with an initial cell number of 10000cells per well. (A) CHO and MCF7 cells, (B) Mock cells; comparisons between (C) P252H and WT, (D) R799C and WT.**

This type of aggregation assay has a great disadvantage, because it only provides us qualitative information. To overcome this limitation in future experiments we could perform a “fast” aggregation assay that allows quantification analysis and that is pivotal to evaluate the initial phases of cell aggregation, where we found the biggest difference between Mock and the other stable cell lines.

### **3.4 Signalling of P252H and R799C mutations and of wild-type MLK3 overexpression**

In Figure 24 we present a brief summary of the western blots performed to evaluate the levels of protein expression of some important targets of MLK3 or of other proteins that could also be affected by MLK3. Most of the values presented are tendencies and not definitive conclusions since some of these results need to be repeated to get definitive conclusions. This confirmation in some cases was not possible due to the limitation of the time to present this thesis. However, we decided to include them since some results could be interesting for discussion, even knowing that they need extra confirmation.

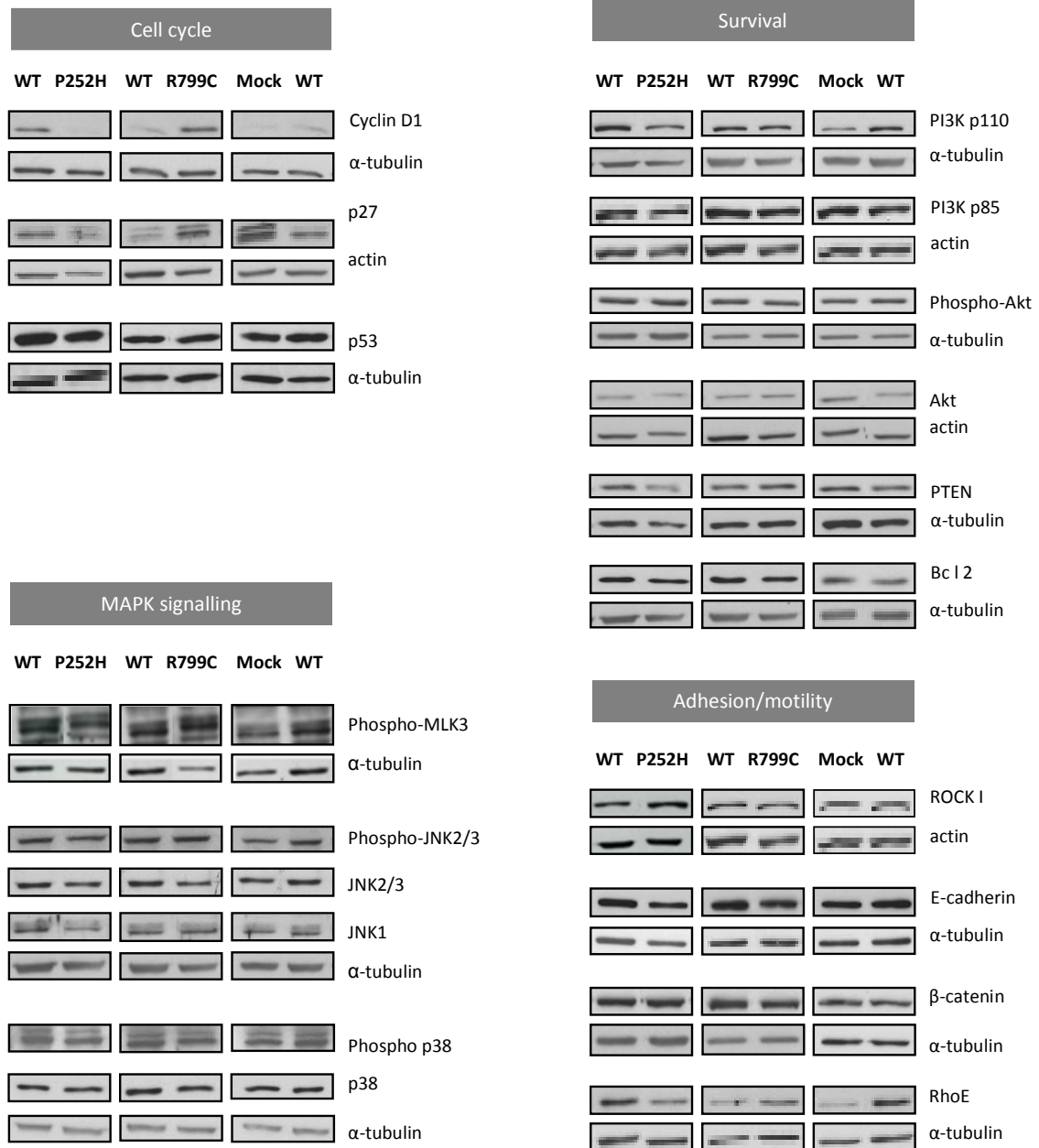


**Figure 24 - Western Blot analysis in HEK293 stable cell lines.**

After performing the western blots, protein expression levels were analysed with Quantity One software and the final results are summarized in Table VII.

**Table VII - Expression levels of the proteins tested by western blot.** An increase or a decrease in protein expression was only considered when there was, at least, a difference, of 1,2 fold comparing to control. Many protein quantifications here presented have an interrogation point (?) because there are some doubts in the final result, which requires new experiments.

Function	Protein	P252H	R799C	WT
Cell cycle	<b>Cyclin D1</b>	↓ 1,7x (p<0,05)	↑ 4x (p<0,05)	↑ 3x
	<b>p27</b>	↓ 1,3x	↑ 2,3x	↓ 1,3x
MAPK signalling	<b>phMLk3</b>	≈	↑ 1,6x	?
	<b>phJNK</b>	↑ 1,7x ?	↑ 1,3x ?	≈ ?
	<b>JNK</b>	↑ 1,2x	≈?	≈ ?
	<b>p53</b>	≈	≈?	↑ 1,5x
	<b>ph p38</b>	↓ 1,5x ?	≈?	↑ 2,2x ?
	<b>p38</b>	?	?	↓ 1,5x
Survival	<b>PI3Kp110α</b>	↓ 1,3 x ?	↑ 1,2 x	?
	<b>PI3Kp85α</b>	≈ ?	≈ ?	≈
	<b>phAkt</b>	↑ 1,2 x	≈	≈
	<b>Akt</b>	≈ ?	↑ 1,4 x ?	≈ ?
	<b>PTEN</b>	≈ ?	≈ ?	≈ ?
	<b>Bcl2</b>	↓ ≈ ?	≈ ?	≈ ?
Adhesion/ migration	<b>ROCK I</b>	↑ 1,5 x (p<0,05)	≈ ?	≈ ?
	<b>E-cadherin</b>	↓ 1,3 x	↓ 1,6 x	≈?
	<b>β-catenin</b>	≈	≈ ?	≈ ?
	<b>RhoE</b>	↓ 1,6 x ?	↑ 1,3 x ?	↑ 2,7 x ?

A detailed description of some important quantifications will be reported below, as well as its association with the cellular effects already presented, whenever possible.

### 3.4.1 MLK3 mutations induces invasion by E-cadherin regulation

The disturbance of intercellular adhesion is one key event for the release of invasive cells from carcinomas [96]. This may be accomplished by loss of function or expression of the epithelial cell-adhesion molecule E-cadherin, which is observed during tumour progression of most carcinomas, and through the activity of cell motility factors [97]. The observed decrease in E-cadherin expression in HEK293 cells expressing R799C and P252H mutations (Table VIII) corroborates the previous data from our group that show the ability of both MLK3 mutant tumours to invade the surrounding adipose tissue and muscle, in contrast to the positive control H-RasV12-expressing tumours [11]. However, based on a higher decrease in E-cadherin expression in R799C we still cannot explain why P252H mutation showed the most aggressive behaviour, with invasion of backbone, bone marrow and spinal cord, but of course, we must take into account many other important factors. This effect may be due to differences in cell migration, since P252H shows an increased migration potential in comparison to R799C.

**Table VIII - Information about E-cadherin protein expression levels of MLK3 mutants.**

Protein	P252H	R799C
E-cadherin	↓ 1,3x	↓ 1,6x

### 3.4.2 P252H and R799C mutations do not share similar patterns of p27 and cyclin D1 expression

P27 is a cyclin-dependent kinase inhibitor (CDKI) that belongs to the Cip/Kip family, which also includes p21. Quiescent cells present an increase in p27 protein levels, which is rapidly inverted after stimulation with mitogens (review in [98]). The most well-known function of p27 is its binding to cyclin E/CDK2 complex and consequently inhibition of this kinase activity. However, p27 role is not only restricted to cell cycle regulation. In fact, in normal human colonic mucosa or during colorectal carcinogenesis, the relation between p27 expression levels and cell proliferation was excluded [99]. In our study the alterations in p27 expression levels also do not seem to be associated to cell proliferation, whereas all stable cell lines have similar proliferation rates.

In an interesting study authors showed that down-regulation or loss of p27 was found to occur significantly associated to metachronous metastases, and not to primary colorectal adenocarcinomas, indicating a role for p27 in the development of metastasis and consequently on the late stages of progression of colorectal cancer [100]. This reduction of p27 levels was also found in advanced gastric cancer. Advanced gastric cancer presented a p27 reduction of about 41% against 15,6% in early gastric cancer [101]. In our study, cells expressing P252H mutation presented low levels of p27 when compared to cells expressing wild-type MLK3 (Table IX). This is an interesting result since it may explain the worse behaviour of this mutant and its ability to invade the bone marrow. As it is established that low p27 expression correlates with worse prognosis, some clinical trials are already taking into account an evaluation of p27 expression, through immunohistochemistry, in advanced solid tumours, upon treatment with specific drugs. (ClinicalTrials.gov NCT00388089 and NCT00389805). Strategies to increase p27 levels will probably bring good results to cancer therapy.

**Table IX - Summary of results from proliferation assay and from both p27 and cyclin D1 protein expression levels of MLK3 mutants.**

	P252H	R799C
<b>Proliferation assay</b>	≈	≈
<b>Cyclin D1</b>	↓ 1,7x (p<0,05)	↑4x (p<0,05)
<b>p27</b>	↓ 1,3x	↑2,25x

However, a total distinct cellular phenotype is expected when p27 shows an increased level of expression as verified for the MLK3 mutant R799C. In fact, it was suggested that high levels of p27 expression may suppress metastasis in colon cancer cells [102]. P27 overexpression in HT29 colorectal cancer cell line leads to partial growth inhibition when compared to those of control vector clones [102]. Authors also observed an increase in sodium butyrate induced-differentiation by counting cells positive for the enzyme intestinal alkaline phosphatase [99], which is a well-known marker of differentiation in HT29 cells and other colon cancer cell lines [102, 103]. In order to determine if that p27 overexpression was affecting other cell cycle related proteins the authors investigated other cyclins and CDKs [102]. As expected the kinase activity of E/CDK2 complex was lower, but interestingly among other proteins, only cyclin D1



expression was altered, from about 1.9 fold to 3.6-fold increase in its expression levels, what may suggest the existence of a feedback loop between p27 and cyclin D1 [102].

Interestingly, we also found a tight correlation of p27 and cyclin D1 in our MLK3 mutants. In one hand, cells expressing the R799C MLK3 mutation display high levels of p27 and cyclin D1 (Table IX). This positive correlation was already identified in some human breast cancer cells and adenomatous polyps [99, 104]. On the other hand, P252H MLK3 mutant displays low levels of p27 and cyclin D1 (Table IX). Interestingly, when an antisense cyclin D1 cDNA construct was overexpressed in the human colon cancer cell line SW48OE8 it led to a decreased expression of p27 [105].

Furthermore, it was already established a correlation between p27 expression and tumour grade; i.e., tumours high p27 expression are well or moderately differentiated carcinomas, whereas tumours with lower p27 expression are poorly differentiated carcinomas [99]. Together these data bring new insights that both MLK3 mutations studied (P252H and R799C) followed different pathways towards cancer. R799C mutation may be related to differentiation, while P252H may confer other important properties such as promotion of cell migration.

There are some other evidences that may corroborate these findings (results not published). Although we did not evaluated the protein levels of BMP-6, our group showed that *BMP-6* gene seems to be 1,7 fold up-regulated in cells expressing R799C mutation when compared to cells expressing P252H that show a decreased of 1,4 fold down-regulation of *BPM-6*. *BPM-6* is known to positively regulate the differentiation of primary skin keratinocytes grown in culture and among other BMP is a potent regulator of osteoblast differentiation [106, 107].

Of course, to validate our hypothesis, that the different MLK3 mutants regulate colon differentiation in a distinct manner we need to evaluate the expression of markers, such as vimentin in HEK293 cells pellet embedded in paraffin, through the search of epithelial markers, such as CD10, BerEP4, cytokeratin (CK) 7, CK-Cam5.2., CK18 as already performed by Nalvarte and colleagues [108].

### 3.4.3 P252H mutation induces cell migration

Curiously MLK3 inhibition, through siRNA, decreases ROCK expression levels, meaning that these two proteins are somehow related (Figure 25).

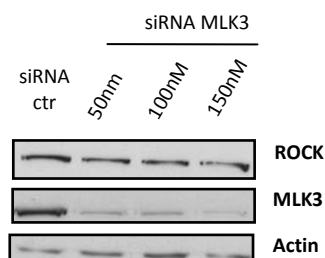


**Figure 25 - Western blot analysis of MLK3 and ROCK expression, upon MLK3 inhibition with siRNA, in HEK293 Mock stable cell line**

The Rho-associated coiled-coil forming kinase, ROCK, is one of two major effectors for Rho. This serine/threonine kinase phosphorylates a variety of substrates: myosin-binding subunit of myosin phosphatase and myosin light chain, enhancing actomyosin contractility, and LIM-kinase that inactivates cofilin leading to filaments stabilization (review in [8]). Therefore ROCK has a crucial role in cell migration.

Most reported data show that Rho/ROCK pathway-related proteins are related to cancer progression. In bladder cancer, for example, higher levels of RhoA, RhoC, ROCK-I and ROCK-II were found in tumour tissue with positive lymph nodes metastases when compared to non-tumoral tissue and primary tumours without lymph nodes metastasis [109], demonstrating that their level of expression was associated with poor differentiation, muscle invasion, lymph node metastasis and shortened survival. In breast cancer, Rho C overexpression was reported to be associated to an aggressive form of cancer and seems to have an important role on the production of angiogenic factors [110]. The data reported in these two tumour models, bladder and breast, plus our own (previously discussed) it seems that poor differentiated and aggressive carcinomas shows an increase in ROCK levels and a decrease in p27 protein levels.

In fact, we can suggest that MLK3 P252H mutation induces poor differentiated tumours, which is associated with its p27 and ROCK expression levels (Table X) and is reflected in a tumour with higher ability to migrate, as verified previously, and produces metastasis. But this hypothesis needs to be proven.

**Table X - Summary of results from migration assay and from both ROCK and RhoE protein expression levels of cells expressing P252H mutation.**

	<b>P252H</b>
<b>Migrated distance</b>	↑1,3x
<b>ROCK</b>	↑1,5x (p<0,05)
<b>RhoE</b>	↓1,6x ?

Besides the levels of ROCK I, we also determined the levels of RhoE for both MLK3 mutants. RhoE interacts with ROCK I and inhibits ROCK I-induced actin stress fiber formation and myosin phosphatase phosphorylation. Thus, in MLK3 P252H mutation the results of both ROCK I and RhoE expressions are in agreement with the inhibitory effect of RhoE on ROCK (Table X) expression. Actually, we verified that MLK3 P252H mutant induces low levels of RhoE accompanied by a significant increase in ROCK expression. To verify if, besides inducing ROCK expression levels, P252H mutation also induces Rho activity, it will be interesting to perform Rhotekin pull down assays (Cell Biolabs).

#### **3.4.4 R799C mutation decreases cell migration**

As mentioned in the introduction chapter, MLK3 limits activated Gαq signalling to Rho by binding to p63RhoGEF [66]. This interaction is induced by MLK3 phosphorylation on residues Thr<sup>277</sup> and Ser<sup>281</sup> and is inhibited by effects of the JNK pathway on MLK3, through a feed back loop [32].

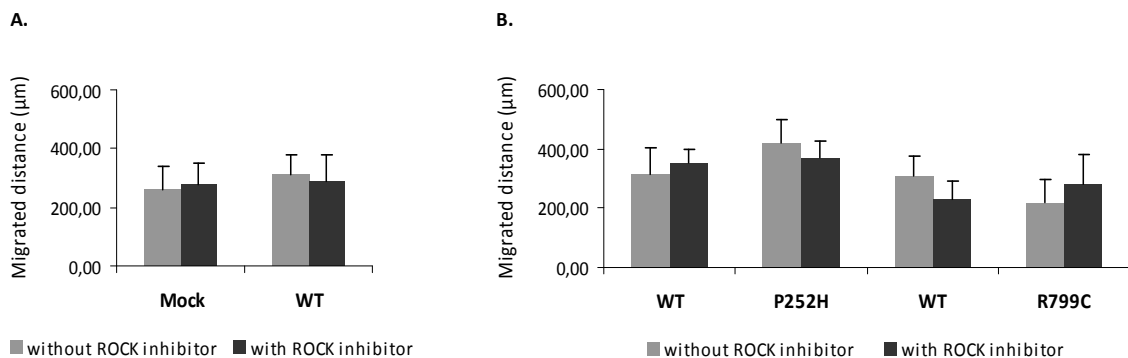
In cells expressing R799C MLK3 mutation, MLK3 phosphorylation is increased, what induces the downstream activation of JNK, as we may observe through an increase in phosphorylated JNK (Table XI). Although JNK may be affecting MLK3 levels in a feedback loop, its activation (only 1,3 fold increase) might not be enough to provoke the complete dissociation between MLK3 and p63RhoGEF and Rho may still activated. This explanation may justify the slight decrease in the distance migrated by these cells, when comparing to the control. However, phospho-JNK antibody has to be tested again.

**Table XI - Summary of results from migration assay and from phospho-MLK3 and phospho-JNK protein expression levels of cells expressing R799C mutation.**

	R799C
Migrated distance	↓1,3x
Phospho MLK3	↑1,6x
Phospho JNK	↑1,3x ?

### 3.4.5 Effects of ROCK inhibitor

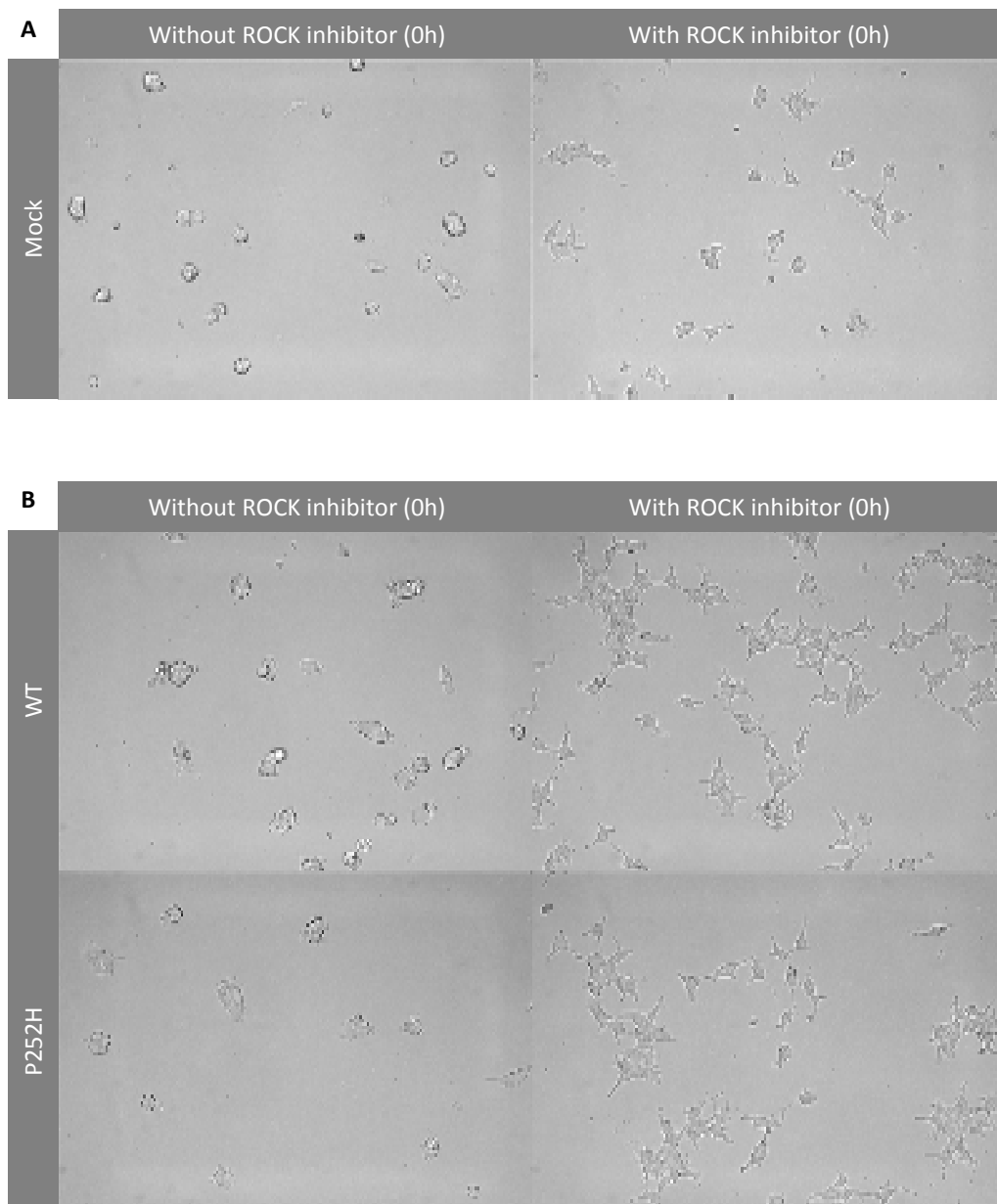
In order to verify if the migratory behaviour of cells was dependent on ROCK expression we studied the effect of ROCK inhibition in the MLK3 P252H mutation. Cells expressing P252H MLK3 mutant showed an increase in cell migration and presented the highest levels of ROCK. In contrast to what we expected, the distance migrated was not significantly affected by the ROCK pharmacological inhibitor Y27632 (Figure 26). But this data has a clear technical limitation since we should have performed protein extract to confirm, by western blot, that ROCK was in fact being inhibited. It had also been interesting to evaluate MLK3 levels, upon ROCK inhibition, to better understand the relation between these two proteins.



**Figure 26 - Migrated distance by the different HEK293 stable cell lines either with or without treatment with ROCK inhibitor - Y27632.** Comparison between (A) Mock and WT cells; (B) WT and MLK3 mutants cells.

However, if we presume the the ROCK pharmacological inhibitor Y27632 was effective and the distance migrated was not significantly altered, we wonder what was being

affected by ROCK inhibition. To study the effect of ROCK inhibition on cell morphology we added Y27632 to cells at low confluence. Almost immediately after ROCK inhibitor was added we observed a complete alteration of the cells phenotype (Figure 27). This effect of ROCK inhibition on cell morphology was already described in the literature and showed to dramatically increase cell spreading and the number of lamellipodia around the perimeter of the cell [111, 112].



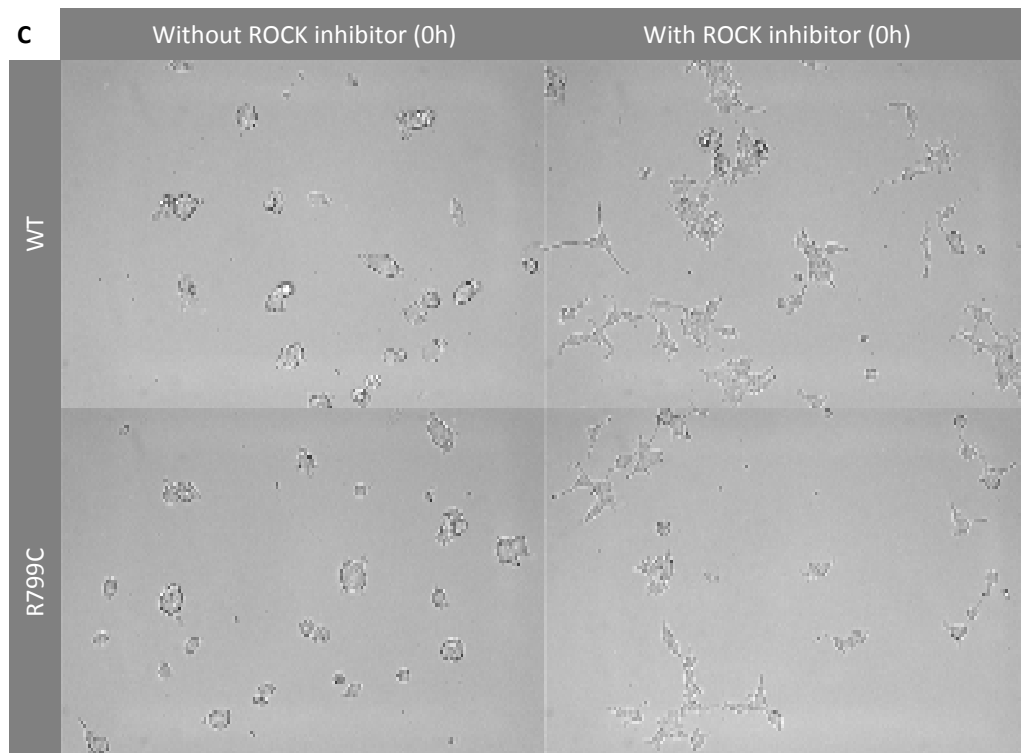


**Figure 27 - Effect of ROCK inhibitor - Y-27632 on cells morphology.** (A) Mock cells. Comparison between (B) WT and R799C, (C) WT and P252H.

In summary and unlikely to what we hypothesized initially, ROCK inhibition did not affect the overall process of cell migration. This is not surprising since it is well known that migration is a very complex process resulting from the combination of different actions: myosin-actin contractability, G protein signaling, microtubule dynamics and the turnover of focal adhesions, thus, ROCK inhibition could only partially affected the overall process [113]

### 3.4.6 MLK3 mutations and WNT signalling pathway

WNT signalling pathway has been highly conserved during evolution. It is involved in embryonic development of all species, in the regeneration of tissues in adult organisms and in many other functions. In many cancers, namely in colorectal cancer components of this pathway presents either mutations or altered expression (review in [114])

Unpublished results from our group show that cells expressing P252H mutations have an upregulation of *FZD10* (1,3 fold), while in cells expressing the MLK3 R799C mutation show a 1,2 fold down-regulation of *FZD10* . High-levels of *FZD10* mRNA expression occurs in different human cancer cell lines and seems to be related to the

activation of a non-canonical WNT/ $\beta$ -catenin signalling [115]. Cancer cells immunopositive for FZD10 showed significantly less nuclear accumulation of  $\beta$ -catenin, compared to FZD10-immunonegative cancer cells, what suggests that FZD10 has an important role in the switch of the canonical WNT signal transduction to a non-canonical WNT pathway [116]. Furthermore, we also demonstrated that cells expressing MLK3 P252H mutation presents a decrease in *LEF1* mRNA levels (data not yet published by the group). Down-regulation of LEF1 also inhibits WNT canonical pathway, suggesting again an induction of the non-canonical pathway, by cells expressing P252H mutation [117]. Interestingly, it was also reported that whenever the non-canonical WNT pathway is activated there is ROCK activation followed by reduced levels of p27 protein [118]. In our experimental work, we verified the same tendency; cells expressing P252H MLK3 mutation present higher levels of ROCK protein and lower levels of p27 protein, suggesting that this MLK3 mutation induces a switch from a canonical WNT pathway to an activation of a non-canonical WNT pathway.

In contrast, cells expressing R799C mutation present high levels of cyclin D1, what may suggest an activation of the WNT canonical pathway. However, it is important to confirm, by immunohistochemistry, that  $\beta$ -catenin expression is at the nucleus.

Although a lot of questions remain to be answered, we can already summarize some important data by the following representation of the WNT pathway. P252H mutation induces activation of the non-canonical WNT pathway, while R799C mutation induces WNT canonical pathway activation (Figure 28).

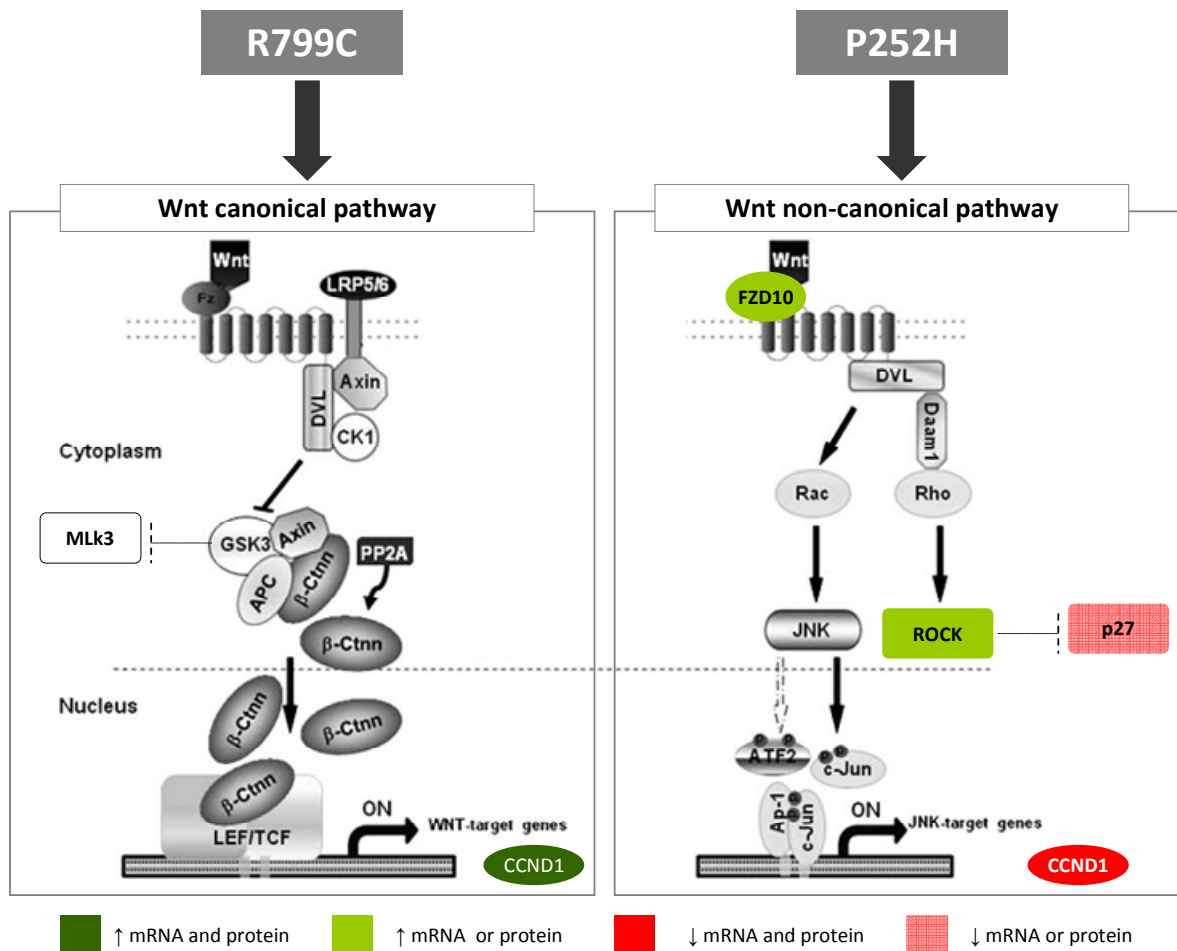


**Figure 28 - Schematic representation of WNT canonical and non-canonical pathways in which mutant forms of MLK3 may exert an effect (adapted from Saadeddin 09).** For p27 and ROCK we have only information regarding their protein expression levels.

### 3.4.7 Wild-type MLK3 overexpression

In HEK293 cells expressing wild-type MLK3 there is a tendency to an increased expression p53 (Table XII). Mutations of *p53* occur in about 50% of all human tumours [119]. However, an increase of expression of wild-type p53 is associated to some kind of protection in response to various types of stress, such damages in DNA or mitotic spindle (reviewed in [119]). For instance, there is an increase in p53 after exposure of the skin to UV light, allowing DNA repair before replication that would make DNA damage permanent [120].



**Table XII - Summary of results from cell viability assay and from both p53 and phospho-p38 protein expression levels of cells overexpressing wild-type MLK3.**

	WT
<b>Cell viability</b>	↓1,2x
<b>p53</b>	↑1,5x
<b>Phospho -p38</b>	↑2,2x ?

MLK3 overexpression seems to induce a decrease in cell viability, when comparing to Mock cells. This effect is very well described, mainly in neurons and in our particular case may be related to the observed increase of phospho-38 expression (Table XII). As p38 signalling is involve in response to stress stimulus, an up-regulation of this pathway could eventually lead to decrease in cell survival, upon a stimulus of FBS1%. This effect is probably related to an induction of apoptosis, however this suggestion requires confirmation. P38 indeed induces apoptosis, by regulating some proteins of Bcl-2 family. For instance it regulates the translocation of Bax, a pro-apoptotic protein, from cytosol to mitochondria, and also phosphorylates Bim, another pro-apoptotic protein, upon a variety of apoptic stimuli [121, 122].

Chapter 5

Concluding remarks and future perspectives

This experimental work brings a new insight on the functionality of the MLK3 mutations P252H and R799C, but unfortunately it is not possible to take much defined conclusions yet. However, this work presents results that promote us to perform further research on the topic but now in a more focus manner. Due to the time constraints, we were not able to perform some experiments at least twice and to initiate other interesting ones that might corroborate our results. Thus, further studies are required in order to validate the results here presented. Some suggestions were already proposed in the previous chapter.

In the first part we intended to prove the functional value of P252H mutation in a colorectal cancer context. Our results prove it, as observed by the down-regulation of some MLK3 targets, upon inhibition of P252H allele of RKO cell line.

Secondly we established HEK 293 stable cell lines, expressing the wild-type MLK3 or MLK3 mutants. We wanted to verify a genotype-phenotype correlation that means that depending on the localization of MLK3 mutation the cellular effects and signalling pathways were different. The results suggested that MLK3 mutants behave differentially, inducing the activation of different signalling pathways. Both mutations are able to induce invasion, but only P252H may induce cell migration. This effect of P252H may be eventually more associated to an increased ability to induce a metastatic phenotype. R799C mutation seems to induce differentiation. These differences between both mutations may be explained by their possible differential activation of WNT signalling pathway. *MLK3* mutations alter colorectal cancer developmental pathways and by this may also have a crucial role in tumourigenesis.

Chapter 6

References

1. Gallo, K.A., et al., *Identification and characterization of SPRK, a novel src-homology 3 domain-containing proline-rich kinase with serine/threonine kinase activity*. J. Biol. Chem., 1994. **269**(21): p. 15092-15100.
2. Ing, Y., et al., *MLK-3: identification of a widely-expressed protein kinase bearing an SH3 domain and a leucine zipper-basic region domain*. Oncogene, 1994. **9**(6): p. 1745-1750.
3. Du, Y., et al., *Cdc42 induces activation loop phosphorylation and membrane targeting of mixed lineage kinase 3*. J. Biol. Chem., 2005. **280**(52): p. 42984-42993.
4. Swenson, K.I., K.E. Winkler, and A.R. Means, *A new identity for MLK3 as an NIMA-related, cell cycle-regulated kinase that is localized near centrosomes and influences microtubule Organization*. Mol. Biol. Cell, 2003. **14**(1): p. 156-172.
5. Teramoto, H., et al., *Signaling from the small GTP-binding proteins Rac1 and Cdc42 to the c-Jun N-terminal kinase/stress-activated protein kinase pathway. A role for mixed lineage kinase 3/protein-tyrosine kinase 1, a novel member of the mixed lineage kinase family*. J. Biol. Chem., 1996. **271**(44): p. 27225-27228.
6. Dorow, D.S., et al., *Complete nucleotide sequence, expression, and chromosomal localisation of human mixed-lineage kinase 2* Eur. J. Biochem., 1995. **234**(2): p. 492-500.
7. Tibbles, L.A., et al., *MLK-3 activates the SAPK/JNK and p38/RK pathways via SEK1 and MKK3/6*. EMBO J., 1996. **15**(24): p. 7026-7035.
8. Narumiya, S., M. Tanji, and T. Ishizaki, *Rho signaling, ROCK and mDia1, in transformation, metastasis and invasion*. Cancer Metastasis Rev., 2009. **28**((1-2)): p. 65-76.
9. Gallo, K.A. and G.L. Johnson, *Mixed-lineage kinase control of JNK and p38 MAPK pathways*. Nat. Rev. Mol. Cell Biol., 2002. **3**(9): p. 663-672.
10. Zhang, H. and K.A. Gallo, *Autoinhibition of mixed lineage kinase 3 through its Src homology 3 domain*. J. Biol. Chem., 2001. **276**(7): p. 45598-45603.
11. Velho, S., et al., *Mixed lineage kinase 3 gene mutations in mismatch repair deficient gastrointestinal tumours*. Hum. Mol. Genetic., 2010. **19**(4): p. 697-706.
12. Sachetto-Martins, G., L.O. Franco, and D.E.d. Oliveira, *Plant glycine-rich proteins: a family or just proteins with a common motif?* Biochim. Biophys. Acta, 2000. **1492**(1): p. 1-14.
13. Bocca, S.N., et al., *Survey of glycine-rich proteins (GRPs) in the Eucalyptus expressed sequence tag database (ForEST)*. Genet. Mol. Biol., 2005. **28**(3): p. 608-624.
14. Li, S.S., *Specificity and versatility of SH3 and other proline-recognition domains: structural basis and implications for cellular signal transduction*. Biochem. J., 2005. **390**(Pt3): p. 641-653.

15. Huse, M. and J. Kuriyan, *The conformational plasticity of protein kinases*. Cell, 2002. **109**(3): p. 275-282.
16. Bossemeyer, D., *Protein kinases - structure and function* FEBS Lett., 1995. **369**(1): p. 57-61
17. Leung, I.W.-L. and N. Lassam, *The kinase activation loop is the key to mixed lineage kinase-3 activation via both autophosphorylation and hematopoietic progenitor kinase 1 phosphorylation*. J. Biol. Chem., 2001. **276**(3): p. 1961-1967.
18. Kamps, M.P., S.S. Taylor, and B.M. Sefton, *Direct evidence that oncogenic tyrosine kinases and cyclic AMP-dependent protein kinase have homologous ATP-binding sites*. Nature, 1984. **310**(5978): p. 589-592.
19. Burbelo, P.D., D. Drechsel, and A. Hall, *A conserved binding motif defines numerous candidate target proteins for both Cdc42 and Rac GTPases*. J. Biol. Chem., 1995. **270**(49): p. 29071-29074.
20. Vacratsis, P.O., et al., *Identification of in vivo phosphorylation sites of MLK3 by mass spectrometry and phosphopeptide mapping*. Biochem., 2002. **41**(17): p. 5613-5624.
21. Lew, J., *MAP kinases and CDKs: kinetic basis for catalytic activation*. Biochemistry, 2003. **42**(4).
22. Leung, I.W.-L. and N. Lassam, *Dimerization via tandem leucine zippers is essential for the activation of the mitogen-activated protein kinase kinase kinase, MLK-3*. J. Biol. Chem., 1998. **273**(49): p. 32408-32415.
23. Vacratsis, P.O. and K.A. Gallo, *Zipper-mediated oligomerization of the mixed lineage kinase SPRK/MLK-3 is not required for its activation by the GTPase Cdc42 but is necessary for its activation of the JNK pathway. Monomeric SPRK L410P does not catalyze the activating phosphorylation of Thr258 of murine mitogen-activated protein kinase 4*. J. Biol. Chem., 2000. **275**(36): p. 27893-27900.
24. Hall, F.L., et al., *Characterization of the cytoplasmic proline-directed protein kinase in proliferative cells and tissues as a heterodimer comprised of p34<sup>cdc2</sup> and p58<sup>cyclin A</sup>*. J. Biol. Chem., 1991. **266**(26): p. 17430-17440.
25. Mishra, R., et al., *Glycogen synthase kinase-3 $\beta$  induces neuronal cell death via direct phosphorylation of mixed lineage kinase 3*. J. Biol. Chem., 2007. **282**(42): p. 30393-30405.
26. Rilling, H.C., et al., *Prenylated proteins: the structure of the isoprenoid group*. Science, 1990. **247**(4940): p. 318-320.
27. Chadee, D.N., T. Yuasa, and J.M. Kyriakis, *Direct activation of mitogen-activated protein kinase kinase kinase MEKK1 by the Ste20p homologue GCK and the adapter protein TRAF2*. Mol. Cell. Biol., 2002. **22**(3): p. 737-749.
28. Kiefer, F., et al., *HPK1, a hematopoietic protein kinase activating the SAPK/JNK pathway*. EMBO J., 1996. **15**(24): p. 7013-7025.

29. Sathyanarayana, P., et al., *Activation of the Drosophila MLK by ceramide reveals TNF- $\alpha$  and ceramide as agonists of mammalian MLK3*. Mol. Cell, 2002. **10**(6): p. 1527-1533.
30. Brancho, D., et al., *Role of MLK3 in the regulation of mitogen-activated protein kinase signaling cascades*. Mol. Cell. Biol., 2005 **25**(9): p. 3670-3681.
31. Barthwal, M.K., et al., *Negative regulation of mixed lineage kinase 3 by protein kinase B/AKT leads to cell survival*. J. Biol. Chem., 2003. **278**(6): p. 3897-3902.
32. Schachter, K.A., et al., *Dynamic positive feedback phosphorylation of mixed lineage kinase 3 by JNK reversibly regulates its distribution to triton-soluble domains*. J. Biol. Chem., 2006. **281**(28): p. 19134-19144.
33. Zhang, H., et al., *Hsp90/p<sup>50cdc37</sup> Is Required for Mixed-lineage Kinase (MLK) 3 Signaling*. J. Biol. Chem., 2004. **279**(19): p. 19457-19463.
34. Zhang, Y. and C. Dong, *Regulatory mechanisms of mitogen-activated kinase signaling*. Cell. Mol. Life Sci. , 2007. **64** (21): p. 2771 – 2789.
35. Craig, E.A., et al., *MAP3Ks as central regulators of cell fate during development*. Dev. Dyn., 2008. **237**: p. 3102–3114
36. Hartkamp, J., J. Troppmair, and U.R. Rapp, *The JNK/SAPK activator mixed lineage kinase 3 (MLK3) transforms NIH 3T3 cells in a MEK-dependent fashion*. Cancer Res., 1999. **59**(9): p. 2195-2202.
37. Chadee, D.N. and J.M. Kyriakis, *MLK3 is required for mitogen activation of B-Raf, ERK and cell proliferation*. Nat. Cell Biol., 2004. **6**(8): p. 770-776.
38. Kyriakis, J.M., *Protein Kinase Functions*, J.R. Woodgett, Editor. 2000, Oxford University Press: Oxford. p. 40-156.
39. Shen, Y.H., et al., *Cross-talk between JNK/SAPK and ERK/MAPK Pathways: sustained activation of JNK blocks ERK activation by mitogenic factors*. J. Biol. Chem., 2003. **278**(29): p. 26715-26721.
40. Chadee, D.N., et al., *Mixed-lineage kinase 3 regulates B-Raf through maintenance of the B-Raf/Raf-1 complex and inhibition by the NF2 tumor suppressor protein*. Proc. Natl. Acad. Sci. U.S.A., 2006 **103**(12): p. 4463-4468.
41. Wan, P.T.C., et al., *Mechanism of activation of the RAF-ERK signaling pathway by oncogenic mutations of B-RAF*. Cell, 2004. **116**(6): p. 855-867.
42. Chadee, D.N. and J.M. Kyriakis, *A novel role for mixed lineage kinase 3 (MLK3) in B-Raf activation and cell proliferation*. Cell Cycle, 2004. **3**(10): p. e73-e75.
43. Lu, K.P., S.D. Hanes, and T. Hunter, *A human peptidyl-prolyl isomerase essential for regulation of mitosis*. Nature, 1996. **380**(6574): p. 544-7.
44. Lu, K.P. and A. R.Means, *Expression of the noncatalytic domain of the NIMA kinase causes a G2 arrest in Aspergillus nidulans*. EMBO J., 1994. **13**(9): p. 2103 - 2113.

45. Kanthasamy, A., et al., *Novel cell death signaling pathways in neurotoxicity models of dopaminergic degeneration: Relevance to oxidative stress and neuroinflammation in Parkinson's disease*. Neurotoxicology, 2009.
46. Mota, M., et al., *Evidence for a role of mixed lineage kinases in neuronal apoptosis*. J. Neurosci., 2001. **21**(14): p. 4949-4957.
47. Xu, Y., et al., *Different protection of K252a and N-acetyl-L-cysteine against amyloid- $\beta$  peptide-induced cortical neuron apoptosis involving inhibition of MLK3-MKK7-JNK3 signal cascades*. J. Neurosci. Res., 2009. **87**(4): p. 918-927.
48. Wang, R., et al., *Inhibition of MLK3-MKK4/7-JNK1/2 pathway by Akt1 in exogenous estrogen-induced neuroprotection against transient global cerebral ischemia by a non-genomic mechanism in male rats*. J. Neurochem., 2006. **99**(6): p. 1543-1554.
49. Cha, H., et al., *Phosphorylation of golgin-160 by mixed lineage kinase 3*. J. Cell. Sci. , 2004. **117**(Pt5): p. 751-760.
50. Mukherjee, S., et al., *Fragmentation of the Golgi apparatus: an early apoptotic event independent of the cytoskeleton*. Traffic, 2007. **8**(4): p. 369-378.
51. Figueroa, C., et al., *Akt2 negatively regulates assembly of the POSH-MLK-JNK signaling complex*. J. Biol. Chem., 2003. **278**(48): p. 47922-47927.
52. Hehner, S.P., et al., *Mixed-lineage kinase 3 delivers CD3/CD28-derived signals into the I $\kappa$ B kinase complex*. Mol. Cell. Biol., 2000. **20**(7): p. 2556-2568.
53. Royds, J.A., et al., *Response of tumour cells to hypoxia: role of p53 and NF $\kappa$ B*. Clin. Mol. Pathol., 1998. **51**(2): p. 55-61.
54. Cilloni, D., et al., *The NF-kappaB pathway blockade by the IKK inhibitor PS1145 can overcome imatinib resistance*. Leukemia, 2006. **20**(1): p. 61-67.
55. Cole, E.T., et al., *Mixed lineage kinase 3 negatively regulates IKK activity and enhances etoposide-induced cell death*. Biochim. Biophys. Acta, 2009. **1793**(12): p. 1811-1818.
56. Buchsbaum, R.J., B.A. Connolly, and L.A. Feig, *Interaction of Rac exchange factors Tiam1 and Ras-GRF1 with a scaffold for the p38 mitogen-activated protein kinase cascade*. Mol. Cell. Biol., 2002 **22**(12): p. 4073-4085.
57. Kelkar, N., et al., *Interaction of a mitogen-activated protein kinase signaling module with the neuronal protein JIP3*. Mol. Cell. Biol., 2000. **20**(3): p. 1030-1043.
58. Whitmarsh, A.J., et al., *A mammalian scaffold complex that selectively mediates MAP kinase activation*. Science, 1998. **281**(5383): p. 1671-1674.
59. Yasuda, J., et al., *The JIP group of mitogen-activated protein kinase scaffold proteins*. Mol. Cell. Biol., 1999 **19**(10): p. 7245-7254.
60. Verhey, K.J., et al., *Cargo of kinesin identified as JIP scaffolding proteins and associated signaling molecules*. J. Cell Biol., 2001 **152**(5): p. 959-970.



61. Nagata, K.-i., et al., *The MAP kinase kinase kinase MLK2 co-localizes with activated JNK along microtubules and associates with kinesin superfamily motor KIF3*. EMBO J., 1998. **17**(1): p. 149-158.
62. Setou, M., et al., *Kinesin superfamily motor protein KIF17 and mLin-10 in NMDA receptor-containing vesicle transport*. Science, 2000. **288**(5472): p. 1796-1802.
63. Sathyanarayana, P., et al., *Drosophila mixed lineage kinase/slipper, a missing biochemical link in Drosophila JNK signaling*. Biochim. Biophys. Acta, 2003. **1640**(1): p. 77-84.
64. Stronach, B. and N. Perrimon, *Activation of the JNK pathway during dorsal closure in Drosophila requires the mixed lineage kinase, slipper*. Genes Dev., 2002 **16**(3): p. 377-387.
65. Noselli, S., *JNK signaling and morphogenesis in Drosophila*. Trends Genet., 1998. **14**(1): p. 33-38.
66. Swenson-Fields, K.I., et al., *MLK3 limits activated Gαq signaling to Rho by binding to p63RhoGEF*. Mol. Cell, 2008. **32**(1): p. 43-56.
67. Palazzo, A.F., et al., *mDia mediates Rho-regulated formation and orientation of stable microtubules*. Nat. Cell Biol., 2001. **3**(8): p. 723-729.
68. Lambert, J.M., et al., *Role of MLK3-mediated activation of p70 S6 kinase in Rac1 transformation*. J. Biol. Chem., 2002. **277**(7): p. 4770-4777.
69. Cha, H., et al., *Inhibition of mixed-lineage kinase (MLK) activity during G2-phase disrupts microtubule formation and mitotic progression in HeLa cells*. Cell. Signal., 2006. **18**(1): p. 93-104.
70. DeSouza, C.P.C., et al., *Mitotic histone H3 phosphorylation by the NIMA kinase in Aspergillus nidulans*. Cell, 2000. **102**(3): p. 293-302.
71. Almoguera, C., et al., *Most human carcinomas of the exocrine pancreas contain mutant c-K-ras genes*. Cell, 1988. **53**(4): p. 549-554.
72. Chandana, S.R., et al., *Inhibition of MLK3 decreases proliferation and increases antiproliferative activity of Epidermal Growth Factor Receptor (EGFR) inhibitor in pancreatic cancer cell Lines*. Cancer Growth and Metastasis, 2010. **3**: p. 1-9.
73. Dimou, A.T., K.N. Syrigos, and M.W. Saif, *Novel agents for the treatment of pancreatic adenocarcinoma: any light at the end of the tunnel?* JOP, 2010. **11**(4): p. 324-327.
74. Conley, B.A., et al., *Role of mixed lineage kinase 3 in response of head and neck squamous cancer cell lines to epidermal growth factor receptor (EGFR) inhibition*, in 2009 ASCO Annual Meeting 2009.
75. Chen, J., E. Miller, and K. Gallo, *MLK3 is critical for breast cancer cell migration and promotes a malignant phenotype in mammary epithelial cells*. Oncogene, 2010: p. 1-13.

76. Simpson, K.J., et al., *Identification of genes that regulate epithelial cell migration using an siRNA screening approach*. Nat. Cell Biol., 2008. **10**(9): p. 1027-1038.
77. Rozengurt, E. and J.H. Walsh, *Gastrin, CCK, signaling, and cancer*. Annu. Rev. Physiol., 2001. **63**: p. 49-76.
78. Mishra, P., et al., *Mixed lineage kinase-3/JNK1 axis promotes migration of human gastric cancer cells following gastrin stimulation*. Mol. Endocrinol., 2010. **24**(3 ): p. 598-607.
79. Shibata, W., et al., *c-Jun NH2-terminal kinase 1 is a critical regulator for the development of gastric cancer in mice*. Cancer Res., 2008. **68**(13).
80. Wroblewski, L.E., et al., *Stimulation of MMP-7 (matrilysin) by Helicobacter pylori in human gastric epithelial cells: role in epithelial cell migration*. J. Cell Sci., 2003. **116**(14): p. 3017-3026.
81. Rangasamy, V., et al., *Estrogen suppresses MLK3-mediated apoptosis sensitivity in ER<sup>+</sup> breast cancer cells*. Cancer Res., 2010. **70**(4): p. 1731-1740.
82. Conzen, S.D., *Nuclear receptors and breast cancer*. Mol. Endocrinol., 2008. **22**(10): p. 2215-222.
83. Conn, P.M. and W.F.J. Crowley, *Gonadotropin-releasing hormone and its analogs*. Annu. Rev. Med., 1994. **45**: p. 391-405.
84. Kraus, S., et al., *Gonadotropin-releasing hormone induces apoptosis of prostate cancer cells: role of c-Jun NH2-terminal kinase, protein kinase B, and extracellular signal-regulated kinase pathways*. Cancer Res., 2004. **64**(16): p. 5736-5744.
85. Kim, B.-C., et al., *Genipin-induced apoptosis in hepatoma cells is mediated by reactive oxygen species/c-Jun NH2-terminal kinase-dependent activation of mitochondrial pathway*. Biochem. Pharmacol., 2005. **70** (9): p. 1398-1407.
86. Hong, H.-Y. and B.-C. Kim, *Mixed lineage kinase 3 connects reactive oxygen species to c-Jun NH2-terminal kinase-induced mitochondrial apoptosis in genipin-treated PC3 human prostate cancer cells*. Biochem. Biophys. Res. Commun. , 2007. **362**(2): p. 307-312.
87. Saunders, D.E., et al., *Paclitaxel-induced apoptosis in MCF-7 breast-cancer cells*. Int. J. Cancer, 1997. **70**(2): p. 214-220.
88. Schiff, P.B. and S.B. Horwitz, *Taxol stabilizes microtubules in mouse fibroblast cells*. Proc. Natl. Acad. Sci. U.S.A., 1980. **77**(3): p. 11-24.
89. Lee, L.-F., et al., *Paclitaxel (taxol)-induced gene expression and cell death are both mediated by the activation of c-Jun NH2-terminal kinase (JNK/SAPK)*. J. Biol. Chem., 1998. **273**(43): p. 28253-28260.
90. Garnett, M.J. and R. Marais, *Guilty as charged: B-RAF is a human oncogene*. Cancer Cell, 2004 **6**(4): p. 313-319.
91. Lai, S.-L., A.J. Chien, and R.T. Moon, *Wnt/Fz signaling and the cytoskeleton: potential roles in tumorigenesis*. Cell Res., 2009. **19**(5): p. 532-545.

92. Barltrop, J.A., et al., *5-(3-carboxymethoxyphenyl)-2-(4,5-dimethylthiazolyl)-3-(4-sulfoxyphenyl)tetrazolium, inner salt (MTS) and related analogs of 3-(4,5-dimethylthiazolyl)-2,5-diphenyltetrazolium bromide (MTT) reducing to purple water-soluble formazans as cell-viability indicators*. *Bioorg. Med. Chem. Lett.*, 1991. **1**(11): p. 611-614.
93. Berridge, M.V. and A.S. Tan, *Characterization of the cellular reduction of 3-(4,5-dimethylthiazol-2-yl)-2,5-diphenyltetrazolium bromide (MTT): Subcellular localization, substrate dependence, and involvement of mitochondrial electron transport in MTT reduction* *Arch. Biochem. Biophys.*, 1993. **303**(2): p. 474-482.
94. Yang, H., et al., *Nutrient-sensitive mitochondrial NAD<sup>+</sup> levels dictate cell survival*. *Cell* 2007. **130**(6): p. 1095-1107.
95. Boterberg, T., et al., *Cell Aggregation Assays*, in *Metastasis Research Protocols: Volume II: Analysis of Cell Behavior In Vitro and In Vivo* S.A. Brooks and U. Schumacher, Editors. 2001. p. 33-34.
96. Takeichi, M., *Cadherins in cancer: implications for invasion and metastasis*. *Curr. Opin. Cell Biol.*, 1993. **5**(5): p. 806-811.
97. Behrens, J., *The role of cell adhesion molecules in cancer invasion and metastasis*. *Breast Cancer Res. Treat.*, 1993. **24**(3): p. 157-184.
98. Lloyd, R.V., et al., *p27<sup>kip1</sup>: a multifunctional cyclin-dependent kinase inhibitor with prognostic significance in human cancers*. *Am. J. Pathol.*, 1999. **154**(2): p. 313-323.
99. Ciaparrone, M., et al., *Localization and expression of p27<sup>KIP1</sup> in multistage colorectal carcinogenesis*. *Cancer Res.*, 1998. **58**(1): p. 114-122.
100. Thomas, G.V., et al., *Down-regulation of p27 is associated with development of colorectal adenocarcinoma metastases*. *Am. J. Pathol.*, 1998. **153**(3): p. 681-687.
101. Kim, D.H., et al., *Reduced expression of the cell-cycle inhibitor p27<sup>Kip1</sup> is associated with progression and lymph node metastasis of gastric carcinoma*. *Histopathology* 2000. **36**(3): p. 245-251.
102. Yamamoto, H., et al., *Comparative effects of overexpression of p27<sup>Kip1</sup> and p21<sup>Cip1/Waf1</sup> on growth and differentiation in human colon carcinoma cells*. *Oncogene*, 1999. **18**(1): p. 103-115.
103. Hodin, R.A., et al., *Cellular growth state differentially regulates enterocyte gene expression in butyrate-treated HT-29 cells*. *Cell Growth Differ.*, 1996. **7**(5): p. 647-653.
104. Fredersdorf, S., et al., *High level expression of p27<sup>Kip1</sup> and cyclin D1 in some human breast cancer cells: Inverse correlation between the expression of p27<sup>Kip1</sup> and degree of malignancy in human breast and colorectal cancers*. *Proc. Natl. Acad. Sci. U.S.A.*, 1997. **94**(12): p. 6380-6385.
105. Arber, N., et al., *Antisense to cyclin D1 inhibits the growth and tumorigenicity of human colon cancer cells*. *Cancer Res.*, 1997. **57**(8): p. 1569-1574.

106. Friedman, M.S., M.W. Long, and K.D. Hankerson, *Osteogenic differentiation of human mesenchymal stem cells is regulated by bone morphogenetic protein-6*. J. Cell. Biochem., 2006. **98**(3): p. 538-554.
107. McDonnell, M.A., et al., *Antagonistic effects of TGFbeta1 and BMP-6 on skin keratinocyte differentiation*. Exp. Cell Res., 2001. **263**(2): p. 265-273.
108. Nalvarte, I., et al., *Overexpression of enzymatically active human cytosolic and mitochondrial thioredoxin reductase in HEK-293 cells. Effect on cell growth and differentiation*. J. Biol. Chem., 2004. **279**(52): p. 54510-54517.
109. Kamai, T., et al., *Significant association of Rho/ROCK pathway with invasion and metastasis of bladder cancer*. Clin. Cancer Res., 2003. **9**(7): p. 2632-2641.
110. vanGolen, K.L., et al., *RhoC GTPases overexpression modulates induction of angiogenic factors in breast cells*. Neoplasia, 2000. **2**(5): p. 418-425.
111. Worthylake, R.A. and K. Burridge, *RhoA and ROCK promote migration by limiting membrane protrusions*. J. Biol. Chem., 2003. **278**(15): p. 13578-13584.
112. Worthylake, R.A., et al., *RhoA is required for monocyte tail retraction during transendothelial migration*. J. Cell Biol., 2001. **154**(1): p. 147-160.
113. Horwitz, A.R. and J.T. Parsons, *Cell Migration - Movin' On*. Science, 1999. **286**(5442): p. 1102 - 1103.
114. Klaus, A. and W. Birchmeier, *Wnt signalling and its impact on development and cancer*. Nat. Rev. Cancer, 2008. **8**(5): p. 387-398.
115. Terasaki, H., et al., *Frizzled-10, up-regulated in primary colorectal cancer, is a positive regulator of the Wnt-beta-catenin-TCF signaling pathway*. Int. J. Mol. Med., 2002. **9**(2): p. 107-112.
116. Nagayama, S., et al., *Inverse correlation of the up-regulation of FZD10 expression and the activation of beta-catenin in synchronous colorectal tumours*. Cancer Sci., 2009. **100**(3): p. 405-412.
117. Ishitani, T., et al., *The TAK1-NLK-MAPK-related pathway antagonizes signalling between beta-catenin and transcription factor TCF*. Nature, 1999. **399**(6738): p. 798-802.
118. Croft, D.R. and M.F. Olson, *The Rho GTPase effector ROCK regulates cyclin A, cyclin D1, and p27<sup>Kip1</sup> levels by distinct mechanisms*. Mol. Cell Biol., 2006. **26**(12): p. 4612-4627.
119. Oren, M., *Regulation of the p53 tumor suppressor protein*. J. Biol. Chem., 1999. **274**(51): p. 36031-36034.
120. McNutt, N.S., et al., *Abnormalities of p53 protein expression in cutaneous disorders*. Arch Dermatol, 1994. **130**(2): p. 225-232.
121. Cai, B., et al., *p38 MAP kinase mediates apoptosis through phosphorylation of Bim<sub>EL</sub> at Ser-65*. J. Biol. Chem., 2006. **281**(35): p. 25215-25222.

122. Shou, Y., et al., *p38 mitogen-activated protein kinase regulates Bax translocation in cyanide-induced apoptosis*. J Toxicol Sci, 2003. **75**(1): p. 99-107.

Chapter 7

Appendix

## Appendix I - *MLK3* sequence into pLENTI vector

TCGTAACAACCTCCGCCCCATTGACGCAAATGGGCGGTAGGCGTG TACGGTGGGAGGTCTATATAAG  
CAGAGCTCGTTTAGTGAACCGTCAGATCGCCTGGAGACGCCATCCACGCTGTTTTGACCTCCATAGA  
AGACACCGACTCTAGAGGATCCACTAG TCCAGTGTGGTGAATTGATCCCTCACC ATG

481 **V e c t o r** ATGGAGCCCTTGAAGAGCCTCTTCCTCAAGAGCCCTCTAGGGTCATG  
541 GAATGGCAGTGGCAGCGGGGGTGGTGGGGCGGTGGAGGAGGCCGGCCTGAGGGGTCTCC  
601 AAAGGCAGCGGGTTATGCCAACCCGGTGTGGACAGCCCTGTTGACTACGAGCCAGTGG  
661 GCAGGATGAGCTGGCCCTGAGGAAGGGTGACCGTGTGGAGGTGCTGTCCCGGGACGCAGC  
721 CATCTCAGGAGACGAGGGCTGGTGGCGGGCCAGGTGGGTGGCCAGGTGGGCATCTTCCC  
781 GTCCAACATATGTGTCTCGGGGTGGCGGCCCGCCCCCTGCGAGGTGGCCAGCTTCCAGGA  
841 GCTGCGGCTGGAGGAGGTGATCGGCATTGGAGGCTTTGGCAAGGTGTACAGGGGCAGCTG  
901 GCGAGGTGAGCTGGTGGCTGTGAAGGCAGCTCGCCAGGACCCCGATGAGGACATCAGTGT  
961 GACAGCCGAGAGCGTTCGCCAGGAGGCCCGGCTCTTCGCCATGCTGGCACACCCCAACAT  
1021 CATTGCCCTCAAGGCTGTGTGCCTGGAGGAGCCCAACCTGTGCCTGGTGTGGAGTATGC  
1081 AGCCGGTGGGCCCTCAGCCGAGCTCTGGCCGGGCGGCGGTGCCTCCCCATGTGCTGGT  
1141 CAACTGGGCTGTGCAGATTGCCCGTGGGATGCACTACCTGCACTGCGAGGCCCTGGTGCC  
1201 CGTCATCCACCGTATCTCAAGTCCAACAACATTTTGTGCTGCAGCCCATTGAGAGTGA  
1261 CGACATGGAGCACAAGACCCTGAAGATCACCGACTTTGGCTGGCCGAGAGTGGCACAA  
1321 AACCACACAAATGAGTGCCGCGGGCACCTACGCCTGGATGGCTCCTGAGTATCAAGGC  
1381 CTCCACCTTCTCTAAGGCGAGTGACGTCTGGAGTTTTGGGTGCTGCTGTGGAACTGCT  
1441 GACCGGGGAGGTGCCATACCGTGGCATTGACTGCCTTGTGTGGCCTATGGCGTAGCTGT  
1501 TAACAAGCTCACACTGCCCATCCCATCCACCTGCCCGGAGCCCTTCGCACAGCTTATGGC  
1561 CGACTGCTGGGCGCAGGACCCCAACCGCAGGCCCGACTTCGCCTCCATCCTGCAGCAGTT  
1621 GGAGGCGCTGGAGGCACAGGTCTACGGGAAATGCCGCGGACTCCTTCCATTCCATGCA  
1681 GGAAGGCTGGAAGCGCGAGATCCAGGGTCTCTTCGACGAGCTGCGAGCCAAGGAAAAGGA  
1741 ACTACTGAGCCGCGAGGAGGAGCTGACGCGAGCGGCGCGGAGCAGCGGTACAGGCGGA  
1801 GCAGCTGCGGCGGCGGAGCACCTGCTGGCCCAGTGGGAGCTAGAGGTGTTTCAAGCGCGA  
1861 GCTGACGCTGCTGCTGCAGCAGGTGGACCGCAGCGACCGCACGTGCGCCGCCCGCGCGG  
1921 GACATTCAAGCGCAGCAAGCTCCGGGCGCGGACGGCGGCGAGCGTATCAGCATGCCACT  
1981 CGACTTCAAGCACCGCATCACCGTGCAGGCCTCACCCGGCCTTGACCGGAGGAGAAACGT  
2041 CTTCGAGGTCGGGCTGGGGATTGCCCCACCTTTCCCGGTTCCGAGCCATCCAGTTGGA  
2101 GCCTGCAGAGCCAGGCCAGGCATGGGGCCGCCAGTCCCCCGACGCTCTGGAGGACTCAAG  
2161 CAATGGAGAGCGGCGAGCATGCTGGGCTTGGGTCCCAGTTCGCCCAAGCCTGGGGAAGC  
2221 CCAGAATGGGAGGAGAAGGTCCCGCATGGACGAAGCCACATGGTACCTGGATTGAGATGA  
2281 CTCATCCCCCTTAGGATCTCCTTCCACACCCCCAGCACTCAATGGTAACCCCCCGCGGCC  
2341 TAGCCTGGAGCCGAGGAGCCCAAGAGCCTGTCCCCGAGAGCGCGGTAGCAGCTCTGG  
2401 GACGCCCAAGCTGATCCAGCGGGCGCTGCTGCGCGGCACCGCCCTGCTCGCCTCGCTGGG  
2461 CCTTGGCCGCGACCTGCAGCCGCCGGGAGGCCAGGACGCGAGCGCGGGGAGTCCCCGAC  
2521 AACACCCCCACGCCAACGCCCGCGCCCTGCCCGACCGAGCCGCCCCCTTCCCCGCTCAT  
2581 CTGCTTCTCGTCAAGACGCCCGACTCCCCGCCACTCCTGCACCCCTGTTGCTGGACCT

2641 GGGTATCCCTGTGGGCCAGCGGTCAGCCAAGAGCCCCGACGTGAGGAGGAGCCCCGCGG  
 2701 AGGCACTGTCTACCCCCACCGGG **GACATCACGCTCTGCTCCTG** GCACCCCAGGCACCCC  
 2761 ACGTTCAACCACCCTGGGCCTCATCAGCCGACCTCGGCCCTCGCCCCTTCGCAGCCGCAT  
 2821 TGATCCCTGGAGCTTTGTGTCAGCTGGGCCACGGCCTTCTCCCCTGCCATCACCACAGCC  
 2881 TGCACCCCGCCGAGCACCCCTGGACCTTGTTCCGGACTCAGACCCCTTCTGGGACTCCCC  
 2941 ACCTGCCAACCCCTTCCAGGGGGGCCCCCAGGACTGCAGGGCACAGACCAAAGACATGGG  
 3001 TGCCCAGGCCCGTGGGTGCCGGAAGCGGGGCCTGA **V e c t o r**



AAGGGC TCGAGTCTAGAGGGCCC GCGGTTCGAAGGTAAGCCTATCCCTAACCCCTCCTCGGTCTC  
 GATTCTACGCGTACCGGTTAGTAATGAGTTTGA TTAATTCTGT

Legend:

1F1 / clon1R	Clon3F/clon3R	<i>Clon5F/2725Rv</i>
Clon2F/clon2R	Clon4F/clon4R	2725Fw/V5(2)